POLITECNICO DI TORINO

Collegio di Ingegneria Chimica e dei Materiali

Master of Science Course
in Materials Engineering

Master of Science Thesis

Design of a 3D printed nanocellulose based moisturizer for wound dressing applications

Tutor/s

prof. Marco Sangermano
prof. Paul Gatenholm

Candidate

Cristian Ghibaudo

July 2018

Index

Sommario esteso

Introduzione e concetto

Il progetto Onskin è svolto nel centro BBV con la collaborazione di Stora Enso, Advanced Polymer Technology AB, Medibiome, Cellink e Sahlgrenska University Hospital e l'obiettivo è lo sviluppo di medicazioni innovative basate su cellulosa microfibrillata (MFC) e materiali sostenibili. Nel precedente WP è stata condotta una mappatura dei bisogni focalizzata sulla guarigione della ferita nei trapianti di pelle e una definizione dei requisiti della medicazione è stata condotta. Nel WP1, lo sviluppo del concetto iniziale ha portato alla definizione di un innovativo bendaggio, come mostrato in Figura 1. L'obbiettivo del lavoro è anche dimostrare la possibilità di utilizzare MFC e lo stampaggio 3D come metodo di produzione. [1]

Il concetto sviluppato consiste in quattro moduli come segue:

1. Modulo idratante (M1)
2. Modulo assorbente (M2)
3. Modulo barriera (M3)
4. Modulo di supporto (M4)

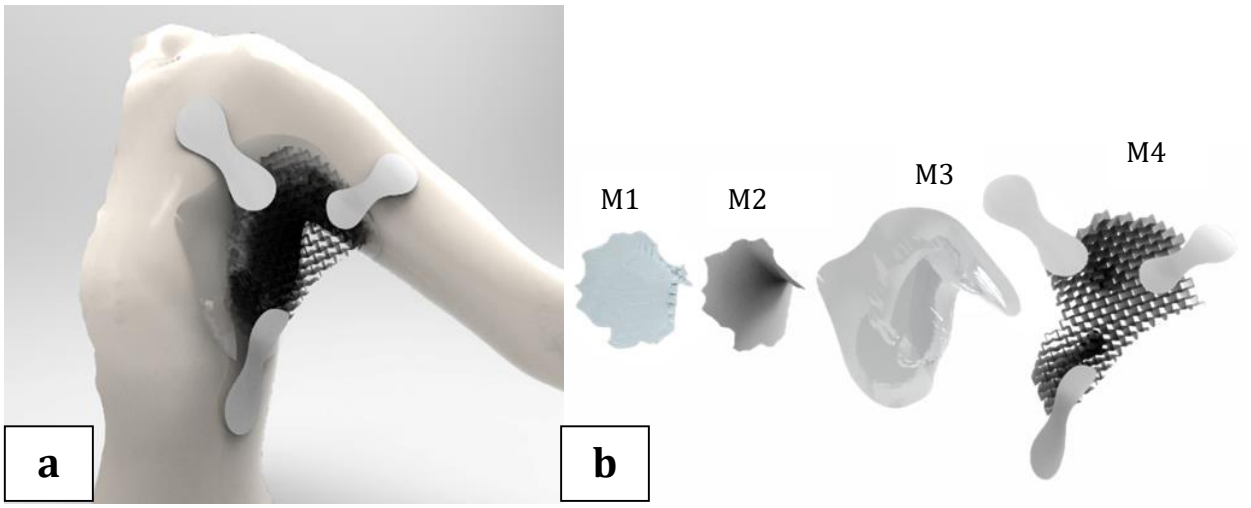

Figura 1 a) Concetto di medicazione della ferita per l'applicazione dell'ascella [1] b) concetto visivo di moduli separati[1]

Ogni modulo deve soddisfare requisiti diversi e ha proprietà diverse, lo scopo di questo lavoro è quello di sviluppare un prototipo del modulo idratante per poi essere combinato con il resto dei moduli. Il requisito preliminare per tutti i moduli è quello di utilizzare materiali sostenibili e biocompatibili.

Concetto e requisiti del modulo idratante

Lo scopo di questo lavoro è dimostrare la possibilità di utilizzare MFC come materiale e usare 3D biprinting come metodo per la produzione di bendaggi tecnologici. I requisiti per il modulo idratante necessario nel concetto di medicazione della ferita sono elencati nella Tabella 1. In questo lavoro sono stati privilegiati i primi quattro requisiti e sono stati condotti diversi test su diversi MFC per valutare la capacità di soddisfarli. Quando la caratterizzazione del materiale è

terminata, quella che soddisfa meglio i requisiti (1-4) saranno considerati gli altri requisiti (5-10) per la selezione finale del materiale e della struttura per il prototipo finale.

Tabella 1. Requisiti del modulo idratante

N	Requisiti	Descrizione
1	Mantenere idratato	La ferita deve essere mantenuta idratata per almeno 7 giorni per una corretta guarigione
2	Rimuovere il liquido prodotto dalla ferita	Il liquido prodotto dalla ferita deve essere rimosso per prevenire rischi di infezione
3	Meccanicamente stabile sotto moderate forze di compressione e taglio	Il materiale deve essere stabile sotto una moderata compressione e forze di taglio per mantenere la struttura
4	Conservare la forma per non spostarsi dal bordo della ferita	Il materiale non deve restringersi troppo e rimanere in posizione per mantenere la ferita sempre idratata
5	Essere compatibile con il metodo di stampaggio 3D	Il materiale deve essere stampabile in 3D per avere la possibilità di creare una struttura che riproduca la forma della ferita e prevenga il sollevamento del trapianto di pelle
6	Essere skin friendly	Il materiale non deve causare reazioni allergiche o irritazione alla pelle del paziente
7	Essere sterile	Il materiale deve essere sterile prima dell'uso
8	Poter essere applicato senza causare dolore al paziente	Il modulo deve essere facile da applicare senza causare dolore al paziente
9	Disponibile su richiesta	Il modulo deve essere disponibile al personale medico subito dopo l'intervento
10	Permettere le normali azioni giornaliere del paziente	Il modulo non deve essere invasivo per consentire alle attività quotidiane ai pazienti, ridurre il costo medico e migliorare la vita durante la guarigione della ferita

Il bendaggio deve avere una durata di almeno 7 giorni, questo significa che anche le proprietà del materiale devono durare per 7 giorni. I campioni sono stati sottoposti a test che hanno valutato le proprietà dei materiali e forniranno i dati necessari per comprendere la migliore soluzione per la produzione del prototipo del modulo. Successivamente, il materiale viene stampato con diverse strutture e la funzionalità delle strutture viene valutata considerando la capacità di estrarre il fluido prodotto dalla ferita, l'interazione con il secondo strato verrà anche valutata. Nella prima parte della tesi viene fornita una descrizione del materiale e della sua produzione, successivamente verranno esposti i metodi di caratterizzazione e metodi di 3D bioprinting, infine una valutazione critica dei risultati ottenuti è conseguita e l'ultima parte è dedicata allo sviluppo del prototipo.

Produzione della nanocellulosa

Disintegrazione meccanica

Per delaminare le nanofibrille, l'energia di legame idrogeno interfibrillare deve essere superato, senza che le fibre vengano tagliate, è anche importante prevenire la coalescenza a seguito della delaminazione, per questo motivo le MFC sono per lo più prodotte con metodi in fase liquida [2]. Uno studio recente [26] utilizza fluidizzatori, mentre una panoramica dei macchinari utilizzati potrebbe essere vista nella Figura 2. La concentrazione di nanocellulosa è in genere bassa, inferiore al 5% in peso, producendo sospensioni viscose che sono difficili da gestire.

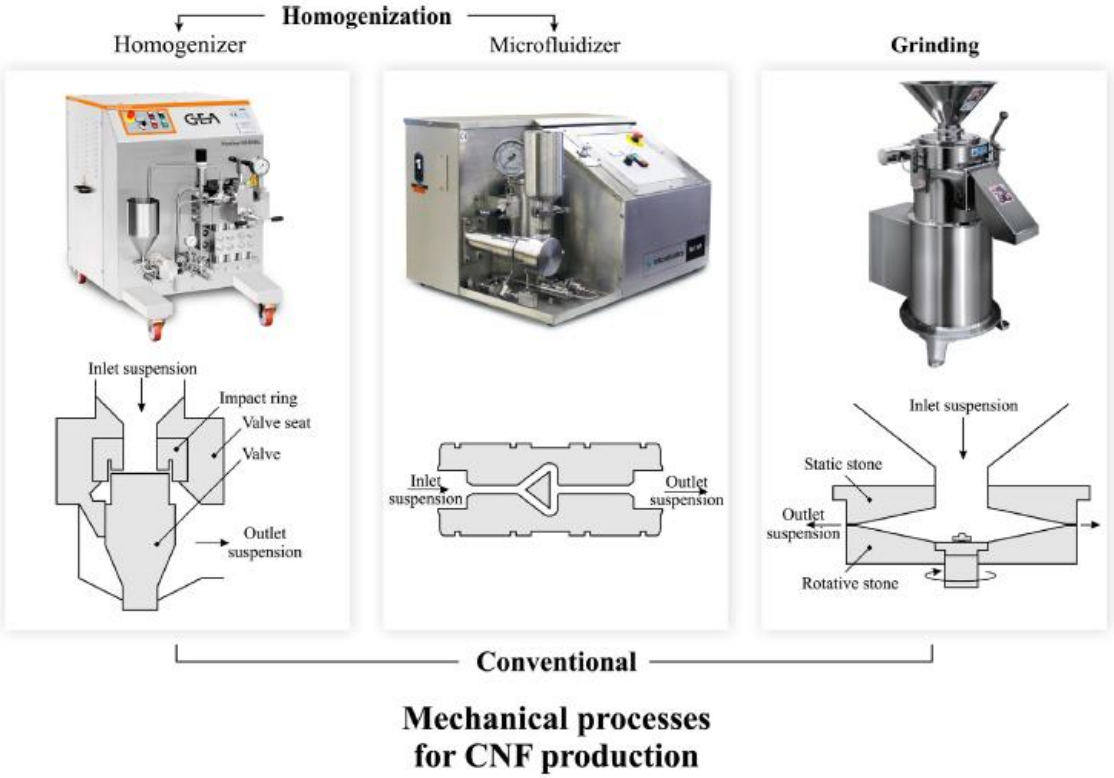

Figura 2. Macchinari usati nella produzione di MFC

Nel processo di omogeneizzazione, la sospensione viene fatta passare attraverso un piccolo spazio tra la valvola di omogeneizzazione e un anello di impatto, così le fibre vengono sottoposte a forze di impatto e di taglio che causano la fibrillazione della cellulosa. Questa apparecchiatura è ampiamente utilizzata nella ricerca per produrre MFC senza pre-trattamenti biochimici. Un inconveniente dell'omogeneizzazione è l'intasamento con fibre lunghe, che rimane la principale sfida per l'upscaling. La soluzione per l'intasamento è sottoporre la cellulosa a un iniziale processo di macinazione in cui la pasta viene passata attraverso un grinder 10 volte e l'MFC ottenuto ha un diametro di 20-90 nm. Durante questo processo l'impasto viene passato tra macine statiche e rotanti, dove la distanza tra di esse può essere regolata, evitando problemi di intasamento.

Per facilitare la fibrillazione, è possibile eseguire la macinazione con presenza di un filler corrosivo, come caolino o carbonato di calcio. In questo caso il materiale risultante è un

composto di MFC e un minerale, questo processo è normalmente designato nell'industria cartaria. Tuttavia, è possibile affermare che la distribuzione delle dimensioni dell'MFC ottenuta con l'ultimo metodo elencato è più elevata rispetto alle altre, il che significa in termini di peso molecolare inferiore e proprietà MFC inferiori [30].

Un ulteriore metodo è il refining dove vengono aumentate la superficie e il volume specifico delle fibre, rendendo le microfibrille più accessibili per ulteriori trattamenti biologici o chimici, nonostante il refining diminuisca la lunghezza delle fibre attraverso il taglio [2].

Pre-trattamento biologico e chimico

I pre-trattamenti sono essenziali in quanto la produzione utilizzando solo la disintegrazione meccanica richiede alti costi energetici, per questo alcuni pre-trattamenti hanno permesso la diffusione di MFC sul mercato. Questi metodi sono principalmente; idrolisi enzimatica, carbossilazione tramite ossidazione mediata da TEMPO e ossidazione periodica-clorite e carbossimetilazione.

Pre-trattamento enzimatico

È stato trovato che il pretrattamento enzimatico con endoglucanasi riduce il consumo di energia e produce MFC con una struttura più uniforme rispetto a quella prodotta con trattamenti che utilizzano acidi [4] [18] [19]. Gli enzimi utilizzati in questo processo sono di tipo endoglucanasi, cioè idrolizzano le regioni amorfe della cellulosa [2]. Nel suo lavoro, Pääkkö et al. (2007) [26] suggerisce una fase di refining prima del trattamento enzimatico per migliorare l'accessibilità delle fibre all'enzima e una fase di refining in seguito. L'ultimo passaggio consiste in diversi step attraverso l'omogeneizzatore. Per avere una buona qualità di MFC dopo il processo enzimatico, è importante eliminare la lignina dalla polpa prima dell'aggiunta di enzimi [18] [19] [26].

Carbossimetilazione

La carbossimetilcellulosa fu preparata per la prima volta nel 1918 e prodotta commercialmente nei primi anni 1920, ma la produzione come nuovo materiale fu riportata da *Wagberg et al. 2008* [36], in cui l'MFC ha un diametro medio delle fibrille di 5-15 nm e una lunghezza fino a 1 micron. Il trattamento carbossimetilico produce MFC con dimensioni di distribuzione leggermente inferiori e più uniformi rispetto a quelle di MFC enzimaticamente pretrattate [9] [37]. Questo trattamento era già praticato in Svezia negli anni '80 da Inventia [38]. Il processo utilizza un omogeneizzatore ad alta pressione, l'ultrasonificazione e la centrifugazione per rimuovere le fibre non fibrillate [2]. Nella Figura 3 è possibile vedere il processo schematico per la formazione delle fibre carbossimetilate.

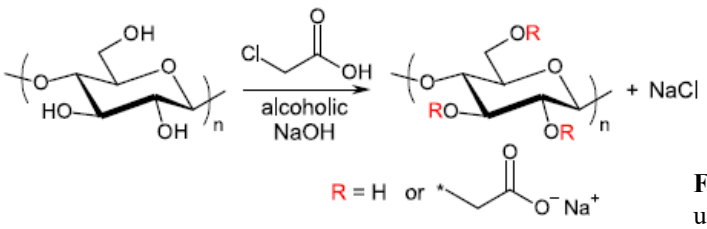

Figura 3. Processo di carbossimetilazione usando acido cloroacetico [2]

Alginato: proprietà

Generalmente, l'alginato è prodotto da alghe marine, da cui viene estratto con un processo chimico e convertito in alginato di sodio. L'alginato può essere prodotto con basso profilo immunogenico, rendendo il materiale interessante per applicazioni biomediche [40].

È un polimero biodegradabile e non tossico [39]. L'alginato è un polisaccaride naturale composto da unità omopolimeriche di 1,4-β-D mannuorato (M) e α-L-gluluranato (G) legati tra loro da un legame covalente. La struttura può variare a seconda della sequenza di blocchi G (G-alginato) o M-blocchi (M-alginato) o alternanza di blocchi M e G, blocchi MG [40] [41].

L'alginato di sodio è il sale di sodio dell'acido alginico, ha un aspetto simile alla gomma. In presenza di ioni bivalenti, come il calcio, subisce un processo di gelificazione, che consiste nella reticolazione delle catene polimeriche con la costruzione di un network polimerico 3D [41]. Grazie alle sue caratteristiche di gelificazione e delle proprietà fisiche, come l'idrofilia, la biocompatibilità e la biodegradabilità, gli idrogel a base di alginato di sodio hanno catturato sempre più interesse nel campo della ricerca [22] [39] [41] [42]. Tuttavia, gli idrogel basati solo sull'alginato di sodio presentano svantaggi, come la scarsa resistenza meccanica e bassa stabilità termica [41].

La struttura e il tipo di giunzione creati influenzano fortemente le proprietà meccaniche dell'alginato reticolato, infatti la catena di alginato mostra una flessibilità diversa, più specificamente, crescente nell'ordine dei blocchi GG, dei blocchi MM e dei blocchi MG [42].

L'attuale medicazione per ferite progettata con alginato di calcio, consente il rilascio di calcio portando allo scambio con il sodio nel liquido delle ferite e produce un contributo riconosciuto all'emostasi clinica [43].

Nel lavoro di *Aarstad et al. (2017)* [40] si suggerisce un modo per combinare MFC e alginato, in modo da utilizzare le migliori proprietà dei due materiali. Questi materiali mostrano una maggiore resistenza alla compressione, il quale si pensa possa essere il risultato della reticolazione mediata da ioni di calcio dell'alginato o di entrambi, in caso di utilizzo di TEMPO-MFC o MFC carbossimetilate. Essi ipotizzano che combinando alginato e MFC, proprietà dei singoli costituenti, cioè rigidità di MFC e compressibilità di alginato, potrebbero essere conservate in gel composito, rendendo possibile il miglioramento delle proprietà meccaniche [40].

In questo lavoro è stato studiato il comportamento del composto alginato MFC, valutando le proprietà meccaniche e reologiche di diverse concentrazioni.

Teoria della guarigione

Progettare e sviluppare una medicazione per ferite è importante per capire il processo di guarigione della ferita e i diversi tipi di forme di essudato e la sua funzione ed effetto sul processo di guarigione. In questa sezione cercheremo di dare alcune informazioni di base per la comprensione delle scelte future riguardanti il materiale e la struttura della medicazione, per uno studio più approfondito dell'argomento è consigliata la lettura dei riferimenti citati.

Processo di guarigione

Il processo di guarigione rappresenta una serie complessa di eventi biologici per ripristinare la funzione di barriera della pelle, prevenire la disidratazione e ridurre il rischio di infezione batterica [45]. Il processo consiste in quattro fasi sistematicamente sovrapposte: emostasi, infiammazione, proliferazione e rimodellamento. Pertanto, la guarigione delle ferite è un processo complesso che coinvolge l'interazione di molti tipi di cellule, componenti della matrice e fattori biologici, ma una caratteristica importante è che l'ambiente della ferita deve essere idratato durante tutto il tempo per una corretta guarigione. Il primo a introdurre la teoria della guarigione delle ferite umide fu *Winter nel 1962* [47], il quale indica i benefici dell'umidità durante la guarigione di una ferita acuta, ma l'eccessiva umidità può essere deleteria, portando a macerazione della pelle e complicazioni della ferita. Gli idrogel di MFC possono essere progettati per mettere a punto l'ambiente umido, ma sono necessari più esperimenti per comprendere il giusto equilibrio di idratazione nelle ferite, poiché non si sa molto sui valori di idratazione corretta [43] [46] [48].

Una differenza importante c'è tra la ferita acuta e cronica in termini di tempo e processo di guarigione [49]-[51]: le ferite acute progrediscono attraverso i normali stadi della cicatrizzazione e di solito guariscono senza complicazioni in una persona sana; le ferite croniche non progrediscono normalmente attraverso gli stadi della guarigione, con conseguenti tempi di guarigione prolungati o addirittura mancata guarigione. Il tempo di guarigione per una ferita cronica può essere compreso tra quattro settimane e 12 settimane. Alcune ferite croniche sono; ulcere da pressione, ulcere alle gambe, ulcere del piede diabetico e ferite maligne [49].

Medicazioni sul mercato

È importante ricordare che non esiste una sola medicazione adatta alla gestione di tutti i tipi di ferite, questa è la prima considerazione da fare per conseguire la scelta giusta della medicazione [43].

Sul mercato si possono trovare molti tipi di medicazione, ma è possibile effettuare una classificazione a seconda del controllo dell'essudato da parte delle medicazioni e può essere suddivisa in due categorie:

1. Controllo diretto:
    - Absorptive dressing
    - Medicazione che modifica l'essudato: controllo batterico, inibitori della proteasi, acido ialuronico
    - Uso della compressione: statico (bendaggio), dinamico (terapia di compressione intermittente)
    - Meccanica; drenaggio, pressione negativa locale (VAC)

2. Controllo indiretto:
    - Alleviazione alla base della causa

La medicazione d'azione della capillarità è il tipo di medicazione a cui ci siamo ispirati, la Figura 4 illustra il concetto di medicazione, queste medicazioni conducono il liquido prodotto dalla ferita lontano dalla superficie della ferita. Di solito sono multi-strato con lo strato interno non aderente che conduce il fluido verticalmente. Strati successivi mantengono e dissipano il fluido attraverso il componente esterno della medicazione del composto. L'efficacia di questo tipo di medicazione è stata dimostrata in ferite con volumi di essudato da moderati a elevati di viscosità da bassa a moderata.

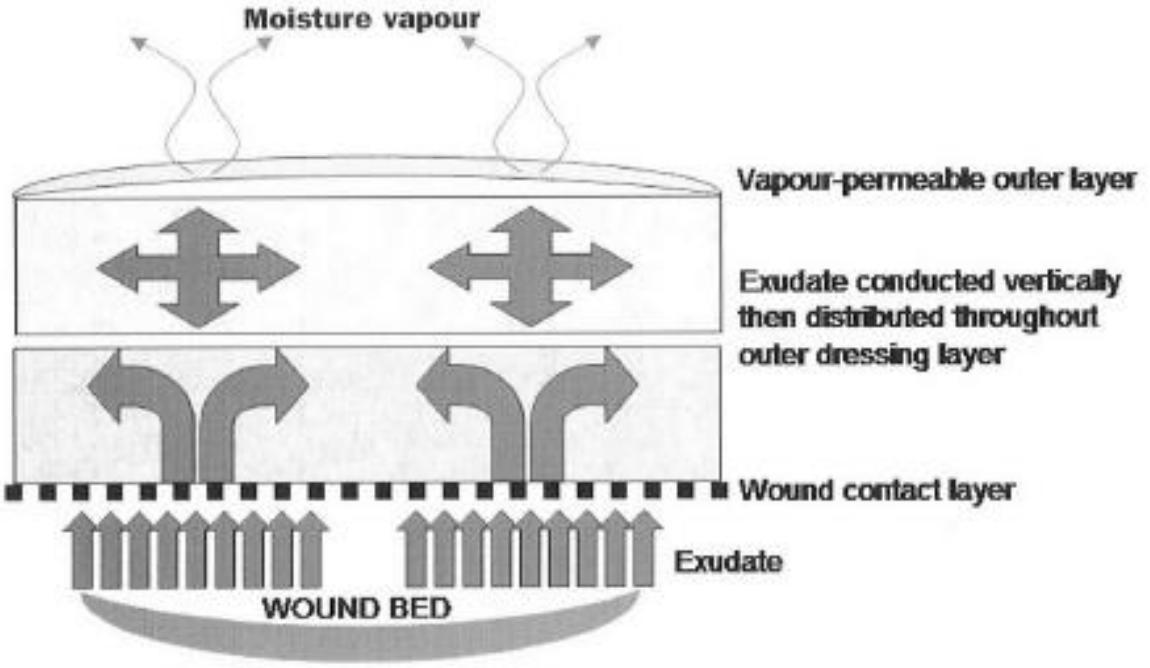

Figura 4. Modello di medicazione ad azione capillare [46]

Lo sviluppo del materiale ideale per la medicazione delle ferite è focalizzato sui requisiti di elasticità, umidità e mantenimento del pH nell'ambiente della ferita. La carbossimetilcellulosa, Hydrofiber®,medicazione (come Aquacel®) è stata ampiamente studiata come promettente materiale per la medicazione delle ferite nel trattamento di ustioni e ulcere, tuttavia l'uso di questo tipo di medicazione richiede cambi di medicazione generalmente frequenti, aumentando il dolore del paziente. Il cambiamento ripetuto e doloroso della medicazione nelle aree delle ustioni e nei siti donatori di trapianti cutanei spesso richiede un'anestesia generale nelle fasi iniziali della guarigione [45].

Hydrofiber® non è né idrocolloidi di nanocellulose né alginati, ma una categoria separata che incorpora i benefici di entrambi, con il difetto di una forte adesione, la prima medicazione Hydrofiber® commercializzata è stata Aquacel® (ConvaTec) 1997. Oltre a Aquacel®, c'è anche Aquacel Ag ® che è impregnato di argento con effetto antimicrobico. Versiva XC® è un'altra medicazione costituita da una combinazione di Hydrofiber® e poliuretano laminato in film che aiuta a evitare la perdita laterale del liquido essudato [52]. Questo tipo di medicazione aiuta la guarigione della ferita proteggendo i bordi della ferita dalla potenziale macerazione e fornendo al controllo passivo delle infezioni [52].

Negli ultimi decenni, gli idrogel sono stati descritti come candidati ottimali da utilizzare nelle medicazioni per ferite poiché soddisfano la maggior parte delle caratteristiche desiderabili di una medicazione ideale; mantenere un livello appropriato di idratazione, per alleviare il dolore, non aderire alla ferita e riprodurre la forma del corpo [43]. MFC potrebbe avere applicazione anche nella medicazione per ferite croniche, la progettazione di una medicazione su misura, con caratteristiche assorbenti e bio-reattive può essere una soluzione che beneficia dello sviluppo delle ultime tecnologie di management della ferita.

Inoltre, la stampa 3D e il coating sono processi a basso costo e possono facilitare la deposizione di specifici materiali di nanocellulosa [53] per consentire la produzione di medicazione per le medicazioni personalizzabile.

Processi di 3D bioprinting

La tecnologia di stampa 3D è la tecnologia di produzione più interessante al giorno d'oggi e per la prospettiva futura, grazie alle sue possibilità di creare prodotti altamente personalizzabili. Grazie a questa caratteristica, ultimamente la stampa 3D viene utilizzata sempre più in campo medico per produrre dispositivi biomedici e tessuti vivi [54]. Una stampante 3D è in grado di produrre prodotti personalizzati con un metodo strato per strato. La recensione di *Carrasco et al. (2015)* [54] mostra le ampie possibilità di utilizzo di fibre di cellulosa e materiali in nanocellulosa in combinazione con i metodi di stampa 3D.

Per uso biomedico, la nanocellulosa è un buon candidato per l'applicazione di biocompositi, tra cui la medicazione e il drug delivery. Tuttavia, qualsiasi tipo di nanocellulosa richiede una valutazione della biocompatibilità prima dell'uso per dispositivi medici [54].

Un ulteriore miglioramento sarebbe l'uso di MFC funzionalizzati con cellule, fattori di crescita, antimicrobici e utilizzare questo materiale come bioink per medicazioni su personalizzate per diversi tipi di ferite. Anche l'elettronica stampata e i biosensori potrebbero essere integrati nella struttura della medicazione delle ferite, per una gestione intelligente e personalizzata [54].

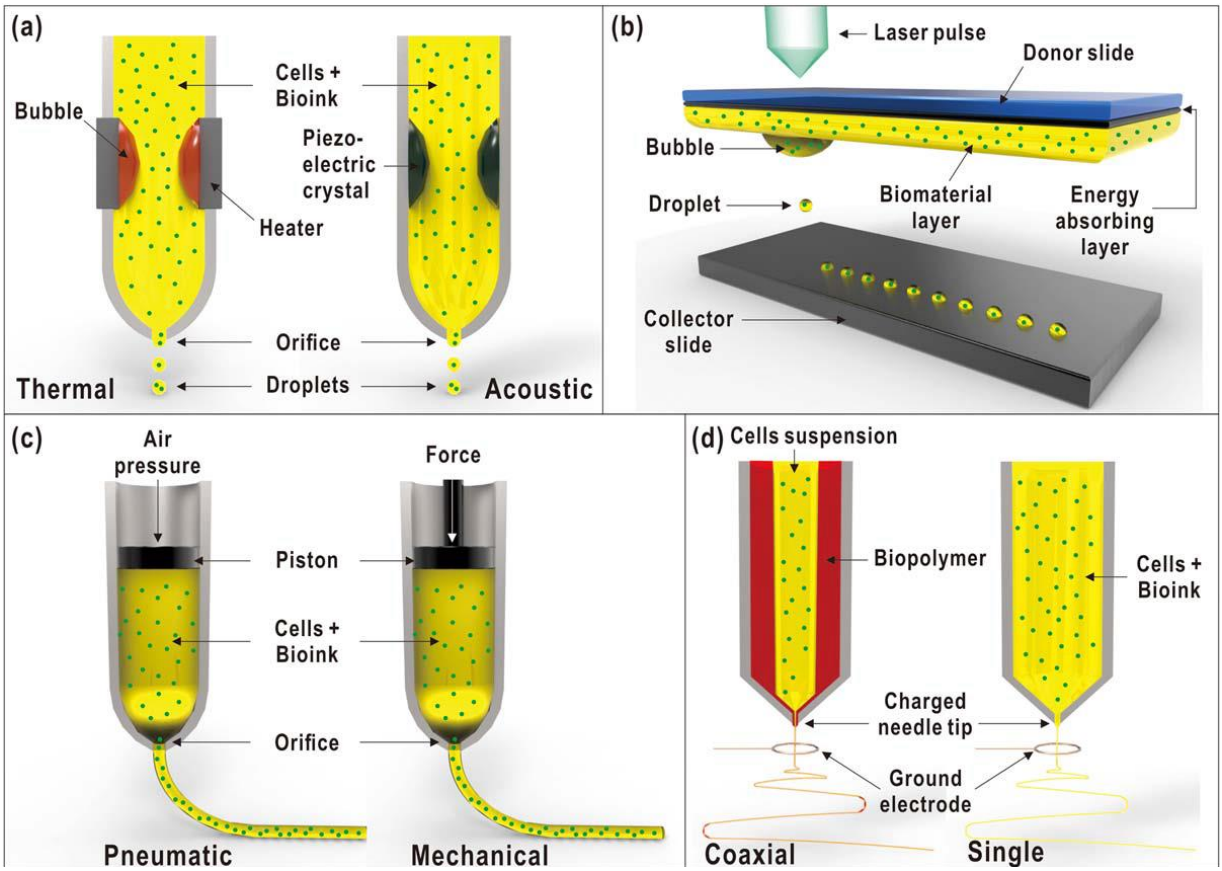

Figura 5. quattro tecnologie di stampaggio 3D, a)inkjet, b) Laser assissited bioprinting, c) extrusion bioprinting, d) bio-electrospray bioprinting. [55].

Gli inchiostri composti da nanocellulosa e alginato mostrano una buona riproduzione della forma, l'alginato come già detto è essenziale per l'integrità della struttura dopo il processo di stampa e la reticolazione [54].

I processi di bioprinting 3D più utilizzati sono:

1. 1. Laser-assisted bioprinting
2. Inkjet bioprinting
3. Extrusion bioprinting
4. Bio-electrospray and cell electrospining bioprinting

Questi processi differiscono per la tecnologia ma anche per le gamme di bioink che possono essere utilizzati.

Extrusion bioprinting

L' Extrusion bioprinting, Figura 5c, è la tecnologia utilizzata in questo lavoro. Queste bioprinters espellono un flusso continuo di bioink sulla piattaforma di stampa grazie ad un sistema pneumatico o meccanico di estrusione, questa soluzione è la più semplice utilizzata per stampaggi senza cellule vive, possiede la più ampia gamma di biomateriali, opolimeri biocompatibili e sferoidi cellulari utilizzabili. Il sistema pneumatico è il più semplice da un punto di vista costruttivo, utilizza l'aria compressa per spingere il bioink da un ugello, mentre il sistema meccanico utilizza forze di compressione fornite da una vite o un pistone. Quest'ultima tecnologia consente di avere un maggiore controllo sul bioink che viene espulso, ma la struttura è più complessa della soluzione pneumatica. L'estrusione bioprinting è il metodo di prototipazione rapida più conveniente. La risoluzione finale dell'oggetto è influenzata da molti fattori della stampante e delle proprietà reologiche del bioink. [55].

Durante il processo di stampa è possibile modificare alcuni parametri per ottenere un'alta risoluzione o un'elevata produttività. Per la stampa di estrusione, quella utilizzata in questo lavoro, i parametri che possono essere modificati sono:

- Dimensione dell'ugello
- Tipo di ugello: conico, dritto
- Pressione
- Velocità di stampa

Cambiando questi parametri, può essere cambiata la risoluzione finale. La stampante utilizzata in questo lavoro è fornita da CELLINK, il BioX. Il BioX ha tre teste di stampa pneumatiche e può essere caricato con materiali diversi.

Preparazione del materiale

Cellulosa microfibrillata e alginato

Gli MFC utilizzati in questo lavoro sono stati forniti da Stora Enso. Sono stati analizzati due diversi tipi, che differiscono per metodi di produzione e concentrazione di massa secca. La prima è una nanocellulosa enzimatica, ha un aspetto opaco e un colore bianco, Figura 6a. Per quanto riguarda le proprietà meccaniche, ha l'impossibilità di essere reticolato senza l'aggiunta di altri componenti, come ad esempio l'alginato.

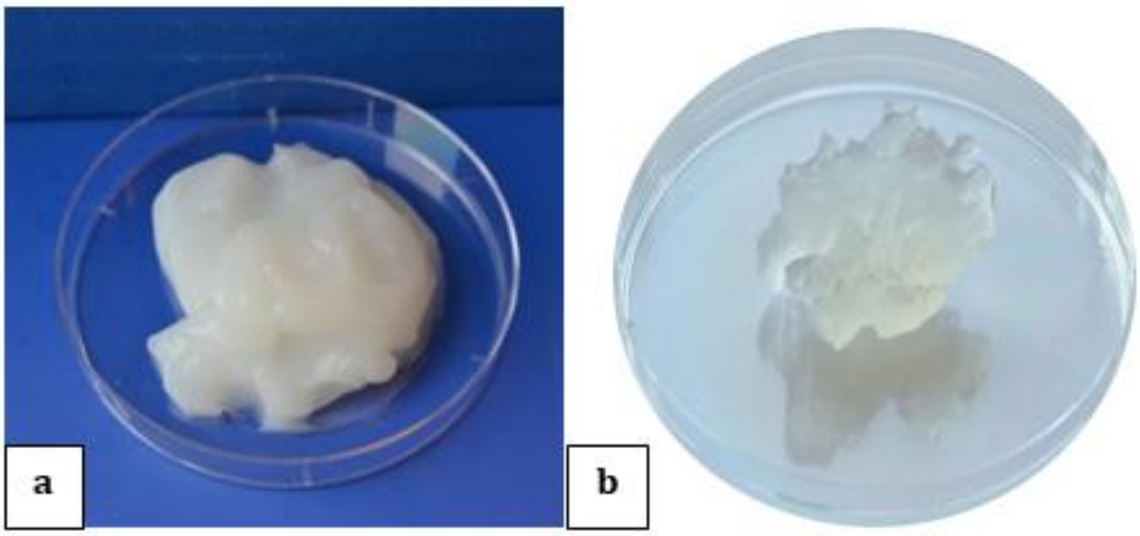

Figura 6. MFC1 e MFC8 nella loro forma grezza

Il secondo tipo è prodotto con un metodo carbossimetilico come sopra descritto, quindi sulla superficie della cellulosa possiamo trovare gruppi carbossimetilici con la possibilità di formazione di una sparsa rete 3D non permanente tra le fibrille a bassa resistenza. L'MFC8 ha un aspetto trasparente, come mostrato in Figura 6b.

L'alginato è un polimero reticolabile, come descritto sopra, ed è stato aggiunto a MFC1 e MFC8 per migliorare le proprietà meccaniche, quando una soluzione con catione bivalente, come Ca^{2+}, viene aggiunta alla composizione.

Sotto la Tabella 2 spiega tutta la composizione utilizzata nel presente lavoro:

Tabella 2. lista dei materiali e delle composizioni utilizzate in questo lavoro

		Dry weight in 10 g of hydrogel		Dry content	
Nome	**Tipo di cellulosa**	**MFC (g)**	**MVG (g)**	**X_{MFC_ink} (%)**	**X_{MVG_ink} (%)**
MFC1_0	Enzimatica	0.3	0	1	0
MFC1_8020			0.075	0.8	0.2
MFC1_6040			0.2	0.6	0.4
MFC1_4060			0.45	0.4	0.6
MFC1_2080			1.2	0.2	0.8
MFC8_0	Carbossimetilica	0.26	0	1	0
MFC8_8020			0.065	0.8	0.2
MFC8_6040			0.173	0.6	0.4
MFC8_4060			0.39	0.4	0.6
MFC8_2080			1.04	0.2	0.8

La preparazione dei bioink è stata effettuata con i seguenti passaggi:

1. Calcolo e peso dell'alginato
2. Aggiunta di MFC all'alginato
3. Miscelazione meccanica dei componenti con una spatola o con uno speed mixer (lo speed mixer aiuta ad avere una distribuzione dell'alginato più omogenea)
4. Miscelazione del bionk con due siringhe collegate attraverso un connettore per 20 volte.

Alla fine del processo, i bioink sono stati lasciati riposare per 24 ore per assicurare la completa dissoluzione dell'alginato, successivamente il bioink è spremuto fuori dalle siringhe attraverso un ugello conico utilizzato nel processo di stampa 3D con un diametro finale di 0,25 mm per garantire la completa dissoluzione dell'alginato in l'inchiostro.

Metodi

I metodi utilizzati in questo lavoro saranno elencati di seguito. La caratterizzazione è stata suddivisa in due categorie principali: caratterizzazione del materiale e caratterizzazione della struttura. L'obiettivo iniziale era definire le proprietà del materiale e selezionare l'opzione migliore per lo sviluppo del prototipo. Il secondo era per la definizione della struttura necessaria per lo sviluppo del prototipo. Ogni test è stato progettato per definire il comportamento del materiale o della struttura in condizioni specifiche e per dimostrare la possibilità del materiale di soddisfare i requisiti necessari per il modulo idratante sopra elencato. Il numero si riferisce ai requisiti elencati nella Tabella 1.

Tabella 3. lista dei metodi utilizzati

Caratterizzazione del materiale		**Requisiti testati**	**Caratterizzazione della struttura**	**Requisiti testati**
Test di ritenzione idrica		1	Test di interazione	1, 8
Test di restringimento		4		
Test reologici			Test di stampabilità	9, 10
	Viscosità	5		
	Crosslinking kinetics	3		
	Test di resistenza a taglio	3 and 4		
Test di compressione		3	Test di estrazione del liquido	2
Citotossicità		6, 7		

Discussione dei risultati

Analizzando i risultati dei test è possibile dedurre quale sia il miglior materiale per creare il prototipo. Prima di tutto l'idrogel deve essere stampabile 3D e quindi avere proprietà di shear thinning. Nell'analisi della viscosità è mostrato che tutte le composizioni sono stampabili in 3D ma alcune sono più facili da stampare rispetto ad altre. Le composizioni con alginato in maggiore quantità hanno mostrato una maggiore viscosità, il che significa che durante il processo di stampa è necessario utilizzare una pressione più alta e una bassa velocità dell'estrusore, infatti per la composizione con circa l'80% di alginato la pressione utilizzata era nell'intervallo di 170 kPa mentre per il la composizione con il 20% di alginato è necessaria solo 20-30 kPa.

Il primo requisito da soddisfare è elencato nella Tabella 1 ed è: mantenere idratato il letto della ferita per almeno 7 giorni. Attualmente Aquacel® viene utilizzato in caso di ferite croniche per mantenere il livello di idratazione elevato nella ferita durante la guarigione. Grazie al test di ritenzione idrica è stato dimostrato che tutti gli idrogel hanno un valore WRT migliore rispetto alla medicazione Hydrofiber®. Tra la composizione con MFC1 e MFC8 e il 20% di alginato il secondo ha valori leggermente più alti, ma il test mostra che entrambi i materiali sono adatti all'applicazione per mantenere il letto della ferita con un livello di umidità adeguato.

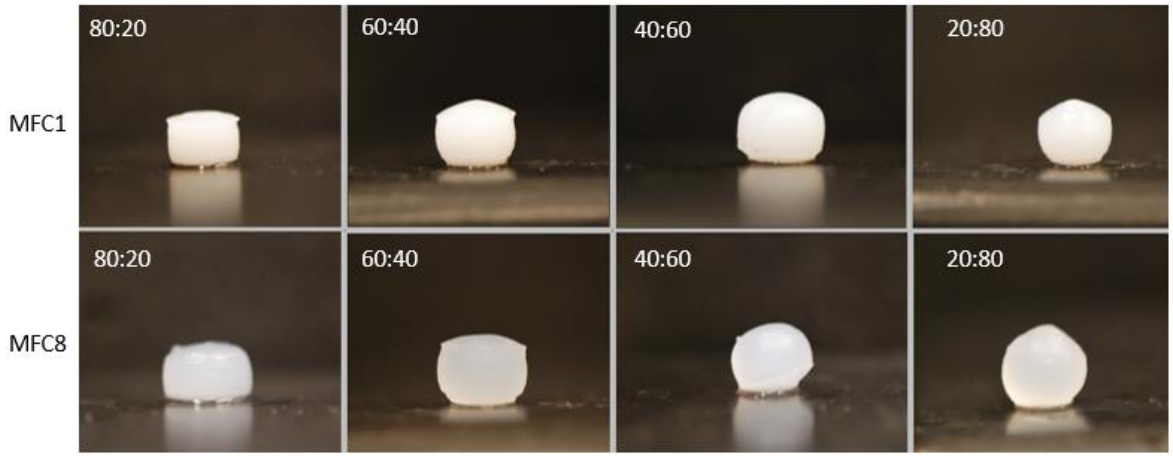

Figura 7.Campioni per i test di compressione. il rigonfiamento aumenta se il contenuto di alginato aumenta

Correlato al test di ritenzione idrica è il test di restringimento, in cui il restringimento è dovuto principalmente all'evaporazione dell'acqua e alla stabilità del reticolo creato, infatti i risultati mostrano materiali reticolati con ST più elevato, questo rende i materiali MFC1_8020 e MFC8_8020promettenti per questa applicazione.

Per quanto riguarda le proprietà meccaniche, è dimostrato che il modulo di compressione è maggiore se l'alginato aumenta, mentre generalmente diminuisce la deformazione percentuale. La prima deduzione dai risultati di compressione è che il materiale senza alginato (MFC8_1) non è adatto per questa applicazione poiché le scarse proprietà meccaniche. Dall'ispezione visiva è importante segnalare un rigonfiamento più elevato per le composizioni con quantità di alginato maggiore, come mostrato nella Figura 7 di seguito.

La composizione con solo il 20% p / v di alginato mostra una buona superficie piatta con un basso rigonfiamento, che si tradurrà in una migliore riproducibilità della struttura da stampare. Il significato del modulo di compressione superiore per valori più elevati di contenuto di alginato è supposto essere causato dalla formazione di rete di alginato che dà forza alla struttura e conseguentemente blocca le fibrille. Una quantità maggiore di alginato creerà una rete più densa e più forte, infatti il carico è principalmente supportato dalla rete di alginato e dopo dalla rete di fibrille manterrà la struttura ma in questo test il punto di rottura delle fibrille non viene raggiunto. La composizione con il 60% e l'80% p / v mostra una elevata rigidità, il che rende i materiali non adatti a questa applicazione poiché presentano anche una bassa elasticità. Considerando la composizione con il 20% p / v dei due materiali, MFC1_8020 e MFC8_8020, la deformazione limite per il mantenimento della struttura è la più adatta per l'applicazione con valori del 49% e 39% rispettivamente, mentre l'MFC8_8020 mostra un modulo di compressione più elevato, 35kPa confronta a 29 kPa, ma minore stress di snervamento, 57 kPa rispetto a 72 kPa.

Grazie al test di cross-linking kinetics è possibile valutare il tempo di cross-linking valutando lo storage modulus in aumento, G ', che è molto veloce, il che significa che la reticolazione è una reazione rapida. Il crosslink parte dalla superficie, formando una pelle esterna al materiale, che limita la diffusione del cross-linker nel bulk per il cross-link completo della struttura. La presenza di fibrille ha facilitato la reticolazione, probabilmente a causa della minore presenza di alginato sulla superficie e più distribuito in tutto il materiale. Inoltre, analizzando la G 'prima della reticolazione è possibile confermare i risultati già visti nel test di viscosità in cui gli idrogel con % di alginato più elevata hanno una viscosità maggiore. Come ultimo risultato è possibile vedere che MFC8_8020 ha G’ finale più alto di MFC1_8020, come allo stesso modo nei risultati di compressione.

L'andamento delle proprietà meccaniche è confermato anche dalla resistenza a taglio dove è possibile vedere il punto di rottura per i materiali MFC1_8020, MFC1_6040, MFC8_8020, MFC8_6040 e MFC8_4060, mentre per gli altri, MFC1_4060, MFC1_2080 e MFC8_2080 non è visibile da quando il test è terminato ad un valore di 10kPa di stress di oscillazione. Per quanto riguarda la composizione interessata MFC1_8020 e MFC8_8020, il valore in cui la G" interseca G' corrisponde al punto di rottura della struttura solida sotto forze di taglio, questo valore ha la stessa tendenza dello stress di snervamento nel test di compressione, poiché è di 4,5 kPa e di 4 kPa rispettivamente.

Il test di citotossicità conferma il materiale è biocompatibile.

Durante la caratterizzazione della struttura, il test di stampabilità mostra che un'altezza superiore a 3 mm rende la struttura troppo rigida e incapace di ricoprire una superficie irregolare, pertanto per il prototipo sono suggerite altezze comprese tra 1,5 e 2 mm. La seconda parte del test suggerisce un riempimento a nido d'ape con una percentuale tra il 20 e il 25% per avere canali ben definiti e una struttura abbastanza forte per essere maneggiata.

La combinazione dei due primi moduli nel test di interazione aiuta a valutare il processo di essiccazione eseguito dal secondo modulo sul primo. Questi test dimostrano che la perdita di acqua è rapida per le prime 20 ore ma poi è quasi nulla, probabilmente perché il secondo modulo assorbe l'acqua libera sullo strato superiore del modulo idratante ma una volta che è saturo il primo strato del modulo assorbente, l’essiccamento è lento e principalmente dovuto all'evaporazione poiché i campioni sono aperti quando devono essere pesati. Questo test mostra

anche che MFC8_8020 è il materiale che ha meno tendenza a perder acqua tra le due composizioni testate.

Nel test di estrazione del liquido, i risultati sono difficili da interpretare poiché è impossibile trovare una velocità di estrazione per le diverse strutture, ma è dimostrato che le strutture possono estrarre il liquido e portarlo nel modulo assorbente.

Sia MFC1_8020 che MFC8_8020 sono adatti all'applicazione per creare il prototipo. Tuttavia, per la fase successiva, la stampa del prototipo, è stata utilizzato solo MFC8_8020, questo anche perché soddisfa il desiderio di avere un modulo trasparente, utile per facilitare l'ispezione visiva della ferita senza la rimozione completa della medicazione. Nella sezione successiva viene eseguita la descrizione della costruzione del prototipo.

Sviluppo del prototipo

Nella Figura 8 sono mostrati i modelli di prototipo piatti. Mostrano buone proprietà meccaniche e, contrariamente al prototipo concavo, sono veloci da produrre con una buona risoluzione, 30 minuti con ugello 0,25 mm. Queste sono le soluzioni che saranno considerate la scelta migliore per il modello finale del prototipo.

Alla fine, il prototipo piatto è stato scelto come il più adatto per l'applicazione, poiché ha il vantaggio di essere più veloce quando è stampato ed è abbastanza flessibile da soddisfare la superficie irregolare del gomito.

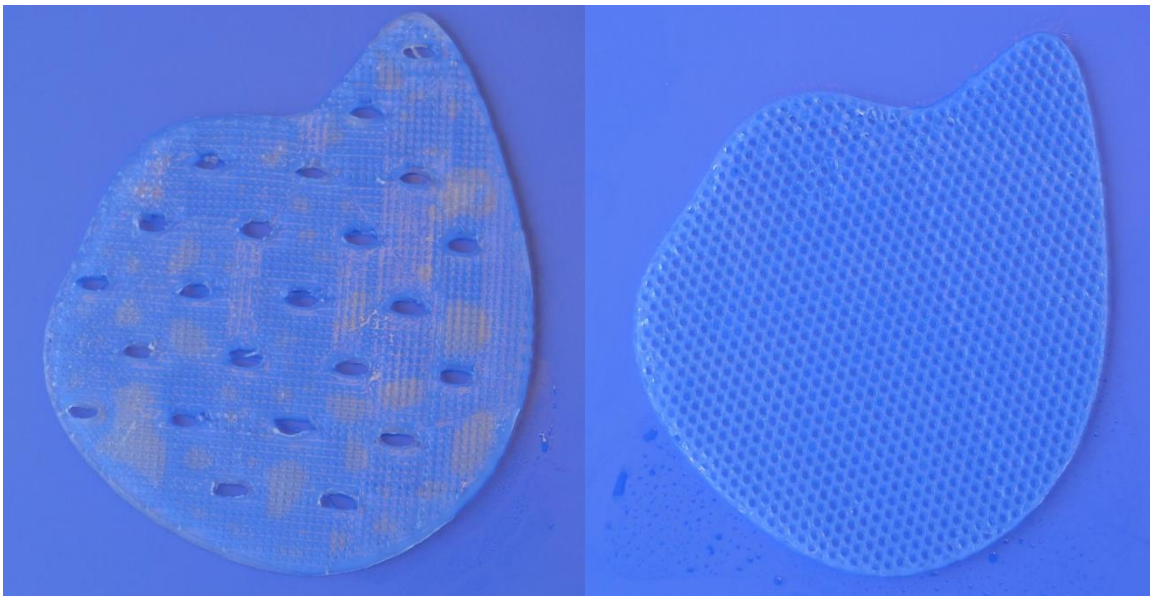

Figura 8. Modelli di prototipo piatto, a) con canali progettati nel file STL, b) con un riempimento a nido d'ape e una percentuale di riempimento del 22 %

Conclusioni e lavori futuri

Alla fine, viene mostrato in questo lavoro la caratterizzazione di idrogel basati su MFC / alginato con test reologici e meccanici. Le proprietà MFC1 e MFC8 sono state valutate e confrontate con diverse quantità di alginato nelle composizioni. Il materiale scelto per questa applicazione è una combinazione di cellulosa microfibrillata, enzimatica o carbossilmetilata e alginato con un rapporto 80:20. Dopo la valutazione del materiale, una caratterizzazione della struttura ha mostrato la migliore soluzione per lo sviluppo di un prototipo. La soluzione migliore è stata trovata nel prototipo piano con il 22% di riempimento e schema a nido d'ape, il prototipo finale è mostrato nella Figura 9. Per concludere, è stata dimostrata la possibilità di utilizzare MFC come materiale per applicazioni di medicazione e processi di stampa 3D. I requisiti elencati nella Tabella 1 sono soddisfatti sia dal materiale che dalla struttura, come mostrato nella Tabella 4.

Tabella 4. Requisiti soddisfatti del modulo idratante

N	RequisitI	Soddisfatto grazie a
1	Mantenere idratato	Materiale (MF1_8020/MFC8_8020)
2	Rimuovere il liquido prodotto dalla ferita	Struttura (prototipo piatto a nido d'ape di riempimento del 22%)
3	Meccanicamente stabile sotto moderate forze di compressione e taglio	Struttura (prototipo piatto a nido d'ape di riempimento del 22%) Materiale (MF1_8020/MFC8_8020)
4	Conservare la forma per non spostarsi dal bordo della ferita	Materiale (MF1_8020/MFC8_8020)
5	Essere compatibile con il metodo di stampaggio 3D	Materiale(MF1_8020/MFC8_8020)
6	Essere skin friendly	Materiale(MF1_8020/MFC8_8020)
7	Essere sterile	Materiale(MF1_8020/MFC8_8020)
8	Poter essere applicato senza causare dolore al paziente	Struttura (prototipo piatto a nido d'ape di riempimento del 22%) Materiale(MF1_8020/MFC8_8020)
9	Disponibile su richiesta	Struttura (prototipo piatto a nido d'ape di riempimento del 22%)
10	Permettere le normali azioni giornaliere del paziente	Struttura (prototipo piatto a nido d'ape di riempimento del 22%)

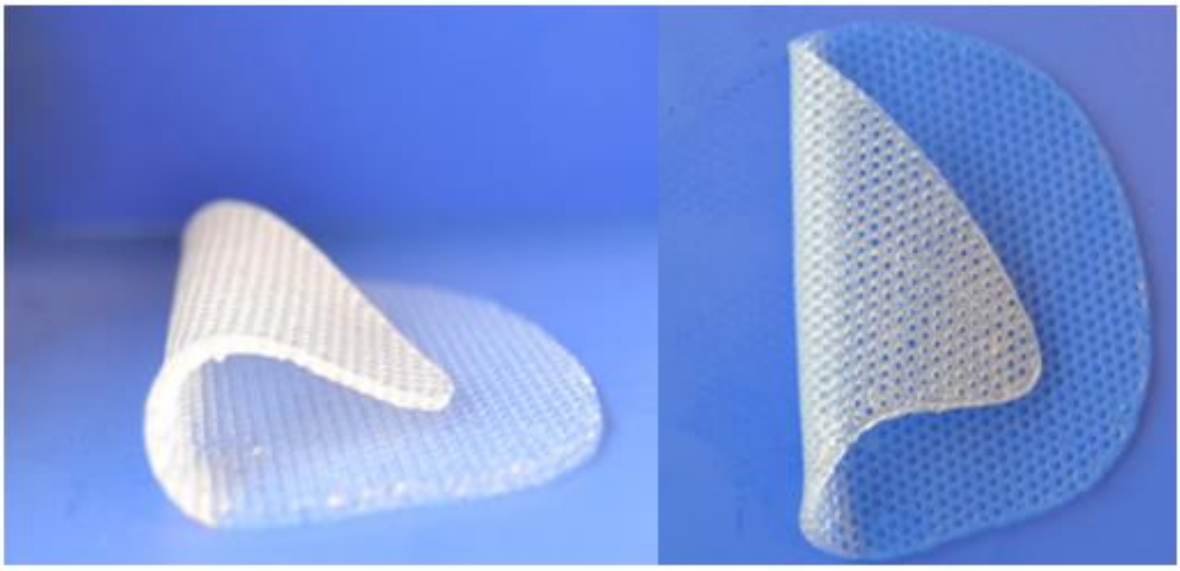

Figura 9 Prototipo piatto a nido d'ape di riempimento del 22%, è flessibile e piegevole

Inoltre, per quanto riguarda i desideri elencati nella Table 2, è possibile vedere che si ottiene un desiderio usando MFC8_8020 come materiale, poiché è più trasparente di MFC1_8020. Gli altri tre desideri; (i) livello di umidità personalizzato, (ii) rimozione di essudati personalizzata e (iii) prevenire la crescita batterica, potrebbero essere utilizzati come ispirazione per il lavoro futuro. Esistono già sul mercato materiali che impediscono la crescita batterica, come Aquacel Ag®, ma potrebbe essere molto utile la possibilità di combinare queste proprietà con un livello di idratazione personalizzato del materiale che potrebbe essere utilizzato su richiesta grazie alla tecnologia di stampa 3D. Per raggiungere questo obiettivo è importante innanzitutto indagare e definire il giusto livello di idratazione necessario per una corretta guarigione. Infine, è possibile ottenere una rimozione personalizzata dell'essudato, ma è necessario indagare più sui fenomeni di trasporto del liquido attraverso il modulo idratante, infatti in questo lavoro è stata dimostrata la funzionalità ma non abbiamo definito quantitativamente la rimozione degli essudati. Nella Figura 10 è possibile vedere il modulo prototipo applicato alla parte interna del gomito, è immediatamente evidente la grande trasparenza del modulo.

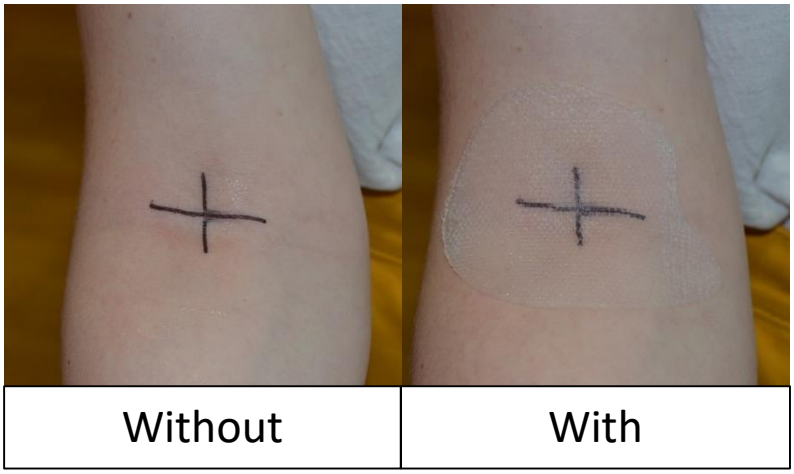

Figura 10. Prototipo applicato alla parte interna del gomito, si può notare l'elevata trasparenza del materiale

Chapter 1

1. Introduction

The Onskin project is led by the BBV center with the cooperation of Stora Enso, Advanced Polymer Technology AB, Medibiome, Cellink and Sahlgrenska University Hospital and the aim is to develop innovative wound dressings based on microfrillary cellulose (MFC) and sustainable materials. In the previous WP a need mapping was conducted focusing on wound's healing in skin transplants and a definition of the wound dressings requirements was conducted, in the WP1 initial concept, Figure 1, was developed also in order to prove the possibility of using MFC and the 3D-printing technology in the project.[1]
The concept developed consist in four modules as follow:

1. Moisturizing module (M1)
2. Absorbent module (M2)
3. Barrier module (M3)
4. Support module (M4)

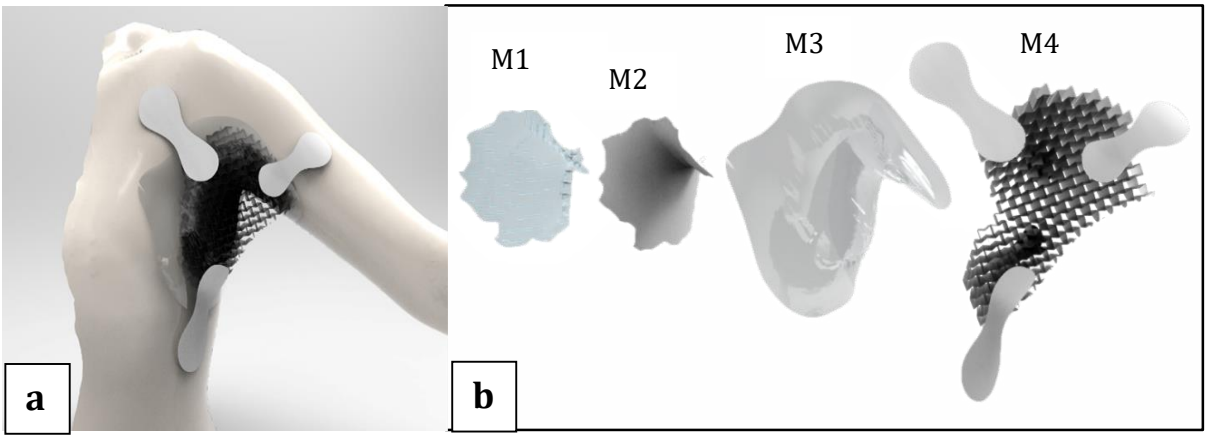

Figure 1. a) Wound dressing concept for the armpit application [1] and b) visual concept of separated modules [1]

Each module has to satisfy different requirements and has different properties, aim of this work is to develop a wound dressing prototype satisfying the requirements and bonding the modules. The prior requirement for all the modules is to use materials be sustainable and biocompatible in this project.

1.1. Moisturizer module concept & requirements

The aim of this paper is to prove the possibility of using MFC as material and 3D-bioprinting as method for wound dressing production. To reach this, it is important to define the requirements in order to fulfil the moisturizer module need in the wound dressing concept, those are listed in the Table 1. In this work the four first requirements were prioritized and different tests on different MFC were conducted to evaluate the ability to satisfy them. When the characterization of the material is finished, the one that satisfy better the requirements (1-4) the other requirements (5-10) will be consider for the final selection of the material and structure for the prototype. Furthermore, some desires were defined, as listed in Table 2, these are not the requirements for the wound dressing, thus they not have to be prioritized but it important to take in consideration for the final assessment.

Table 1. Moisturizer module requirements [1]

Number	Requirement	Description
1	Keep moist	The wound bed must to be kept moist for at least 7 days to have a proper healing
2	Remove wound exudate	The wound exudate produced from the wound must to be removed
3	Mechanically stable under moderate compression and shear forces	The material must be stable under moderate compression and shear forces to maintain the structure
4	Retain the shape to prevent the maceration	The material must not shrink to much to stay in place and maintain the wound bed moist all the time
5	Be 3D printable	The material must be 3D printable in order to have the possibility of create a structure that reproduce the wound shape and preventing maceration and lifting of the skin transplant
6	Be skin friendly	The material must not cause allergic reaction or irritation to the patient's skin
7	Be Sterile	The material must be sterilize before the use
8	Be applied without causing any pain to the patient	The module must to be easy to apply without causing pain to the patient
9	Available on demand	The module must be available to caregiver immediately after surgery
10	Allow the daily tasks of the patient	The module must not be invasive to allow daily activities to the patients to reduce the medical cost and improve the living during the wound healing

The wound dressing should have a lifetime of at least 7 days, this mean that also the material's properties need to last for 7 days.

Table 2. Moisturizer module desires [1]

Number	Desire	Description
1	Customized moisture level	The amount of moist level should be customizable to heal different wound
2	Customized exudate removal	The design of the structure must be customizable to allow the removal of different amount of exudate depending on the wound production.
3	Be transparent	The material is preferred transparent to enable the inspection of the wound healing without removing completely the wound dressing.
4	Prevent bacterial growth	The material should prevent or eliminate the bacterial growth in the wound bed.

The samples undergo to tests which will evaluate the materials properties and will provide necessary data to understand for the module best solution assessment. After that, the material is printed with different structures and the design structures' functionality is evaluated considering extraction fluid ability and interaction with the second layer.

In the first part of the paper a description of the material, characterization methods and 3D bioprinting methods is given, after which a critical evaluation of the results obtained is accomplish and in the last part is dedicated to the prototype development.

Chapter 2

2. Background theory

2.1. Cellulose theory

The cellulose is the most abundant natural polymer that can be used to solve issue due to the extreme use of fossil oil-based product. Cellulose is a vast source for environmentally friendly and biocompatible products and the cellulose come from wood and plants mainly[2]. The most use of cellulose until this days was in the papermaking industry[3]–[5], but lately it is highly demanded for environmental friendly and biocompatible products[3]. In the Figure 2 it is show the cellulose chemical formula.

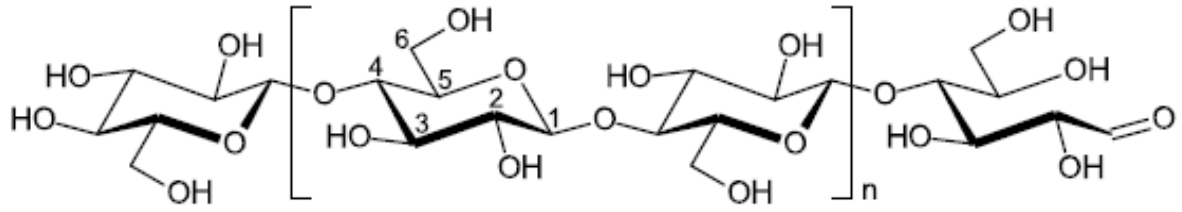

Figure 2. Molecular structure of cellulose polymer [2]

To describe the structure of the cellulose it is necessary to start from the molecular view. It is a linear polymer chain consisting of β-1,4-linked D-glucose rings.[5] The cellulose is a long linear-chain polymer with large number of hydroxyl groups. To satisfy the thermodynamically preferred bond the angle of the acetal oxygen bridges turns every second glucose units of 180° forming a disaccharide that is the structural units called cellobiose[3]. The building blocks of cellulose polymer chain are D-glucopyranose (glucose) molecules. when linked together by beta-1,4-glucosidic bonds they turn into anhydroglucose units. Two anhydroglucose units compose anhydrocellobiose, which is the repeating unit of cellulose polymer. Each anhydroglucose unit has six carbon atoms with three hydroxyl groups (C2,C3 and C6) giving high degree of functionality to cellulose molecule[2], as we will see later there is high possibility of polymer functionalization. The number of anhydroglucose is used to determine the degree of polymerization (DP) (more constituents, higher DP)[2]–[4]. The DP varies from many factors, from the raw material to the treatment to obtain the final product, but normally vary from 300 to 1700, higher value can be reached with cotton and general plant fibers, 800 to 10000, and even with bacteria cellulose[3][4][6].

Cellulose can be derived from a variety of sources such as wood (hardwood and softwood), see fibers (cotton, coir etc.), blast fibres (flax, hemp, jute, ramie etc.) grasses (bagasse, bamboo etc.), marine animals (tunicate), algae, fungi invertebrates and bacteria[7], but wood is the most important source. For the production of cellulose deriving from wood as raw material it is important to extract lignin and hemicellulose, this is done with a large-scale chemical pulping, separation and purification processes[3][4]. Non-wood plants are receiving increasing interest as a source of cellulose since they, generally, comprise less lignin.

The cellulose chains are gather together to form fibrils. The fibrils are the primary structural component in the build of plant cell walls.[8] These fibrils have excellent mechanical properties since the cellulose molecules are arranged in a crystallinity way in the fibrils structure, where both Van der Waals forces and hydrogen bonds hold together the crystals.[8] Its chain give to the fibrils high stiffness, and hydroxyl groups onto it give high hydrophilic properties, this characteristic allow suspension formation with shear thinning properties, even with small concentration of MFC (1 to 4% w/v) [2][4][5][9].

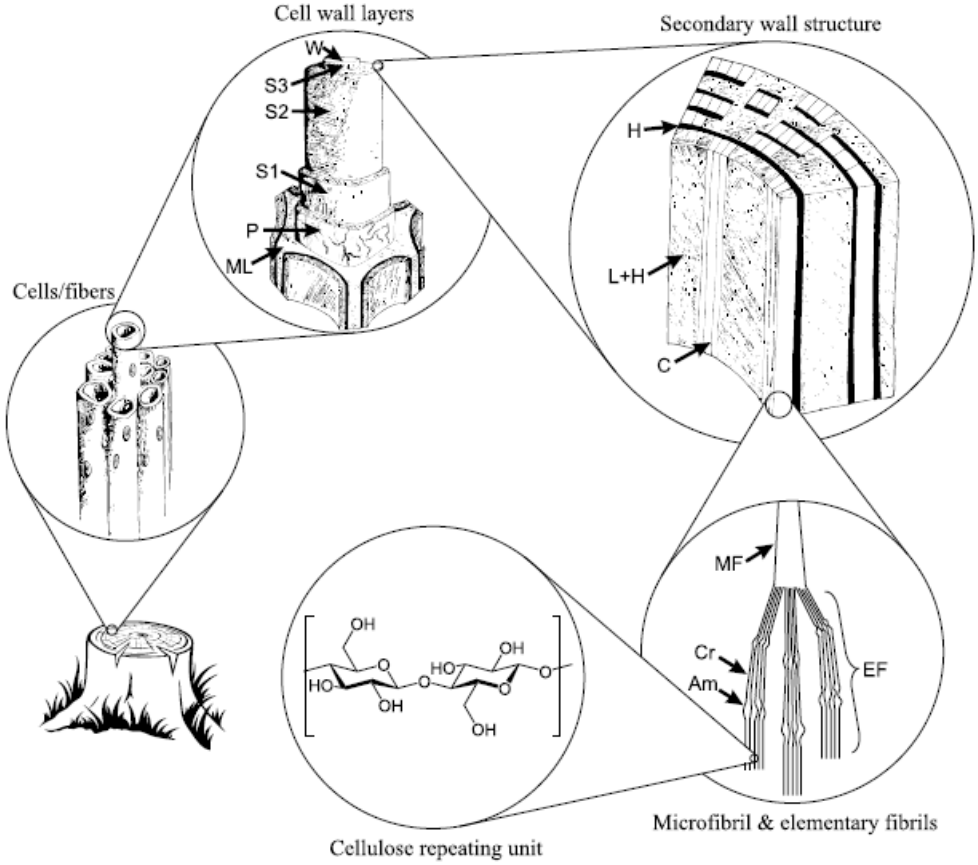

Figure 3. Hierarchical structure from the wood to cellulose polymer [2]

Figure 3 show the hierarchical structure from the elementary unit, cellulose chain, until the macroscopic element, in this case wood.

Considering the lateral dimensions; the elementary fibrils are between 1.5 and 3.5 nm, between 10 and 30 nm are called microfibrils and in the order of 100 nm it is possible to call them microfibrillar bands, while the length is in the range of micrometre[3]. The fibrils dimension depends primarily from cellulose source, for example in the spruce wood microfibrils have a diameter of 10-20 nm[3], and secondly from extraction treatment. A bundle of fibrils creates the fibre, which gives mechanical properties to wood cells[2][3][5][8].

Regarding cellulose properties, it is possible to design them changing or adding functional groups to the cellulose chain, thanks to the hydroxyl groups reactivity [3]. Indeed the repeating of glucose units generates surprising specificity and divers architectures, reactivity and functions[3]. The properties of cellulose are also determined by intermolecular interaction, entanglements, cross-linking reactions, chain-length and from functional groups added to the

chain[3]. For example cellulose chain can obtain additional carboxyl or carbonyl groups after isolation and purification processes[2][3][10][11].

The cellulose properties are thus determinate from the structural organization of chain units and from the groups functionality blended coming from the treatment of raw material. The chirality, degradability and hydrophilicity are due to the hydroxyl groups donor reactivity bond to cellulose units, their most important function is the formation of hydrogen bonds necessary to build a extensively network to allow formation of partially crystalline fibre structure[3].

Using some *top-down* processes is possible to obtain the elementary fibrils that could be used in many applications. The cellulose nanofibrillated (CNF or MFC) material was introduced the first time by *Turbak et al.(1983)*[12] and *Herrick et al(1983)*[13]. The cellulose obtained had lateral dimension in nanometre range, it was obtained by passing a softwood pulp aqueous suspension several times through a high-pressure homogenizer. During the treatment, high shearing forces produce strongly entangled network contain both crystalline and amorphous domains. They generally possess high aspect ratio and form gels in water with shear thinning and thixotropic behaviour.

The possibility of using microfibrillated cellulose (MFC) as a renewable and biodegradable natural material has attracted a lot of interest in the research and development of the material[4][14]. The cellulose is a versatile source since it can be modified by chemical treatment to obtain a lot of variety of commercial derivatives[3][15]. Mainly two type of nanocellulose are distinguished: (i) the one obtained by acid treatment, referred as cellulose nanocrystals (CNC) and the one produced mainly by mechanical disintegration, cellulose nanofibrillated (CNF) or microfibrillated cellulose (MFC)[2]–[4][8]. Since the terminology is not unique yet in literature it could be found different name for the same material, in this report we will use the abbreviation MFC to indicate microfibrillated cellulose. Besides cellulose, into the raw source normally there is also hemicellulose, lignin and a comparably small amount of extractives and inorganic salts. Hardwood is more complex and heterogeneous structure than softwood, which normally has fibres 3-4 times longer. Softwood required less mechanical treatment than hardwood to produce equivalent fibrillation level. It is also important to say that the use of never-dried cellulose comparing to once-dried makes the fibrillation more favourable, since drying promotes hydrogen-bonding between nanofibrils known as hornification [16][17] . Another type of cellulose is the bacterial cellulose (BC). The MFC and CNC are produce by disintegration by a top-down process, while the BC are produce with a bottom-up process from low molecular weight sugars by bacteria, thus the large scale of production of the last cellulose remain questionable. All the cellulose type exhibits hydrophilicity, relatively large surface area, broad potential of surface chemical modification.

The MFC is already a ready material available as commercial product and more interest in industrial applications, but commercialization in the past had to solve the main challenge of isolating CNF since there is a high demand of energy during the disintegration process. In the 2000s and 2010s many chemical and biological or enzymatic pre-treatment of hydrolysis[18][19] help to reduce drastically the demand of energy for the process[2]–[4][20][21].

The MFC has the great capacity of forming a suspension with water, due to the high hydrophilicity, with shear thinning properties, this made this material perfect suitable to be used as ink in the 3D printing process[22][23].

2.2. Production of cellulose nanofibrils

Pulp fibers are produced using several chemical treatment to remove the lignin[4]. Therefore, the first step is to remove the lignin various cooking and bleaching methods, similar to the one used in the papermaking industry. The final fibers are almost pure cellulose containing less than 10w/w% hemicellulose[4][5]. The pulp was usually passed through a high pressure homogenizer five to ten times to obtain MFC gel-like material, this determines an high demand of energy, 12,000-70,000 kWh/tonne[24][25]. The energy demand could be decrease conducting some pre-treatment as enzymatic hydrolysis, again refining and finally homogenization [26][27] or homogenization carboxylmethylation, followed by homogenization [8] or furthermore TEMPO-mediated oxidation followed by blending [28]. In the review of *Lindström et al*.[4] is possible to see the value of energy necessary to produce a tonne of MFC. The energy request decrease drastically with enzymatic or carboxymethylation pre-treatment, it is of 1800 and 500 kWh respectively. Thus the production process is a combination of different operations by varying which different kinds of MFC are obtained[2]. In Figure 4 is possible to see the great variety of possibility to produce MFC from wood pulp[2].

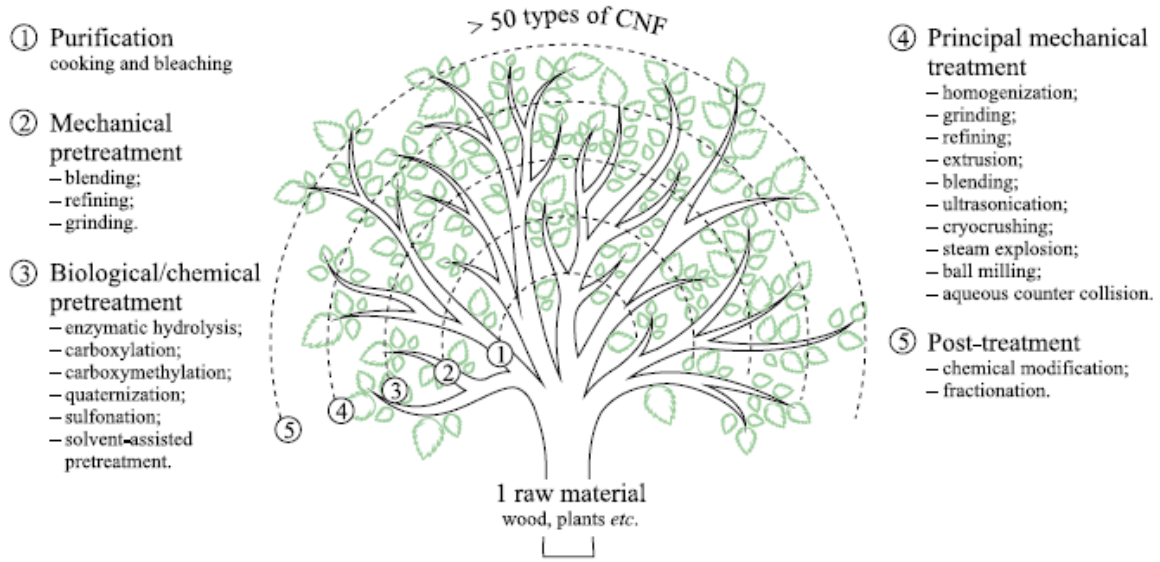

Figure 4. Schematic diagram of MFC production [2]

2.2.1. Mechanical disintegration

To delaminate the nanofibrils the interfibrillar hydrogen bonding energy it has to be exceeded, rather than cut the fibers, it is also important to prevent reverse coalescence, for these reason the MFC are mostly produced using aqueous medium methods[2]. The first methods used from *Turbak and Herrick*[12][13] establish the use of high pressure homogenizers, while more recent work[26] use fluidizers, but the principle is almost the same. An overview of the machinery used could be seen in the Figure 5. The nanocellulose concentration is typically low, less than 5%wt. which result in viscous suspensions that are hard to handle.

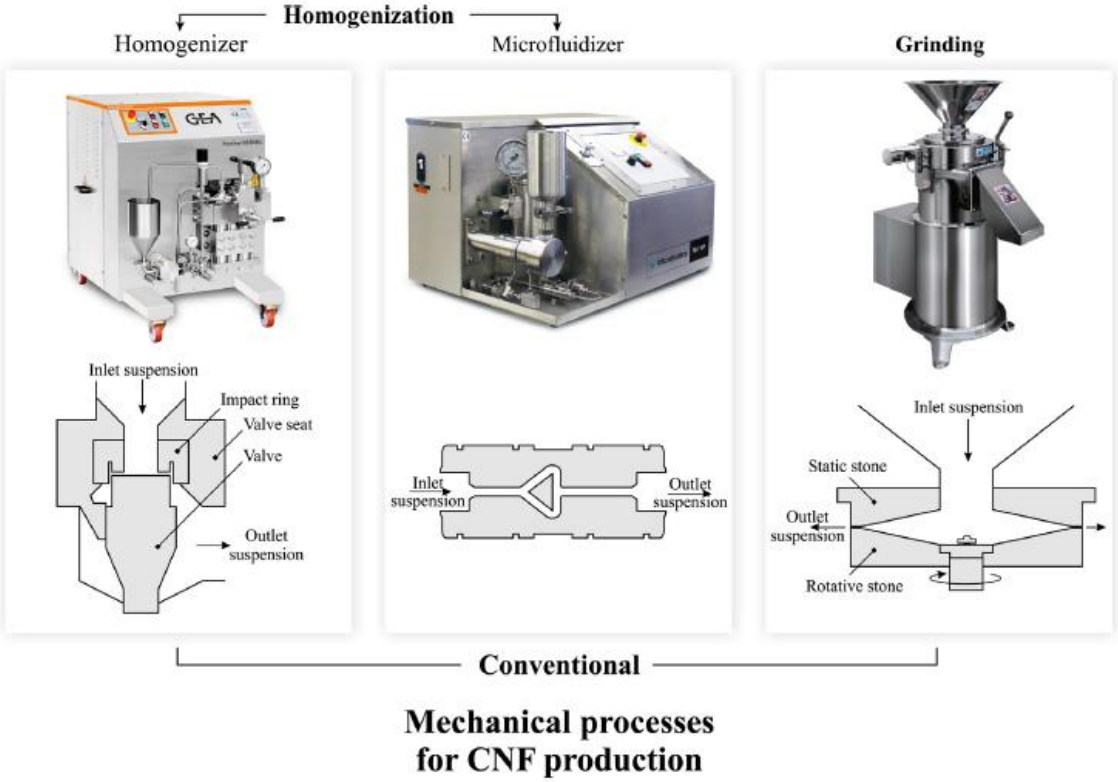

Figure 5. Machinery used in the MFC production

In the homogenization process, a slurry is passed through a tiny gap between the homogenizing valve and an impact ring, thus the fibers withstand impact and shear forces which cause the cellulose fibrillation. This equipment is widely used in research to produce MFC without biochemical pre-treatments[5]. The alternative was proposed by *Zimmermann et al. (2004)*[29] using a microfluidizer to obtain nanofibrils with a diameter from 20 to 100 nm and several ten micrometres as length. The principle of this technique consists of passing cellulose suspension through a thin chamber with a specific geometry, e.g., Z- or Y-shape. A drawback of homogenization is clogging using long fibers, this remain the main challenge for upscaling. The solution for clogging is a previous grinding process where the pulp is passed through a grinder 10 times and MFC obtained has a diameter in the range of 20-90nm. During this process the slurry is passed between static and rotating grinding stones, where the distance between them can be adjusted, avoiding clogging problem.

To facilitate the fibrillation, it is possible to perform grinding with presence of a corrosive filler, like kaolin or calcium carbonate. In this case the resulting material is a

composite of MFC and a mineral, designated for use in the papermaking industry, this method was successfully industrialized and is present on the market under the name FiberLean MFC[2]. Super grinder should be more efficient but is difficult to quantify MFC quality versus the energy used from the several methods[4]. However it is possible to say that the size distribution of the MFC obtained with the latest methods is higher compared to the others, meaning in lower molecular weight and inferior MFC properties[30].

A further method is refining where specific surface and volume of fibers are increased, making microfibrils more accessible for further biological or chemical treatment, despite the refining process decrease the fibers length through cutting[2].

2.2.2. Pre-treatment biological and chemical

The pre-treatments are essential since the production using only mechanical disintegration requires high energetic costs, for this some pre-treatment allowed the diffusion of MFC on market. These methods are mainly; enzymatic hydrolysis, carboxylation via TEMPO-mediated oxidation and via periodate-chlorite oxidation and carboxymethylation.

Enzymatic pre-treatment

It is been found that enzymatic pre-treatment with endoglucanase reduce the energy consumption and produce MFC with a more uniform structure than with the one produced with acid treatments[4][18][19]. The enzymes used in this process can be divided in two categories[4]: (i) cellobiohydrolases, which can catalyse the hydrolysis of crystalline part of the cellulose, (ii) endoglucanases, which hydrolyse amorphous regions of cellulose[2]. In his work, *Pääkkö et al. (2007)*[26] suggest a refining stage before the enzymatic treatment to enhance fibers accessibility to the enzyme and a refining stage afterwards. The last step consists in several passes through the homogenizer. To have a good quality of MFC after the enzymatic process is important eliminate lignin from the pulp before adding enzymes[18][19][26].

Carboxylation via TEMPO-mediated oxidation and via periodate-chlorite oxidation

The introduction of negative charge on fibrils surface induce electrostatic repulsion making easier delamination between fibrils. The negative charge could be induced by carboxyl groups. Since 1993 *Davis and Flitsch (1993)*[31] start to use 2,2,6,6-tetramethylpiperidine-N-oxyl (TEMPO), a water soluble nitroxyl radical for selective oxidation of the primary alcohol groups of into carboxyl groups[4][15][21][32]. This process was used mainly by *Saito et al. (2006)*[28] to oxidize cellulose with TEMPO and hypobromide and hypochlorite at basic pH to produce MFC using blending.

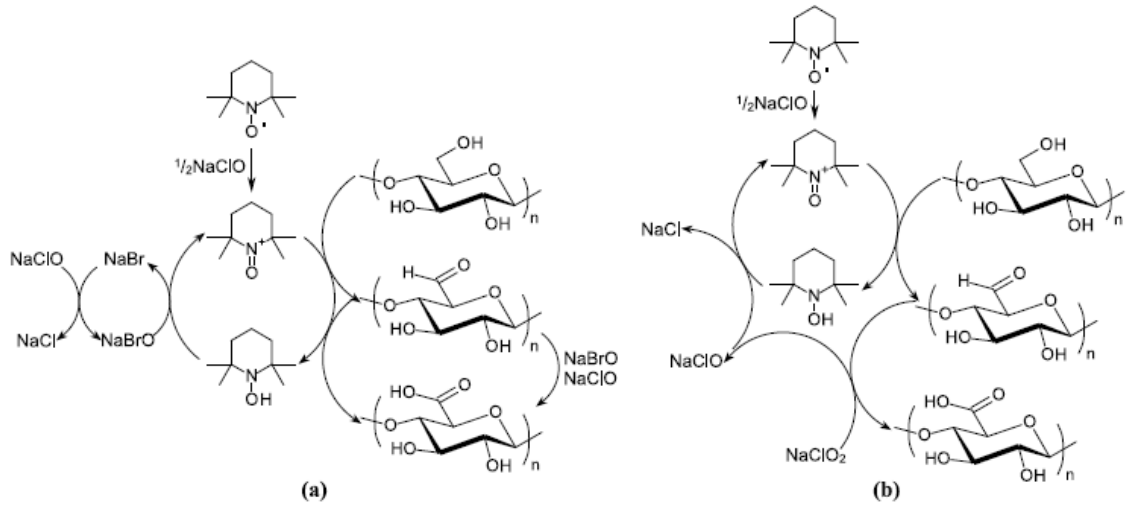

Figure 6. Process of carboxylation by (a) TEMPO/NaBr/NaClO in water at basic pH and (b) TEMPO/NaClO /$NaClO_2$ in water at neutral or slightly acidic pH [2].

The reaction carried out at room temperature for several hours and at the end between nanofibrils was created electrostatic repulsion that allow to reach width of 3-5nm.

Unfortunately if treatment is carried out in a basic environment there is risk of decrease the nanofibrils DP [5][20][28], a solution was proposed by *Satio et al.(2009)*[15] where the reaction was performed under weakly acidic conditions at 60°C for up to 72h, this allow to increase the substitution of the alcohol groups with carboxyl groups without causing depolymerisation of the MFC, the process is schematized in Figure 6.

Another method to substitute carboxyl group on the surface of the fibrils is the sequential periodate-chlorite oxidation of cellulose [33]. This method was used by *Tejado et al. (2012)*[34] where the cellulose secondary alcohols are first oxidized using sodium periodate to aldehyde groups, which are subsequently converted to carboxyl groups using sodium chlorite. With this pre-treatment it can be produced MFC with width of 3-5nm after the homogenizer treatment[35]. As is possible to see in Figure 7 the schematic process[2]

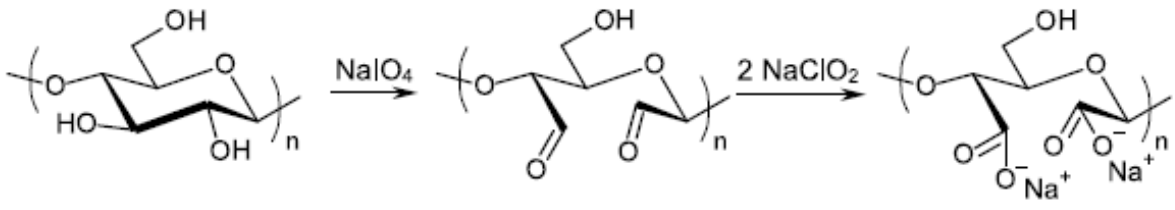

Figure 7. Process of carboxylation via periodate-chlorite oxidation [2]

Carboxymethylation

Carboxymethyl cellulose was first prepared in 1918 and produced commercially in the early 1920s, but the production as a new material was reported by *Wagberg et al. 2008*[36], where the MFC has average diameter of the fibrils of 5-15nm and length of up to 1 micron. The carboxymethyl treatment produces MFC with slightly lower and more uniform distribution dimensions compared to those of enzymatically pre-treated MFC [9][37]. This treatment was already practice in Sweden in the 1980s from Inventia[38]. The process uses a high-pressure homogenizer of carboxymethylated cellulose fibers and ultrasonification and centrifugation to remove the non-fibrillated fibers[2]. In the Figure 8 is possible to see the schematic process for the formation of the carboxymethylated fibers.

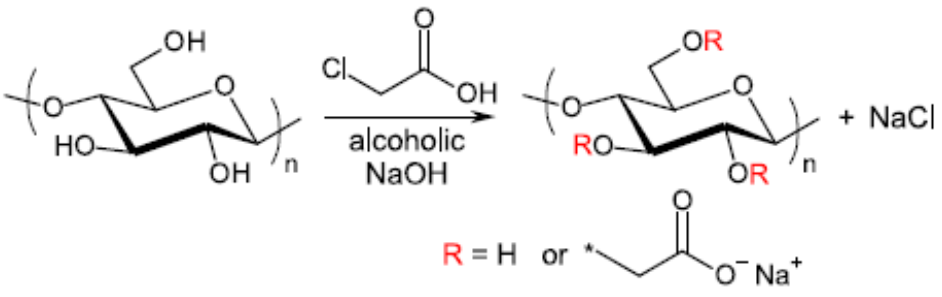

Figure 8. Process of carboxymethylation using chloroaceatic acid [2]

2.3. Alginate: properties and crosslinkability

Generally, the alginate is produced by seaweeds, where it is extracted with a chemical process and converted in sodium alginate. It is a non-toxic biodegradable polymer[39]. It can be found in form of powder or solution. Alginate can be produced under physiological conditions, this with low immunogenic profile, make the material interesting for biomedical application.[40]

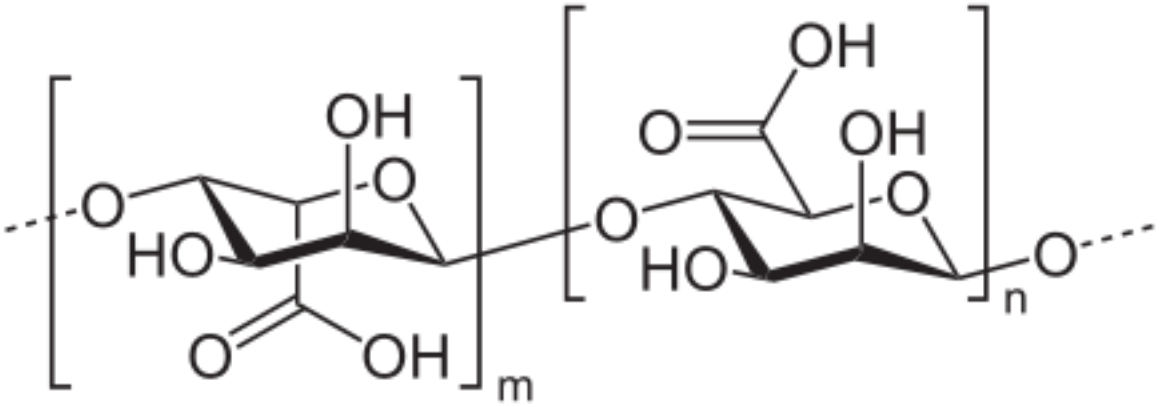

Figure 9. Chemical structure of alginate polymer

The alginate is a natural polysaccharide composed with homopolymeric units of 1,4-β-D mannuorate (M) and α-L-gluluranate(G) linked together by a covalent bond. The structure can vary depending on the sequence of G-blocks (G-alginate) or M-blocks (M-alginate) or alternating of M- and G-blocks, MG-blocks. The structure of the alginate gives different mechanical properties, since the strength of the bonding between the M and G-blocks differs[40][41].

The sodium alginate is the sodium salt of the alginic acid, it has a gum-like aspect. In the presence of divalent ions, such as calcium, strontium, barium, etc., it undergoes to a solidification process, which consist in the cross-link of the polymer chains with the construction of a 3D network[41]. Due to the gelation characteristic and physical properties, such as hydrophilicity, biocompatibility and biodegrability, sodium alginate based-hydrogels have captured more and more interest in the research field[22][39][41][42]. However, hydrogels only based on sodium alginate have the disadvantages of poor mechanical strength and low thermal stability[41].

In calcium alginate, sodium is exchanged with a divalent ion of calcium and it creates a network between polymer chains, bringing to the formation of a strong network. As we said the structure and the type of junction created, highly influence mechanical properties of crosslinked alginate, indeed the alginate chain show different flexibility, more specific, increasing in the order GG-blocks, MM-blocks and MG-blocks[42]. It has been shown that also the molecular weight and concentration of the polymer influence Young's modulus and strength of hydrogels[22][40][42]. In general is possible to say that G-blocks junctions are the one more stable and higher concentration, the number of G-blocks in the chain will be responsible for high gel strength[42]. The rupture strength is a reflection of the strength and the number of junctions, and in general is possible to say that the strongest junctions are the shortest in length[40][42].

Alginate is widely used in many field; food, textile, papermaking, pharmaceutical and biomedical industries[39]–[41]. It can be also used as hydrogel in bioengineering research[22][23] where alginate composites have favorable properties, such as improved porosity, important for the cell proliferation and also giving mechanical strength after crosslinking. In literature there are some work regarding the use of alginate in combination with other biopolymer, such as gelatine[39][41][42] and in the last decade it starts to attract interest also composite hydrogel MFC/alginate for biomedical application and wound dressing[22][40][42].

It has been studied also the calcium introduction in the wound healing process, this will be indicate in more detail later, but we can say that the actual wound dressing designed with calcium alginate, allow calcium releasing leading to exchange with sodium in wound fluids and producing a acknowledged contribution to clinical haemostasis[43]. In in-vitro wound construct, calcium alginate increased the proliferation of fibroblasts but delayed the proliferation of keratinocytes without influencing their motility. This suggests that the calcium realised by dressing will benefits some aspects of wound but not others.[44]

In the work of *Aarstad et al. (2017)* [40] it is suggested a way to combine the MFC and alginate to use the best properties of the two material. These materials show increased compression strength suggested to be the result of calcium ions mediated crosslinking of the alginate or both, in case of using TEMPO-MFC or caboxymethylated-MFC. They hypothesize that by combining alginate and MFC, advantageous properties of individual constituents, i.e., stiffness of MFC and compressibility of alginate, could be preserved into composite gel, making possible to tailor the mechanical properties.[40]

In this work it has been investigated the behave of composite MFC-alginate, evaluating the mechanical and rheological properties of different concentrations.

2.4. Wound healing theory

To design and develop a wound dressing is important to understand the wound healing process and the exudate difference form types and their function and effects on the healing process. In this section we will try to give the basic knowledge for the understanding of future choices regarding material and structure of dressing, for a more depth study of the subject is recommended the reading of references quoted.

2.4.1. Wound healing process

The healing process represents a complex series of biological events to restore skin barrier function, prevent dehydration and reduce risk of bacterial infection[45]. The process consists of four systematically overlapping phases: haemostasis, inflammation, proliferation and remodelling. In the initial phase monocytes have a central role in wound healing; within hours after injury monocytes reach the wound site and differentiate into macrophages to phagocytosis of necrotic tissue and secretion of cytokines and growth factors[43][46]. They also play an important role in the proliferative phase realising soluble mediators that recruit and active fibroblasts. The fibroblasts migrate into the wound site and they are responsible for the synthesis, deposit and organization of the new tissue matrix[43].

Therefore, as explained above wound healing is a complex process involving the interaction of many cell types, matrix components and biological factors, but an important characteristic is that the wound environment has to be moist during all the time for a correct healing. The first to introduce the theory of moist wound healing was *Winter in the 1962*[47], he indicates benefits of moisture during healing of an acute wound, but excessive moisture can be deleterious, leading to skin maceration and wound complication. MFC hydrogels can be designed in order to tune the moist environment, but more experiments are necessary to understand the right moisture balance moisture in wound since not much is known about[43][46][48].

An important difference there is between acute and chronic wound in term of healing time and process[49]–[51]: acute wounds progress through the normal stages of wound healing and usually heal without complication in a healthy person; chronic wounds do not progress normally through the stages of healing, resulting in extended healing times or non-healing. The time for a chronic wound to heal may be between four weeks and 12 weeks, therefore, it is possible that acute wounds become chronic in patients with significant pathologies and/or risk factors. Some chronic wounds are; pressure ulcers, leg ulcers, diabetic foot ulcers and malignant wounds[49].

2.4.2. Acute and chronic exudate wounds

Wound exudate is the natural balsam to seal the wound from bacteria and debris, this with dried surface exudate is normal and welcome sign that healing is progressing, but despite the advances made in the wound care, knowledge about exudate remain rudimentary[50]. The production of exudate is an essential part of the moist wound healing process. However, amount produced and components of exudate in acute and chronic wounds differ.

In an acute wound, exudate is rich of endogenous proteases that contribute to the proliferation and growth of new cells, thus facilitating wound closure and healing[49]. A healthy wound will generate a small level of moisture that is visible on its surface, even if optimal level of exudate required to facilitate the healing is undetermined, and it varies with different types of wounds[50]

Regarding the composition, exudate has a high content of protein and essential nutrients for epithelial cells. A healthy wound contains endogenous protein-degrading enzymes, such as proteases or proteinases, which have the role to assist in preparation of the wound bed and to degrade components of the wound bed and to degrade components of the extracellular matrix, collagen and elastin, prior to wound closure and remodelling. Macrophages continue with wound cleansing by phagocytosing bacteria and debris and by producing elastase and collagenase, so contribute to the process of autolysis[50].

Exudate can be identified by difference in colour and viscosity, normally it has a pale amber colour, but in presence of bacteria may changes to green, brown or black depending from many factors as cited above. Typically, exudate can be describe as[46]:

- Serous: clear and water-like consistency, this exudate includes presence of bacteria;
- Fibrinous: cloudy, contains fibrin protein strands;
- Purulent: almost milky, containing infective bacteria and inflammatory cells;
- Haemo-purulent: as above but with the presence also of blood coming from dermal damage;
- Haemorrhagic: the main component are the red blood cells.

It has been proved that the wound fluid coming from the acute wound has beneficial impact on the wound healing process. Stimulating fibroblast and endothelial cell production, completely in contrast with the chronic wound fluid. Indeed, it has high content of destructive proteinases, slowing down or even blocking the proliferation of key cells in the wound healing process. Chronic wound exudate consists of extravascular fluid (water, salts, proteins carbohydrate, and fatty acids) plus varying quantities of cells, bacteria, cellular and bacteria debris, bacterial exotoxins and endotoxins, bacterial glycocalyx, short-chain volatile fatty acids (which contribute to wound odour and may be cytotoxic) growth factors and free radicals. The dressing will interact with the wound exudate fluid and change the properties of it, influencing the wound healing process[46].

The exudate is mostly produced during the inflammatory and proliferative stages of the healing process, the volume produced will vary not only at different stages of healing but also from different wound types, depending on their origin and location and size[50]. Exudate may be regarded as a transport mechanism. Exudate is derived from plasma, which delivers all necessary ingredients, to tissues and organs of the body. The analysis of wound exudate can

provide information on the status of the wound healing and this can help in the diagnosis of infection[50].

In case of chronic wound a prolonged inflammatory response is observed, this leads to increasing the wound fluid and exudate production. In literature is difficult to find a quantity of exudate produced from the wound, since production depends from many factors: size, location and origin of wound, patient's clinical history, management of wound care[46][49][52].

Indeed, approximately amount of exudate produced are classified as light, moderate and heavy, some more specific data are found but are approximately; volumes of 50g per 100cm^2 per day have been calculated for legs ulcers and burn wounds, corresponding to approximately 5 ml per 10cm^2 wound area[46][49].

For the wound exudate management is important to point out the following step that has to be follow during the wound healing treatment:

1. Optimizing the wound environment;
2. Controlling infective load;
3. Protecting the surrounding skin;
4. Maximizing the patient's quality of life by preventing exudate leakage, controlling odour and reducing wound pain[46].

The excessive fluid is not by itself the cause of delayed wound healing but the nature of it, it is of primary importance to understand the correct management of wound for a proper healing. The goal of effective wound dressing is to remove excess exudate, debris and 'chemicals' from wound bed while maintaining ideal moisture balance to allow cell migration and ultimately wound healing[45][46][50][51].

2.4.3. Dressing for wound care

It is important to remember that there is not a single dressing suitable for the management of all types of wounds, this is the first consideration to make the right choice of dressing usage[43].

On the market many types of dressing can be found, but a classification is possible to be made depending on exudate control by dressings, and can be divided in two categories:

1. Direct control:
    - Absorptive dressing
    - Dressing modifying the exudate: bacterial control, protease inhibitors, hyaluronic acid
    - Use of compression: static (bandage), dynamic (intermittent compression therapy)
    - Mechanical; drainage, topical negative pressure (VAC)
2. Indirect control:
    - Alleviation underlying cause: cardiac failure, dependent oedema, venous disease, lymphoedema

Capillarity action dressing is the type of our dressing idea, Figure 10 illustrates the dressing concept, these dressings conduct fluid away from the wound surface. They are usually multi-layered with the inner, non-adherent layer conducting fluid vertically. Subsequent layers hold and dissipate the fluid throughout outer component of the compound dressing. The efficacy of this dressing type have been shown in wounds with moderate to high exudate volumes of low to moderate viscosity.

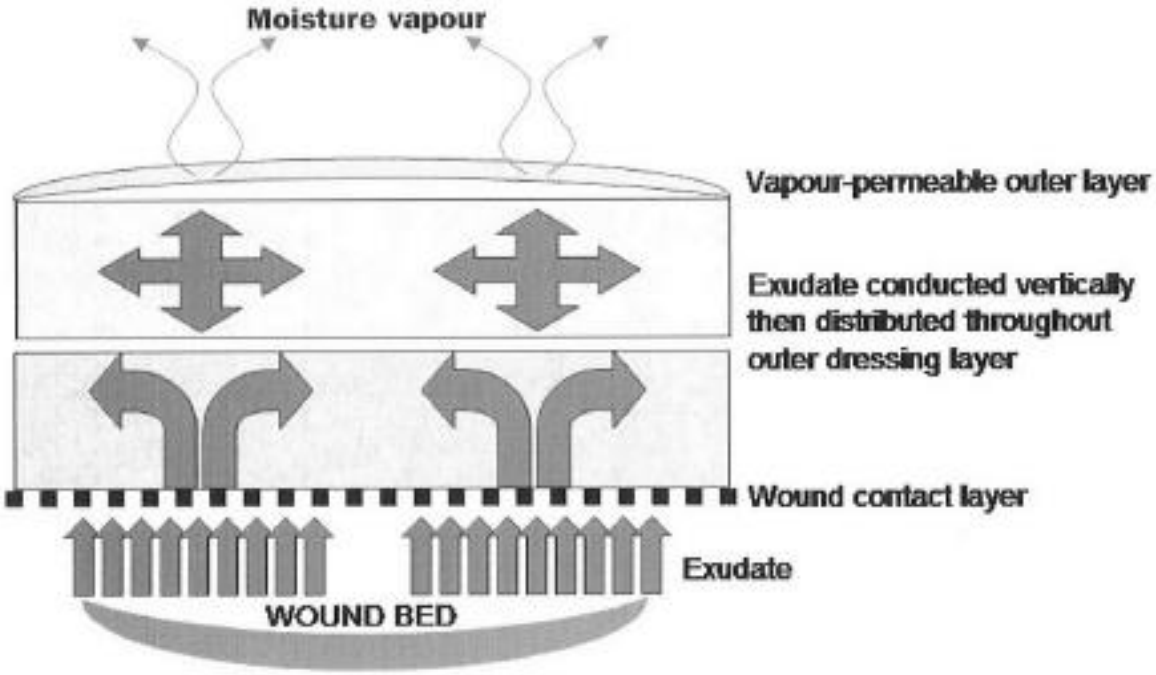

Figure 10. Sketch of capillarity action dressing [46]

Other types of dressing are absorptive dressing, transmission dressing, gel formation dressing(i.e. Aquacel®), bacterial control dressing, topological negative pressure (VAC), that can be used in different occasion depending form the volume and the viscosity of the exudate[46].

The development of ideal wound dressing material is focused on the requirements of elasticity, moisture and pH maintenance in the wound environment. Carboxymethylcellulose Hydrofiber® dressing (as Aquacel®) with integrated ionic silver has been widely studied as a promising wound dressing materials in treatment of burns and ulcers, however using this type of dressing require generally frequent changes of dressing, increasing patient's pain. It is important to notice that repeated, painful dressing change in burn wound areas and skin graft donor sites often need general anaesthesia in initial stages[45].

Introduction of alginate and hydrocolloid dressing in the 1990s with the Hydrofiber® technology lead to significant changes in practice. The material called Hydrofiber® is a pad or ribbon dressing composed of sodium carboxymethylcellulose, which is incorporated in form of a fleece held together by a needle-bonding process, this material can absorb a large amount of wound exudate, transforming itself in a gel. Hydrofiber® are neither hydrocolloids nor alginates, but separate category incorporating the benefits of both, with the defect of a strong adhesion, the first Hydrofiber® dressing to be launched was Aquacel® (ConvaTec) 1997. Further Aquacel®, there is also Aquacel Ag ® which is a silver-impregnated with antimicrobial effect. Versiva XC® is another dressing constituted by a combination of Hydrofiber® and polyurethane film laminate that help to avoid the lateral leakage[52]. This type of dressing help the wound healing protecting wound edges from potential maceration and providing at the wound bed passive infection control[52].

In the last decades, hydrogels have been described as optimal candidates to be used in wound dressings since they fulfil most of the desirable characteristics of an ideal dressing; maintain an appropriate level of moisture in the wound, to relieve pain, to not adhere to wound and to conform body shape[43]. MFC could have application in dressing for chronic wound, the design of a tailor-made wound dressing with barrier, absorbent and bio responsive characteristic may benefit from assembly of complex porous structures in an effective way.

Furthermore, printing and coating are low cost processes and can facilitate the deposition of specific nanocellulose materials[53] to allow the production of wound dressing customizable, bio-based and low cost. Some works regarding MFC dressing has been carried out in patients with burns (acute wounds) and compared with the commercialized dressing Suprathel® (PMI, polymedics, Germany)[45]. However clinical studies concerning the use of MFC in wound healing applications with patients are lacking[45].

2.5. 3D-bioprinting process

3D printing technology is the most interesting manufacturing technology nowadays and for the future perspective, thanks to its high customizable products possibilities. For this characteristic, lately 3D printing is used increasingly in the medical field to produce biomedical device and live tissues[54]. A 3D printer is able to produce personalized product with a bottom-up fabrication by a layer-by-layer method. The 3D bioprinting is intend to be the method of printing with biobased material, as nanocellulose hydrogels, with or without living cell. The 3D bioprinter open the opportunity to print with material that cannot be melted, as in the FDM (fused deposition modelling)[54][55]. The review of *Carrasco et al. (2015)*[54] show the wide applications possibility of using cellulose fibers and nanocellulose material in combination with 3D printing methods.

For biomedical use, nanocellulose with complementary polymers are good candidates for biocomposite applications, among which wound dressing and drug delivery. However, any type of nanocellulose requires a thorough assessment of biocompatibility before the utilization for medical devices[56]. These materials should contain low amount of endotoxin contaminant, such as bacterially derived lipopolysaccharides (LPS). The materials with a content <50 EU/g are considered to be ultrapure and adequate for biomedical use[54].

A further improvement would be use MFC functionalized with cells, growth factors, antimicrobials and use this material as bioink for tailor-made wound dressings. Even printed electronics and biosensors could be integrated into the wound dressing construct, for a intelligent and personalized wound management[54].

Inks composed of nanocellulose and alginate show good shape reproduction the alginate as already mentioned is essential for the integrity of the structure after the printing process and crosslinking[54].

The most used 3D bioprintign process are:

5. Laser-assisted bioprinting
6. Inkjet bioprinting
7. Extrusion bioprinting
8. Bio-electrospray and cell electrospining bioprinting

These processes differ by technology but also by ranges of bioinks that can be used, below there will be a brief description of the different methods. The application of 3D bioprinting is wide and not only limited to replacement of diseased tissue.

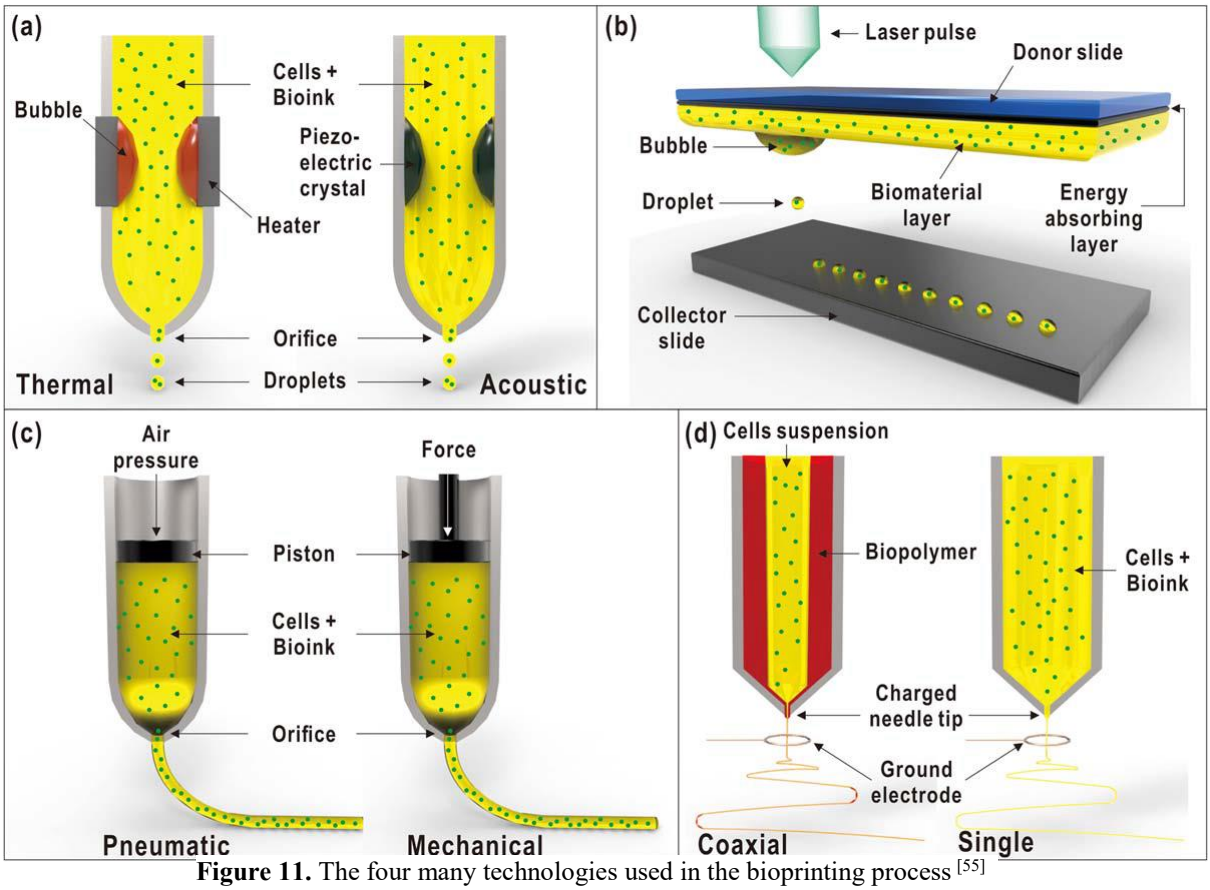

Figure 11. The four many technologies used in the bioprinting process [55]

2.5.1. Inkjet bioprinting

Inkjet biopreinters, Figure 11a, produce a continuous filament or droplets of bioink to build up 3D objects. The inks are forced to flow thanks to thermal or acoustic devices through a nozzle out of the cartridges. The printing bed and movement of the cartridges are controlled mechanically in x,y and z directions in micrometers. Some bioprinters are based on the common inkjet printers but modified to obtain 3D structures. These printers have a wide amount of bioinks available. Thermal inkjet bioprinter use an electrical heating system in their print heads, the heat creates bubbles and eject the bioink out of the nozzle. Another solution is the acoustic inkjet bioprinter which use piezoelectric material to create bubbles in the print heads and eject the ink. Droplets size and ejection directionality can be controlled, the advantage of using acoustic bioprnter is that, in case of printing with living cells, they are not damage from high temperature stresses. These printers have many advantages such as easy access to bioprinting platform, high processing speed, and low cost, but the greatest advantage is that the the target surface does not to be flat, this is very important for in situ bioprinting. However, the major drawbacks is that the bioink has to be in the liquid state and with appropriate viscosity[55].

2.5.2. Laser-assisted bioprinting

Laser-assisted bioprinting (LAB), Figure 11b, is build on the principle of laser-induced forward transfer (LIFT), where a high-energy laser pulse creates high-pressure bubbles in the bioink layer and these bubbles eject it onto determined places. The essential parts of a LIFT are: a pulsed laser beam, a focusing system, a ribbon, an energy-absorbing layer and a bioink layer. The ribbon, which is transparent, works as support for the thin energy absorbing layer (material), while the bioink needs to be in liquid or gel condition to be spreaded over the metal layer. All these different parts have impact on the final resolution of the printed structures, but generally LAB have high resolution, few micrometers. Advantages of using this technology are that high cell density structures can be printed and the bioink, hydrogel, could be printed with any desired viscosity. However, it is important to remember that the use of lasers, especially UV-light, can have negative effect on cells. The high resolution of this technology is an advantage but this imply also low printing speed, which can be inadequate in cases where the hydrogel is subject to fast dehydration[22][55].

2.5.3. Extrusion bioprinting

Extrusion bioprinting, Figure 11c, is the technology used in this work. These bioprinters eject a continuos stream of bioink onto the pprinting bed thanks to pneumatic or mechanical extrusion system, this are the easiest solution used for non-biological purposes, they have the widest range of biomaterials, biocompatible opolymers, and cell spheroids usable. The pneumatic system is the simplest from a contruction point of view, it uses compressed air to force bioink out of a nozzle, while the mechanical system uses compressive forces provided by a screw or a piston. This last technology allows to have more spatial control on the bioink which is ejected, but the structure is more complex than the pneumatic solution. The extrusion bioprinting is the most convenient rapid prototyping method for making structures. The critical issue in extrusion bioprinters is the loss of cell viability due to shear stress applied to the bioink at a small orifice. The final object resolution is affected by many factors of the printer and of the bioink rheology properties[55].

During the printing process some parameter can be changed in order to obtain high resolution or high productivity. For the extrusion printing, the one used in this work, the parameters that can be changed are:

- Nozzle dimension
- Nozzle type: conical, straight
- Pressure
- Printing speed

Changing these parameters, it can be change the final resolution.

The printer used in this work are provided by CELLINK, the BioX. The BioX has three pneumatic printheads and can be loaded with different material. The printer is show in Figure 12.

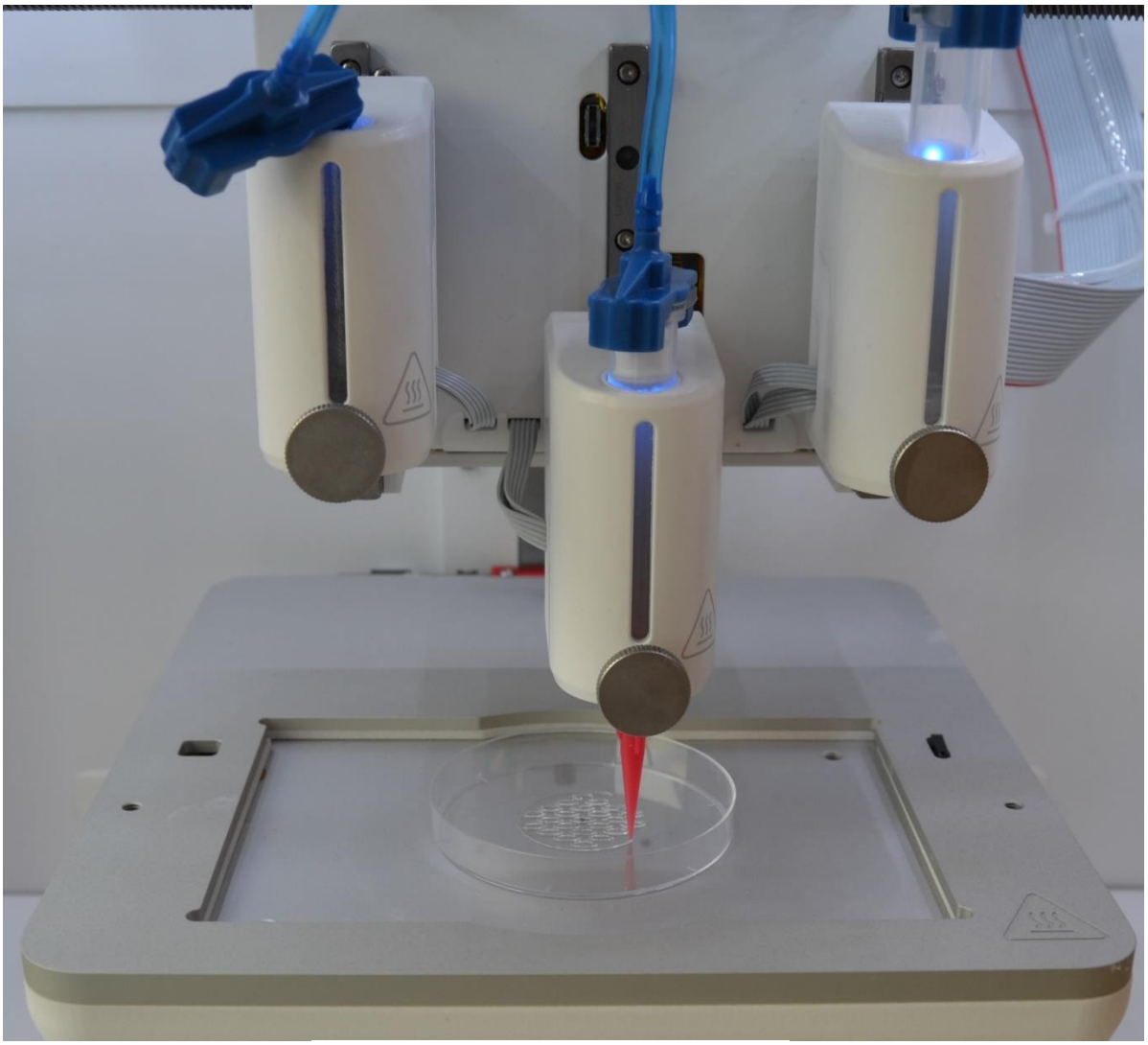

Figure 12. BioX printer with three print head.

2.5.4. Bio-electrospray and cell electrospinning bioprinting

Bio-electrospray and cell electrospinning bioprinting, Figure 11d, utilize eletrric field between two charged electrodes to eject droplets or continuous filament of bioink. Traditionnaly, it has been used for scaffold in tissue engineering without living cells, but lately a modification to the system which use low electric current support the idea that the technology can be used for in situ bioprinting. It has very high resolution, it can create nano-sized droplets or fibers[55].

Chapter 3

3. Materials

3.1. Microfibrillated cellulose and alginate

The MFCs used in this work were provided by StoraEnso. It has been analysed two different types, that differ by production methods and concentration of dry mass, as listed in Table 3.

The first one is an enzymatic nanocellulose, named in this work MFC1, it has a non-transparent aspect and with a white colour, Figure 13a. Regarding the mechanical properties, it has the impossibility to be cross-linked without the addition of other components, i.e. alginate.

The second type is produced with a carboxymethyl method as described above, named MFC8, Figure 13b, thus onto the cellulose surface we can find carboxymethyl groups with the possibility of formation of a sparse 3D non-permanent network between the fibrils with low strength. The MFC8 has a transparent aspect.

Alginate is a crosslinkable polymer, as described above, and it was added to both MFC1 and MFC8 to improve mechanical properties, when a solution with bivalent cation, as Ca^{2+}, is added to the composition.

Table 3. Description of the material utilized

Name	Type of MFC	$X_{MFC} \cdot 100$
MFC1	Enzymatic	3.0
MFC8	Carboxymethylated	2.6

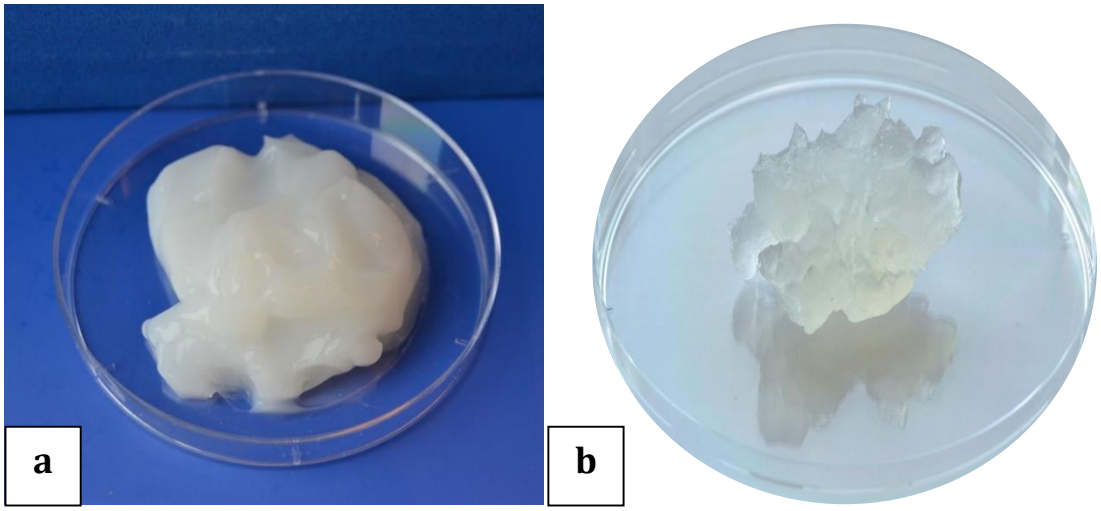

Figure 13. a) MFC1 raw conditions, b) MFC8 raw conditions.

To MFC was added alginate purchased from NOVA MATRIX, the concentration of the G-blocks in the alginate (MVG) is higher than 60%. To prepare the inks the alginate is added as powder to MFC in gel state and mixed several time, to ensure a complete and homogenous

dissolution of the alginate. The composition was initially mixed manually and secondly with two syringes connected. Furthermore, some tests to compare the properties of inks with alginate in powder or in solution were carried on. In this work the mainly composition used was with 80% of dry content correspond to the MFC and 20% correspond to the alginate, but also other compositions, listed below in Table 4, were prepared to evaluate the mechanical properties.

The alginate has been added as powder and the amount was calculated with the following formula (3.1):

$$g_{alginate} = \frac{g_{hydrogel} \cdot X_{MFC}}{X_{MFC\_ink}} - g_{hydrogel} \quad (3.1)$$

Where $g_{hydrogel}$ are the grams of the considered MFC gel, X_{MFC} and X_{MFC_ink} are the fraction of dry mass of cellulose in the hydrogel and the fraction of the dry content corresponding to the cellulose in the ink respectively. The alginate is added as powder to avoid the viscosity decrease, otherwise the ink prepared with alginate solution would not be printable. Below the Table 4 explain all the composition used in the present work:

Table 4. List of material and composition used in this work

		Dry weight in 10 g of hydrogel		Dry content	
Name	**Type of cellulose**	**MFC (g)**	**MVG (g)**	**X_{MFC_ink} (%)**	**X_{MVG_ink} (%)**
MFC1_0	MFC1	0.3	0	1	0
MFC1_8020			0.075	0.8	0.2
MFC1_6040			0.2	0.6	0.4
MFC1_4060			0.45	0.4	0.6
MFC1_2080			1.2	0.2	0.8
MFC8_0	MFC8	0.26	0	1	0
MFC8_8020			0.065	0.8	0.2
MFC8_6040			0.173	0.6	0.4
MFC8_4060			0.39	0.4	0.6
MFC8_2080			1.04	0.2	0.8

The preparation of the inks was carried on with the following steps:

1. Calculation and weight of the alginate
2. Addition the MFC to the alginate
3. Mechanical mixing of the components with a spatula or with a speed mixer (speed mixer help to have a more homogeneous alginate distribution)
4. Mixing of the ink with two syringes connected 20 times.

At the end of the process the inks were let sit for 24h to ensure the complete alginate dissolution ad then squeezed out of the syringes through a conical nozzle used in the 3D printing process with a final diameter of 0.25mm to be ensure complete alginate dissolution in the ink.

3.2. Other materials

Other materials used in the work are:

- Calcium chloride: used as croslinker and prepared from the powder purchased from SigmaAldrich. It has been prepared a solution of 0.5M
- SWF: synthetic wound fluid, it is a solution with protein and used in the absorption and stability test;
- Magnesium nitrate: prepared a super saturated solution from Magnesium nitrate powder purchased from Sigma Adrich used in the water retention and shrinking tests
- Solution of Sodium Chloride 9mg/l

Chapter 4

4. Methods

The methods used in the present work have been divided into methods that characterize material properties and the ones used for characterization of prototype structure.

4.1. Material characterization

The materials used in this section are mainly the ones described above in the material section.

4.1.1. Water retention test

Aim

The main aim of this test is to evaluate qualitatively the material's water retention to establish hydrogels properties when it comes to maintain a moist environment.

To ensure this it is necessary an environment with a constant relative humidity and constant temperature, this will allow to compare samples results between each other. Hydrogels have a high amount of water (around 97%w/v) and ability to hold water bond into the fibrils network is given mainly by hydrogen bonds that are formed between water molecules and charge groups onto cellulose chain. This means that more charge groups onto cellulose surface allow to have more hydrogen bonds and consequently higher water retention. The water holding capability depends also from the strength of this bonds and not only from the numbers of them, therefore highly charged with high number of substituent onto the cellulose surface will give higher water retention.

Procedure

The test is carried on MFC1 and MFC8 with 20% of dry alginate content and some samples are crosslinked with calcium chloride 0.5 M. MFC1 and MFC8 without alginate are used as blank to evaluate the effects of the crosslinking action on the water retention properties of the material. In the case of the MFC8 it was tested also crosslinked without the addition of alginate, since the carboxymethyl groups on the chains allow formation of a weak network between fibrils.

The samples are disks of 20mm in diameter and 2 mm height printed with the 3D printer Inkredible® provided by CELLINK. The printed samples with alginate were crosslinked with 0.5 calcium chloride for 30 min before to start. Then the samples were disposed in a petridish of 60 mm in diameter and then disposed into a 100 mm petridish with a super saturated solution of magnesium nitrate used to keep relative humidity around 50-60% at 37°C[57], as shown in Figure 14. Afterthat all samples were closed to ensure a constant relative humidity and placed in an oven with a constant temperature of 37°C. The data were collected measuring weight with a balance Precisa 2200TX every hour for the first six hours and then after 24 hours.

Aquacel® samples were subjected to same test to compare the ability of the hydrogel to keep a moist environment with a dressing already on the market and utilized from the surgeon. Aquacel® samples were prepared adding water to the dry dressing until a saturated condition was achieved. Table 5 reports the samples with the crosslinked conditions and the number of samples evaluated.

Table 5. Material and number of samples used in the Water Retention Test.

Name	Type Cellulose	% MVG	Crosslinker	N° of samples
Acuacel®	Hydrofiber®	-	-	3
MFC1_0	MFC1	-	-	1
MFC1_8020	MFC1	20	$CaCl_2$ (0.5M)	6
MFC8_0	MFC8	-	-	1
MFC8_1	MFC8	-	$CaCl_2$ (0.5M)	3
MFC8_8020	MFC8	20	$CaCl_2$ (0.5M)	6

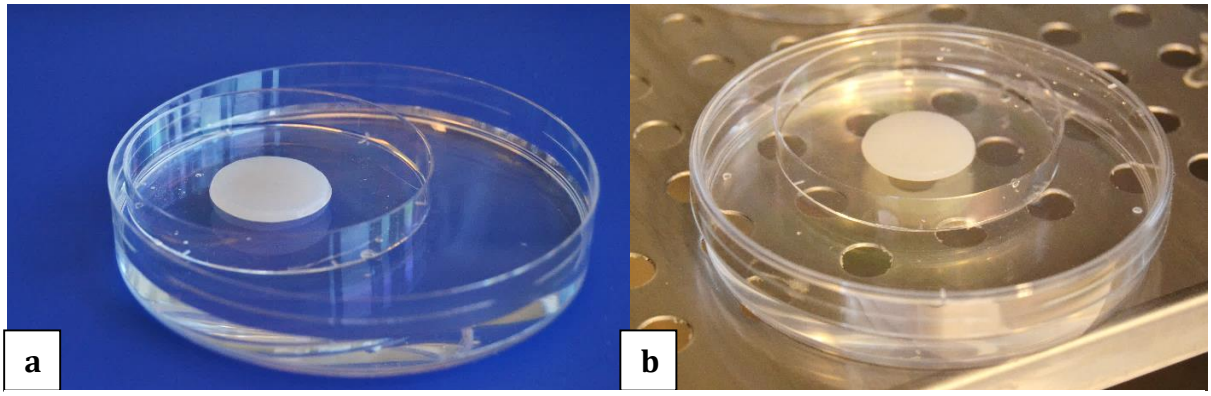

Figure 14. Sample preparation for Water Retention Test: a) configuration of the sample let floating on the Magnesium Nitrate solution; b) sample in the oven

4.1.2. Shrinking test

Aim

The aim of the shrinking test is to evaluate the capacity of hydrogels to keep shape under certain conditions of relative humidity and temperature. To ensure a constant environment relative humidity and temperature were set like during water retention test and samples are prepared in the same way, indeed the two tests can be carried out in the same time with same samples.

Procedure

Preparation and number of samples are equal to the ones in water retention test, while collection of datas was made taking pictures to samples with a Nikon D3100 camera, Figure 15, every hour for the first six hours and then after 24 hours. Images were analysed with the software ImageJ® from National Institute of Health (USA) and the disk area was compared to the initial area to evaluate the shrinkage of the material.

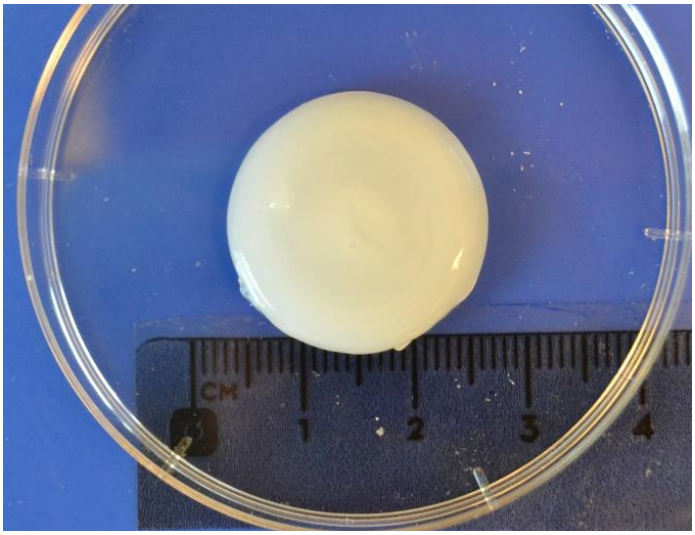

Figure 15. Shrinking test sample

4.1.3. Compression test

Aim

The aim of the compression test is to evaluate the hydrogel mechanical properties under compressive stresses. The test was conducted with Instron equipment at Chalmers University of Technology and using BlueHill® software. The datas collected were analysed and the compressive modulus at small deformation (0-5%) was calculated as the curve stress-strain slope. In order to have precise data, with ImageJ® was calculated the contact area of each sample with the press and then right stress was calculated dividing the load per the sample area.

Procedure

The samples preparation is done printing cylinder with a diameter of 9 mm and height of 4 mm using BioX® 3D bioprinter provided by Cellink. The number of samples and composition are reported in the Table 6. The samples need to be crosslinked to be handle and thus possible to conduct the compression test, for this reason in this test MFC1 and MFC8 without crosslinked network cannot be tested. However, MFC8 without alginate crosslinked and MFC1 and MFC8 with different concentration of alginate, from 20% to 80%, were used. Also a solution of 3%w/v MVG alginate was prepared.

The crosslinking process was conducted with $CaCl_2$ 0.5 M for 1 hour and then the samples were putted in DI over night to ensure the structure stability.

Table 6. Material and number of samples used in the compression test

Name	**Type**	**% MVG**	**Crosslinker**	**N° of samples**
MVG 3%	Alginate	3%w/v	$CaCl_2$ (0.5M)	9
MFC1_8020	MFC1	20	$CaCl_2$ (0.5M)	6
MFC1_6040	MFC1	40	$CaCl_2$ (0.5M)	6
MFC1_4060	MFC1	60	$CaCl_2$ (0.5M)	6
MFC1_2080	MFC1	80	$CaCl_2$ (0.5M)	6
MFC8_1	MFC8	0	$CaCl_2$ (0.5M)	6
MFC8_8020	MFC8	20	$CaCl_2$ (0.5M)	6
MFC8_6040	MFC8	40	$CaCl_2$ (0.5M)	6
MFC8_4060	MFC8	60	$CaCl_2$ (0.5M)	6
MFC8_2080	MFC8	80	$CaCl_2$ (0.5M)	6

Thanks to BlueHill® software it was possible to set the method; it was used a compression rate of 1%/s with a stop at 80% strain or at the load cell limit. In this test was used a 10N load cell since the load on the material was small. In Figure 16 is possible to see the configuration used to test the materials compressive properties.

Figure 16.Configuration of the compression test. The sample is load between the press

4.1.4. Rheological test

All rheological tests were conducted using a rheometer from TAinstrument, Figure 17, more specifically the DiscoveryHR2 model. The configuration, in all of the test, was a plate to plate with serrated or flat geometry depending from the test that was execute.

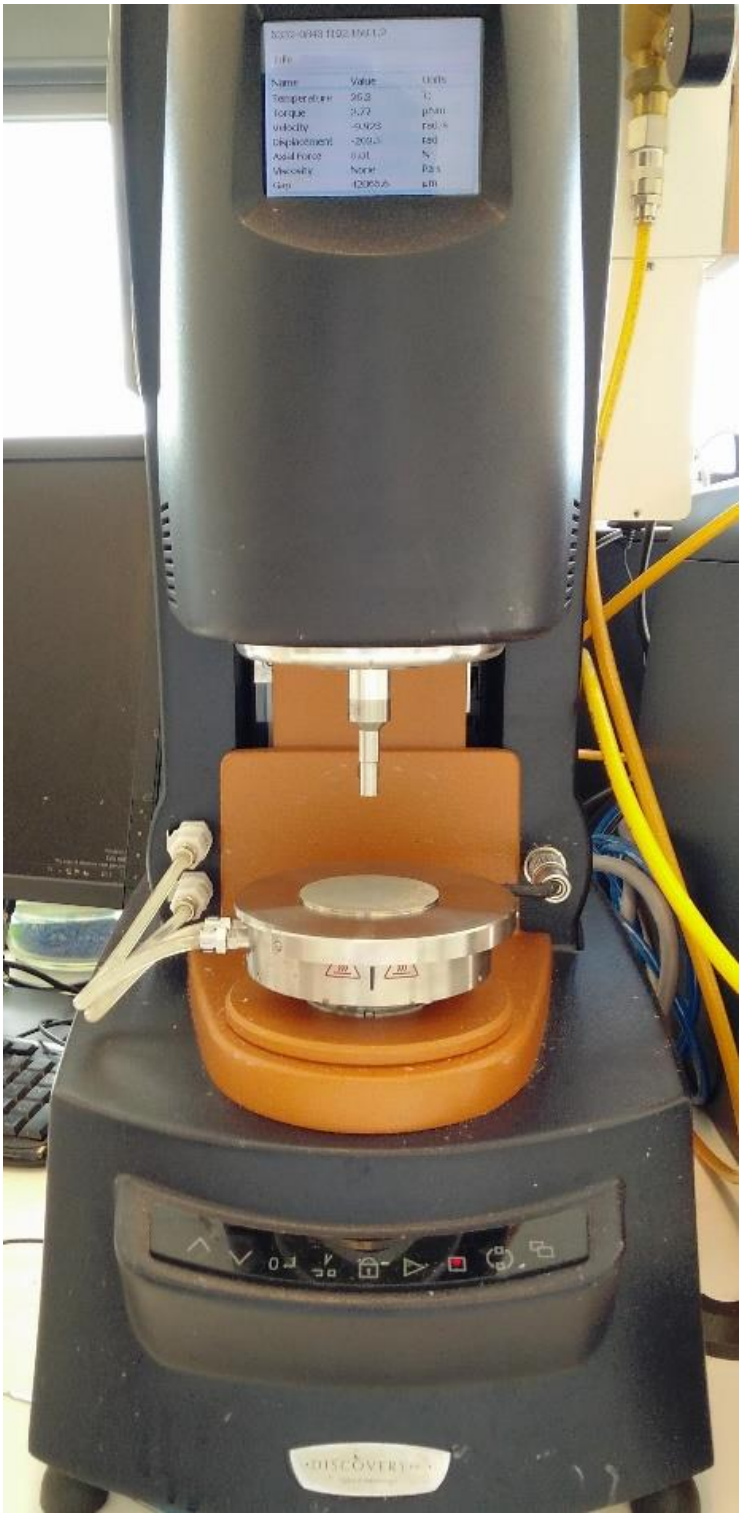

Figure 17. Rheometer used in this work

Viscosity inks test

Aim

To evaluate the inks viscosity a viscosity sweep test was conducted on the material. The hydrogel, not crosslinked, has shear thinning properties, this means that increasing shear rate, viscosity decrease. This is essential in a 3D bio printable inks, since it is necessary that the ink flows under controlled pressure, but it has to maintain the shape when there are not forces applied on it.

Figure 18. Geometry used in the viscosity test. It is a plate to plate geometry flat.

The material rheology need to be studied when dry alginate is added to the composition. Viscosity depends mainly from the chain length and from the entanglements formed into the structure. When a shear force is applied the material start to lose the entanglements structure and thus it starts to flow. In Figure 18 is possible to see the geometry used in the experiment.

Procedure

In this test the geometry used was plate to plate with a flat surface, with 20 mm diameter contact with the material. The material was placed on the bottom plate in order to have enough material that fill the gap between the bottom plate and the geometry.

The parameters were set to have a temperature constant of 25°C and a shear rate that vary from 1.0×10^{-3} to 1500 1/s. The gap between the geometry and the plate was set at 500µm. The materials tested is listed in Table 7 below:

Table 7. Materials used in the viscosity test

Name	**Type**	**% MVG**
MVG 3%	Alginate	3%w/v
MFC1_0	MFC1	0
MFC1_8020	MFC1	20
MFC1_6040	MFC1	40
MFC1_4060	MFC1	60
MFC1_2080	MFC1	80
MFC8_0	MFC8	0
MFC8_8020	MFC8	20
MFC8_6040	MFC8	40
MFC8_4060	MFC8	60
MFC8_2080	MFC8	80

Crosslinking kinetics

Aim

In this test it has been evaluate the crosslinking kinetics of different hydrogel composition measuring the storage modulus during time when the cross linker (calcium chloride) was added. Since the crosslinking of the ink take place as soon calcium ions are in contact with the alginate, there is formation of a cross-linked skin on the hydrogel surface and then the material core is cross-linked with a mechanism of diffusion through the hydrogel network. Therefore, the process take time to be complete, with this test it is evaluated the time necessary for a complete crosslinked structure. In Figure 19a) and 19b) it is showed the geometry used.

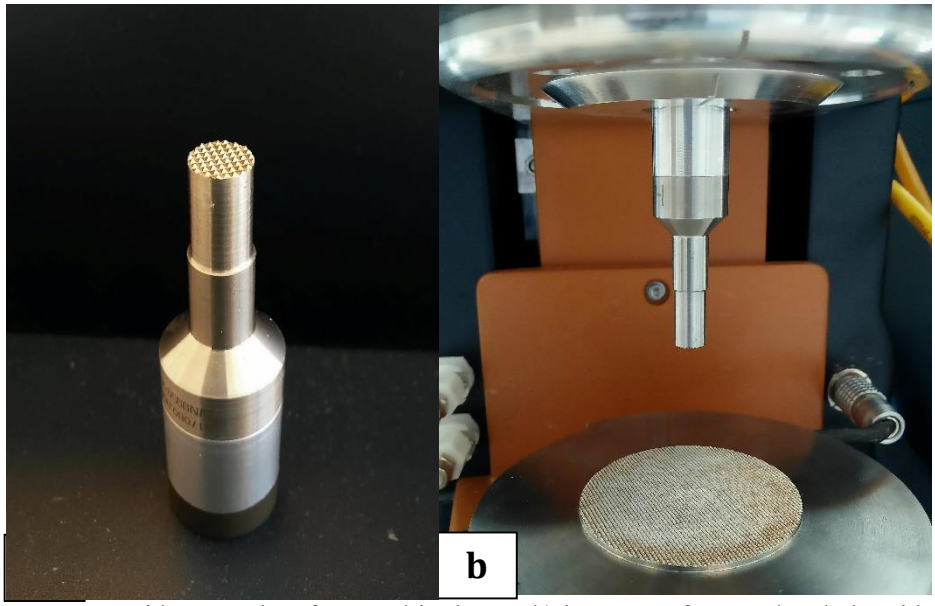

Figure 19. a) Geometry with serrated surface used in the test,b) bottom surface used and alsowith the serrated surface

Procedure

The geometry used in this test was an 8 mm plate to plate with a serrated surface either geometry and either bottom plate. The temperature was set at 25° C for all the tests, and the tests lasted from 10min to 40min, until the material reached linear trend. Oscillation stress was set at 2 Pa and oscillation frequency at 1 Hz for all the test time. After 1 min from the experiment start, calcium chloride (0,5 M) was added to the specimen and the storage modulus value was measured every 3 seconds. The materials tested are listed below in the Table 8.

Table 8. Material used in the Crosslinking kinetics test

Name	**Type**	**% MVG**	**Crosslinker**
MVG 3%	Alginate	3%w/v	$CaCl_2$ (0.5M)
MFC1_8020	MFC1	20	$CaCl_2$ (0.5M)
MFC1_6040	MFC1	40	$CaCl_2$ (0.5M)
MFC1_4060	MFC1	60	$CaCl_2$ (0.5M)
MFC1_2080	MFC1	80	$CaCl_2$ (0.5M)
MFC8_8020	MFC8	20	$CaCl_2$ (0.5M)
MFC8_6040	MFC8	40	$CaCl_2$ (0.5M)
MFC8_4060	MFC8	60	$CaCl_2$ (0.5M)
MFC8_2080	MFC8	80	$CaCl_2$ (0.5M)

Shear resistance

Aim

The aim of the test is to evaluate the hydrogels crosslinked resistance under shear forces. The storage and the loss modulus were measured during a rheological test where oscillation stress is the only parameter increasing while frequency and temperature are kept constant (1Hz and 25°C respectively). This test can give information about the shear forces that the material can withstand before the network created by crosslinking breaks. The geometry used is a 8 mm plate to plate with a serrated surface on the geometry and on the bottom plate, Figure 19.

Procedure

The hydrogels tested are the same that have been tested in the crosslinking kinetics test, Table 8. To prepare the test, the material was placed on the bottom plate and the geometry was lowered to the trim gap (1050µm), at this point, calcium chloride was added (0,5 M) and let sit for 10 minutes.

The measurement starts after the crosslinking time, oscillation stress increased from 0 to 10'000 Pa with a constant temperature of 25°C and constant frequency of 1Hz. The measurement of storage modulus and loss modulus were taken every ten points per decade. The breaking point is identified as the intersection between storage modulus and loss modulus.

4.1.5. Cytotoxicity test

Aim

The aim of the test is to ensure the skin friendly behaviour of the material. The cytotoxicity test was carried out by Medibiome and results are reported in this work to show the material behaviour in presence of human cells.

Procedure

Cytotoxicity protocol is described by ISO 10993-5 Biological evaluation of medical devices— Part 5: Tests for in vitro cytotoxicity. This standard is describing that the choice how to evaluate cytotoxicity depends upon "the nature of the sample to be evaluated, the potential site of use and the nature of the use".

The test specimens are prototypes made of nanocellulose materials presented as hydrogels and will be applied in close contact with human tissue. Based on the physical characteristics of the prototypes, 11 mm in diameter, 2 mm thick with holes and presented in HBSS solution, agar diffusion assay was considered to be most relevant method to assess both the device and its solution.

The choice of human cells owes to that human cells will reflect the clinical reality (humans) closer than mouse cells that are otherwise most commonly used. The cell line tested is MRC-5 cells, human lung fibroblasts that are listed in ISO 10993-5 as an optional cell line to study. Below is reported the preparation method used from Medibiome:

Preparation of test specimens and controls:

• The negative and positive controls were punched aseptically with a punch at 11.3 mm in diameter.

• The prototypes were used as delivered. Also, their solvents, HBSS (Hanks Balanced Salt Solution) were tested to confirm that no cytotoxic compound had dissolved into the solvent. Despite the hypothesis that any substances in the solvent are in equilibrium in the hydrogel as well as outside the hydrogel since the hydrogels contain 98% water in HBSS.

Preparation of media

The cells were propagated according to the instructions from the American Type Culture Collection1.

ATCC complete growth medium: 10% FBS and 1% PEST in EMEM

Procedures – Indirect contact test, Agar Diffusion assay, n=3

1. 3 ml of a 1×10$_5$/ml cell suspension was seeded into culture tissue plates and incubated for 20 hours at 37°C, 5% CO2.

2. 2% agarose was prepared in EMEM and mixed to give a final concentration of 1xEMEM, 10% FBS, 1% PEST, and 1% agarose.

3. The complete media was then removed from cells and instead 3 ml agarose suspension was added and allowed to solidify at RT in a LAF hood (~ 15 min).

4. Once solidified the test specimens and their respective HBSS solution 1 ml and controls were applied and the assemblies incubated for 24 hours at 37°C, 5% CO$_2$.

5. After incubation the test specimens and controls were removed and 3 ml 0.01% neutral red stain was flooded and incubated for 1 hour at 37°C, 5% CO$_2$. Thereafter the stain was removed and the cell cultures were evaluated microscopically in a phase contrast microscope at 10x magnification.

Determination of cytotoxicity – indirect contact test
According to ISO 10993 guidelines:
The positive control should score 3 or 4.
The negative control should score less or equal to 1 and the negative control should have at least 70% viability as indicated by neutral red. If less than 70% or more than 10% degeneration indicate a problem inherent to the cells or culturing technique.

4.1.6. Stability in SWF and NaCl

Aim

In this test some samples were tested to understand if synthetic wound fluid (SWF) or a solution of sodium chloride could degrade the material structure.

Procedure

The samples were prepared printing cylinder with 11 mm diameter and 3 mm height with 4 elliptical channels designed in the STL file. The compositions utilized in this test were MFC1 and MFC8 both with a concentration of 20% of alginate and crosslinked after printing with calcium chloride 0.5 M for 1 hour. After the preparation, the samples were immersed in SWF and in NaCl for 24 hours and placed on a shaking table in oven with constant temperature at 37°C.

Each test consists into visual analysis of six samples for each material (MFC1_8020 and MFC8_8020) to evaluate the samples degradation.

4.2. Structure characterization

Once the material is characterized, the next challenge is to demonstrate the structure functionality, therefore it could absorb liquid from wound bed, it doesn't dry out when it is in contact with the absorbent module. To evaluate this, two main tests were conducted to examine the behaviour of two different materials. Furthermore, the freedom deign was evaluated in order to determine the best prototype solution.

4.2.1. Interaction between modules

Aim

The test purpose is to establish the possibility of combine two module without any interlayer in between to separate, which will change transport properties. For this reason, it is important to investigate the changing in moisture level during time when the two module are in contact. If the moisturizer module will dry out completely in short time it will not provide the right amount of moist in wound bed environment for a correct healing for all the time necessary.

Procedure

The test consists in joining the two modules with a low load to make sure that there is completely contact between the two surface. The samples were prepared in two different ways: (i) the moisturizer module was printed with BioX with a cylindrical shape with 25mm of diameter and 3mm of height, two different materials were tested, MFC1_8020 and MFC8_8020, and then crosslinked with $CaCl_2$ (0.5 M) for 1 hour; (ii) the absorbent module was printed with BioX and only MFC8_8020 was used, crosslinked with $CaCl_2$ (0.03 M) for 1 hour and then freeze, and freeze-dried. Then it is important to ensure an entire contact between the two modules, to do that the two modules were overlapped in a petridish of 60mm and then a cover was added on the top of the absorbent module and the petridish was close with the upper part and sealed with the parafilm, as show in Figure 20, to limit the dry out by evaporation. The samples were weighted separately and together each two hours for the first eight hours and then after 24, 31, 48, 54, 72, 78 and 197 hours, to evaluate the long term effect. In the table below there are listed the material and the number of samples tested.

Table 9. Material and number of samples used in the interaction test

Module	**Name**	**Type cellulose**	**% MVG**	**Crosslinker**	**N° samples**
Moisturizer	***MFC1_8020***	MFC1	20	$CaCl_2$ (0.5 M)	5
	MFC8_8020	MFC8	20	$CaCl_2$ (0.5 M)	5
Absorbent	***MFC8_8020***	MFC8	20	$CaCl_2$ (0.03 M)	10

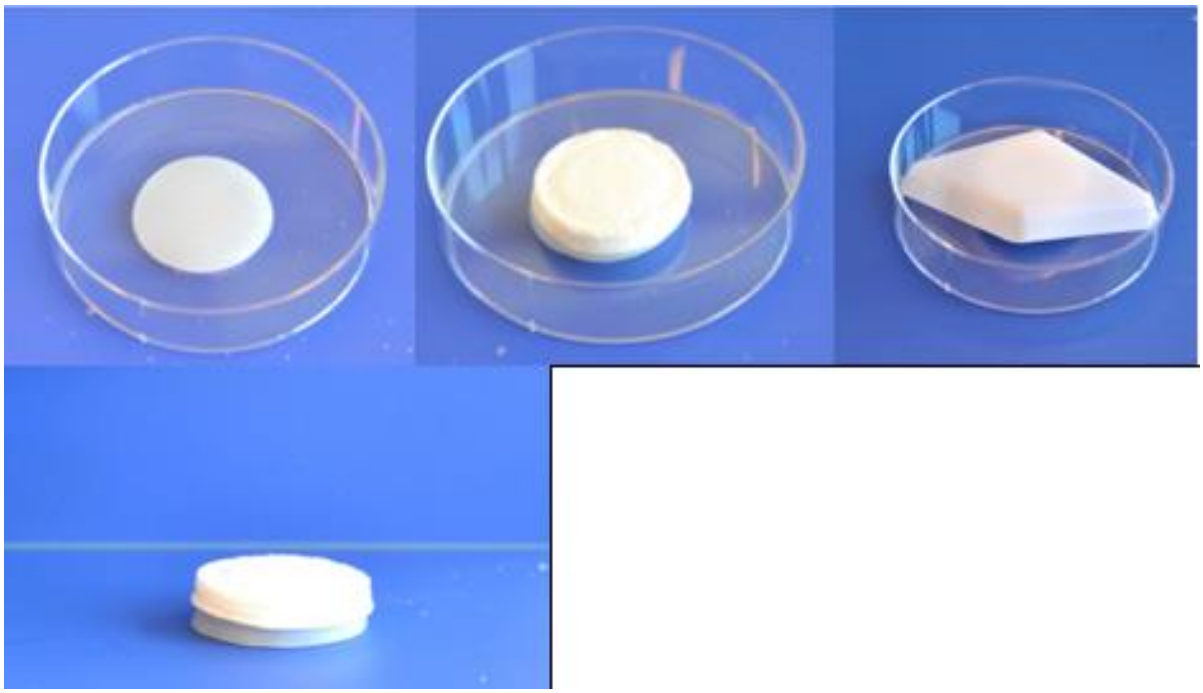

Figure 20. Configuration of the samples used in the Interaction test

4.2.2. Printability

Aim

The main aim of this test is to investigate the inks developed possibility and discovered limits during printing process. As described above the inks material has shear thinning properties thus viscosity has to be low enough to flow when a pressure is applied, but high enough to stand when forces aren't applied. Further, they normally are also thixotropic materials, this means that viscosity changes also with time and restore to high viscosity is not immediate. Different structure and different materials were tested in this experiment to set up the right parameters to obtain the best resolution and to discover the limits. The resolution of the 3D printing depends from many factors; material's properties, pressure, printing speed and mostly important from the dimensions of the nozzle used. In all the printings in this work was used the 0.25mm diameter conical nozzle.

Procedure

There are two different tests;

1. Printing of same structures but with different height to evaluate height limit and to discover the printing parameter; in this test, structure printed was a disk with 25mm of diameter and 1 to 4mm height and 23 elliptical channels.
2. Printing with changing the structure infill to see the smallest channels that can be obtained from the printing process. The disks dimension in this experiment were 11 mm in diameter and 2mm height, the infill was imposed as honeycomb pattern with a percentage vary from 10% until was possible to notice the channels.

The materials used in both cases were MFC1_8020 and MFC8_8020. Figure 21 show the printing process.

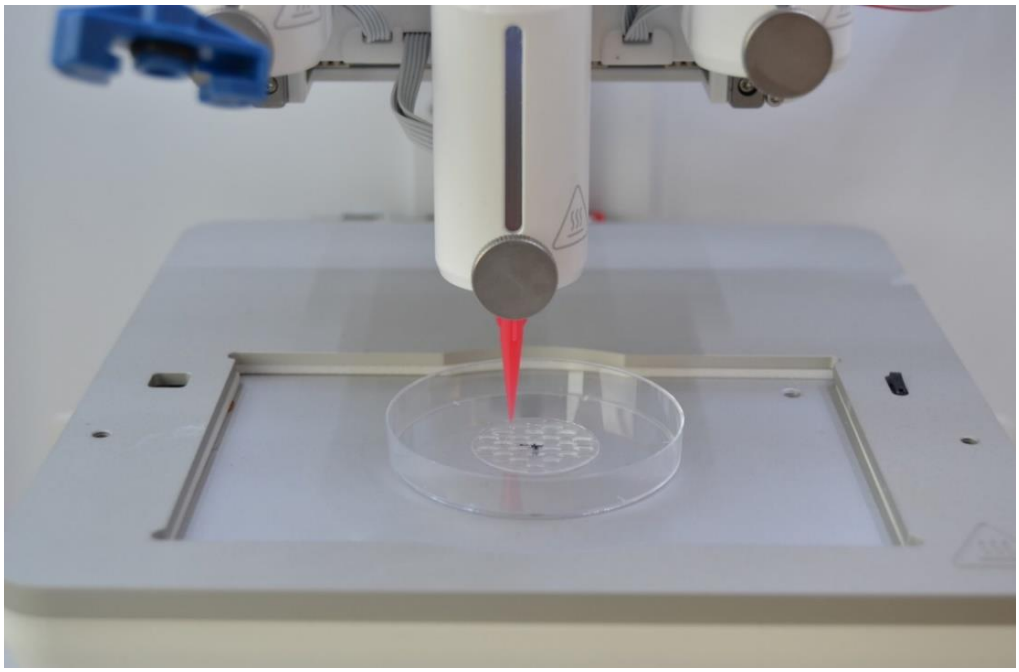

Figure 21. Picture taken during the printing of BioX

4.2.3. Liquid exudate extraction test

Aim

The purpose of liquid exudate extraction test is to evaluate the structure designed effective capability to extract liquid and transport to the second layer, the absorbent module. It was evaluated also the difference between absorption for a structure with many channels (23) and one with few (5).—The strength of the 3D printing process is the high customizable possibility; thus this solution could be take in consideration when it is necessary to design channels for specific cases. In this test, the material is not the most important parameter since the liquid transport is achieved thanks to the capillarity forces created in the channels, for this reason only MFC1_8020 was used as material in the test, even if same structures were printed also with MFC8_8020 to show possibility to reach same resolution.

Procedure

The samples were prepared as said above. The test consists in the weight change measurement of the absorbent module after 10 minutes when it is placed over the moisturizer module, a weight control on the moisturizer module is also accomplish to evaluate if some liquid is lost or gained during the test.

To set the test the moisturizer module was placed on a grid, which was immersed in SWF in a way that the level of the liquid was even to the bottom surface of the moisturizer structure, as shown in Figure 20. After this the absorbent module was placed on the top of the moisturizer module and test started. After 10 minutes each module was weighted separately. In Figure 22 below, it is also possible to see the different structure tested.

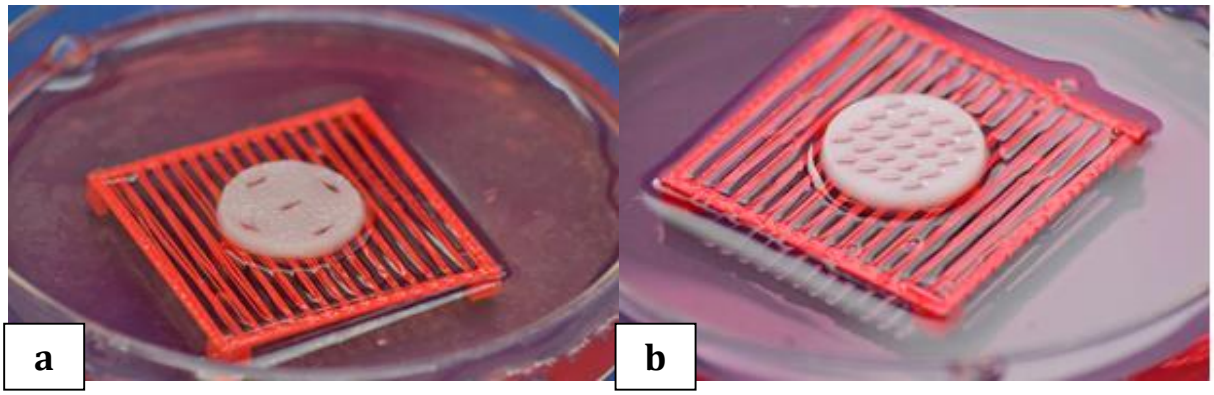

Figure 22. Samples of the liquid extraction test; a) Sample with 5 channels, b) sample with 23 channels

Chapter 5

5. Results

5.1. Material characterization

5.1.1. Water retention test

The data were calculated with the formula (5.1.):

$$WRT_{value} = \frac{W_i}{W_0} \cdot 100 \qquad (5.1)$$

Where W_i and W_o are weight values of samples at time 0 hour and i=1,2,3,4,5,6,24. Thus a higher value means a higher material's water retention. The water retention test results are reported in Table 10 and in Figure 23, the first main difference observed is between Aquacel® and MFC taken in examination.

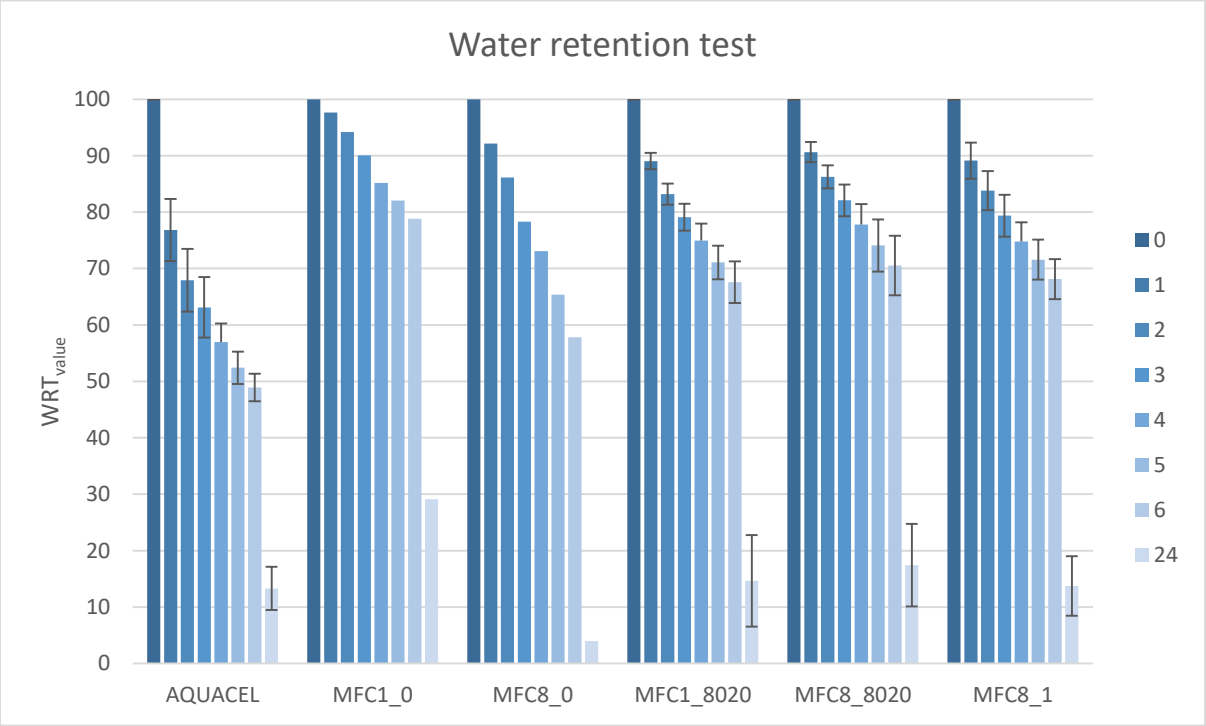

Figure 23. Graph of the WRT results

In Figure 23 are shown the results, Aquacel® showed a faster decrease in the first hour, meaning a high water evaporation, furthermore, general values of Aquacel® are lower than all MFC samples confirming the high hydrophilicity of the material. MFC1_0 and MFC8_0 are used only to show the difference between the material crosslinked and not crosslinked, but they cannot be the material for the final structure since it is impossible to have a freestanding structure without any kind of crosslink.

Regarding the MFC1 there is a difference between composition with alginate and crosslinked (MFC1_8020) and the one without alginate not crosslinked (MFC1_0). The MFC1_8020 show a lower WRT_{value}, while for MFC8 the trend is opposite, showing that crosslinking increases water retention capacity. For MFC8_0 the final weight is very low, almost all water is gone leaving only a dry film of nanocellulose.

Comparing the two compositions crosslinked of MFC1 and MFC8 (MFC1_8020 and MFC8_8020 and MFC8_1) a slightly difference is seen, MFC8_1 show a similar WRT_{value} to MFC1_8020 and slightly lower compared to MFC8_8020, which shown the best properties in this test. The reasons could be due to surface modification of MFC8 nanofibrillis. MFC8 is a carboxylmethyl cellulose with some aldehydic and carboxylmethylic groups on nanofibilis surface. These groups increase possibility of creating hydrogen bond with water, while enzymatic nanocellulose (MFC1) is devoid of these groups. Another reason for MFC8_8020 higher values, could also due to slightly higher initial water content (97,4% w/v comparing with 97% w/v).

Table 10. WRT results, the results are average of the total samples

TIME (h)	0	1	2	3	4	5	6	24
AQUACEL	100	76,83	67,93	63,11	56,95	52,41	48,93	13,30
MFC1_0	100	97,63	94,21	90,06	85,17	82,05	78,83	29,09
MFC8_0	100	92,16	86,13	78,31	73,11	65,38	57,81	3,98
MFC1_8020	100	89,05	83,19	79,10	74,98	71,07	67,58	14,65
MFC8_8020	100	90,62	86,26	82,10	77,78	74,09	70,54	17,42
MFC8_1	100	89,12	83,83	79,36	74,79	71,58	68,12	13,75

5.1.2. Shrinking test

The data were calculated similar to WRT test, in fact, it was used the formula (5.2):

$$ST_{value} = \frac{A_i}{A_0} \cdot 100 \quad (5.2)$$

Where A_i is sample's surface area at i hour (with i=1,2,3,4,5,6,24) and A_0 is the initial sample's surface area. Thus a higher ST_{value} means a lower shrinkage and better property of the material when it comes to maintain shape during time. In Table 11 and in Figure 24 are shown ST_{value} of the materials tested. From the datas is possible to see two major differences:

1. The MFC hydrogels show a lower shrinkage compared with Aquacel®;
2. The hydrogels crosslinked show a lower shrinkage compared with the hydrogel without crosslink agent.

From these results, Figure 24, is possible to deduce that the crosslinking process is essential for the structure to keep the shape and have lower shrinkage during time. Further, for MFC8_1 the shrinkage is lower than MFC8_8020 meaning that alginate has an effect on the hydrogel internal structure.

The crosslink is necessary not only to create freestanding structures but also to reduce the possibility of shrinkage. The materials crosslinked properties with alginate are quite similar for the first 6 hours but then the MFC1_8020 presents high shrinkage after 24 hours, even higher than MFC1 not crosslinked, suggesting that the best material is the MFC8_8020 regarding the shrinkage test.

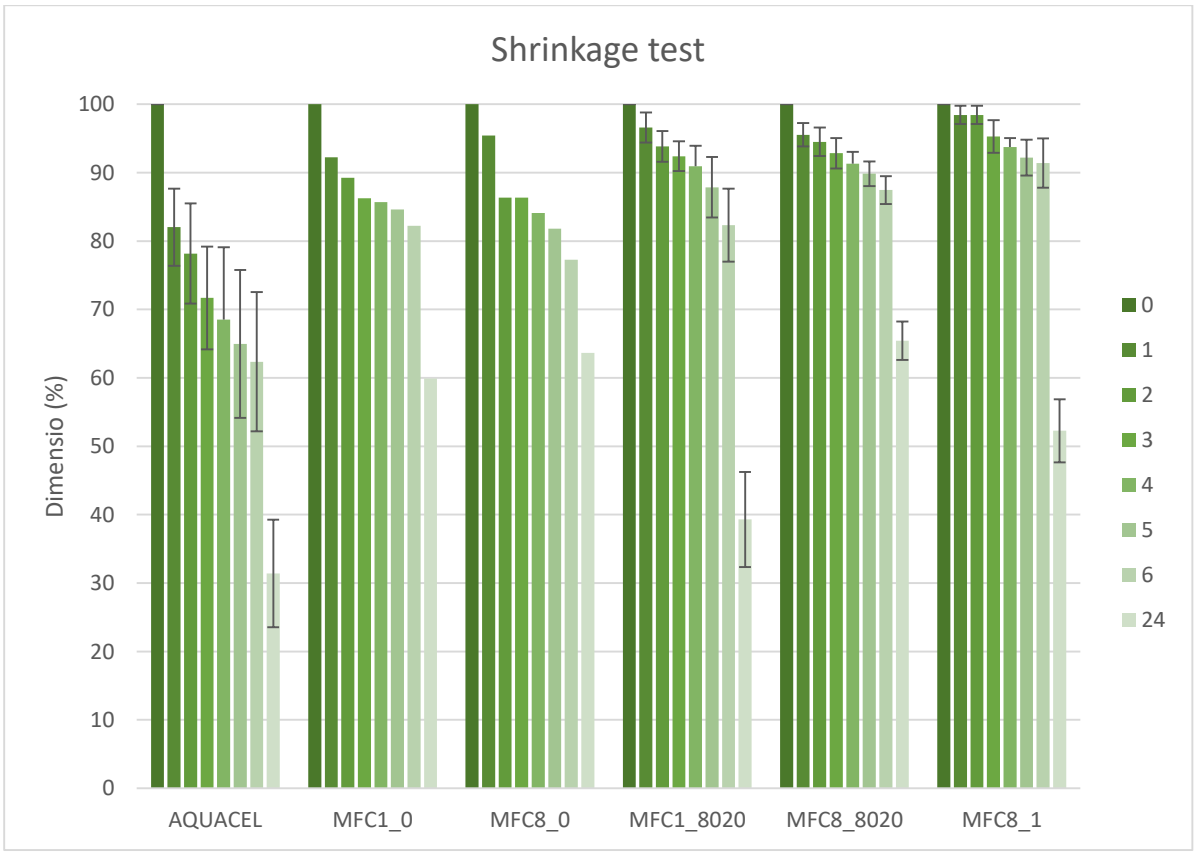

Figure 24. Graph of the ST value.

Table 11. ST value results

TIME (h)	0	1	2	3	4	5	6	24
AQUACEL	100	82,03	78,18	71,70	68,53	64,96	62,37	31,40
MFC1_0	100	92,27	89,23	86,26	85,69	84,60	82,23	59,91
MFC8_0	100	95,45	86,36	86,36	84,09	81,82	77,27	63,64
MFC1_8020	100	96,60	93,83	92,41	90,93	87,87	82,33	39,30
MFC8_8020	100	95,54	94,51	92,84	91,31	89,85	87,47	65,43
MFC8_1	100	98,45	98,45	95,31	93,76	92,21	91,41	52,27

5.1.3. Compression test

Thanks to this test it is possible to obtain information about stiffness and elasticity of the gels calculating slope in different region of the curve compressive stress/compressive strain.

The yield stress and yield strain are the values corresponding to the point where the graph start to be linear, this is the point where the alginate start to break up, the physical network is kept but the long polymeric chain start to flow under a constant load. This are the limit value for the use of the material for the application, at higher stress or strain the structure given to the hydrogels is lost.

In Table 12 are shown values of the compressive modulus for small deformation (0-5%) and yield stress and yield strain of hydrogels evaluated.

Table 12. Results of the compression test

Material	Modulus 0-5% kPa	St.Dev kPa	Yield stress kPa	St.Dev kPa	Yield Strain %	St.Dev %
Alginate	63,5	8	143	20	64,1	6
MFC8_1	7,3	3	4	1	31	4
MFC8_8020	34,8	5	56,7	8	39,3	4
MFC8_6040	57,2	13	67,7	5	40,3	4
MFC8_4060	123,8	11	69,6	5	36,2	3
MFC8_2080	297,4	54	74,2	5	21,3	9
MFC1_8020	28,9	3	72,4	4	49,9	3
MFC1_6040	54,2	6	86,7	5	44,6	2
MFC1_4060	176,8	13	97,9	13	32,4	3
MFC1_2080	318,2	69	82,9	4	20,8	4

These results confirmed what supposed, the alginate network give to the structure a mechanical stability and enough elasticity to be a freestanding structure. Indeed, materials without alginate (MFC8_1) crosslinked with calcium chloride show a lower compressive modulus, this could be explained because the structure formed by the cellulose fibrils with calcium ions is not a stable network as the one formed by the alginate. This is confirmed by the compressive modulus of MFC8_1, which is only 7,3 kPa against 34,5 kPa of MFC8_8020. This demonstrate that a small amount of alginate is important to improve the mechanical properties of the hydrogels. The network of alginate not only increase the compressive modulus but also a large increase in the yield stress is observed, from 4 kPa with a deviation of 1 kPa, to 56,7 kPa with a deviation of 8 kPa, proving a good combination of the two materials.

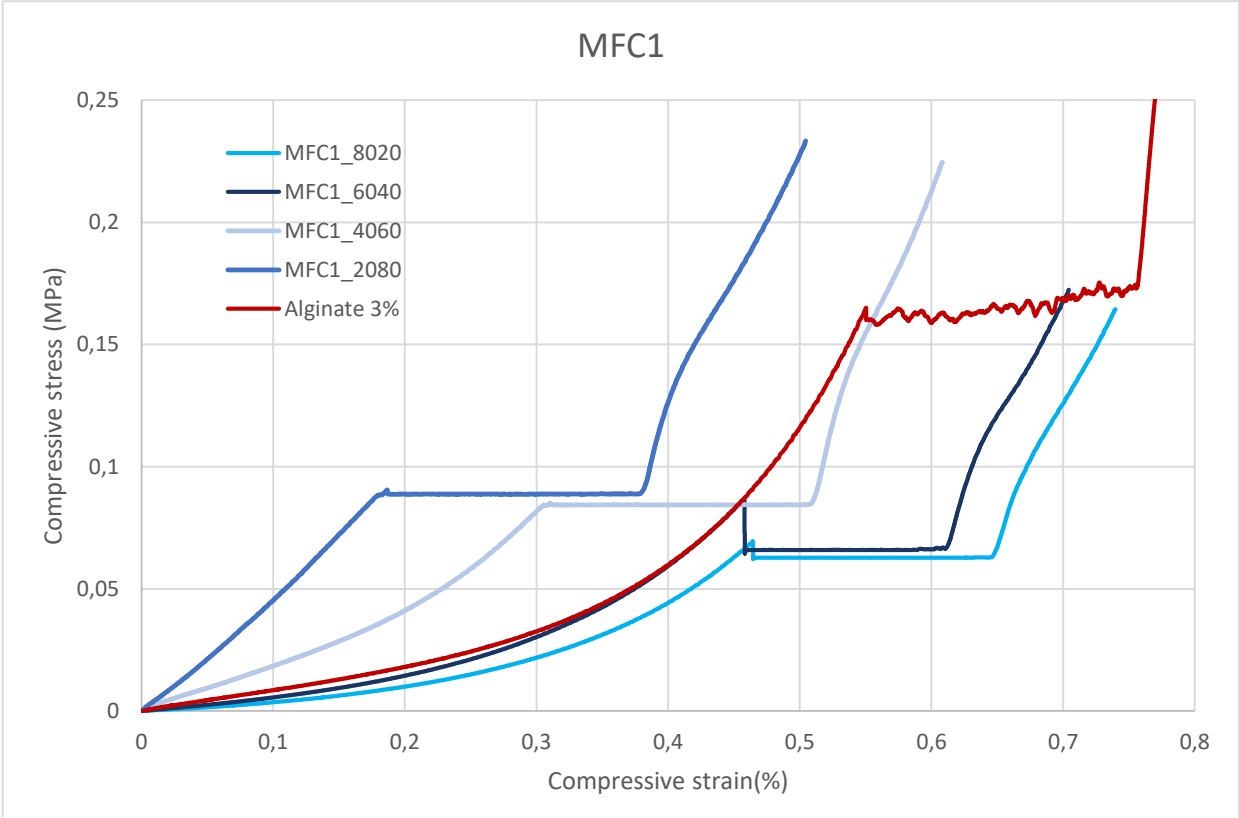

Figure 25. Graph of compression results for the MFC1 derivate hydrogels

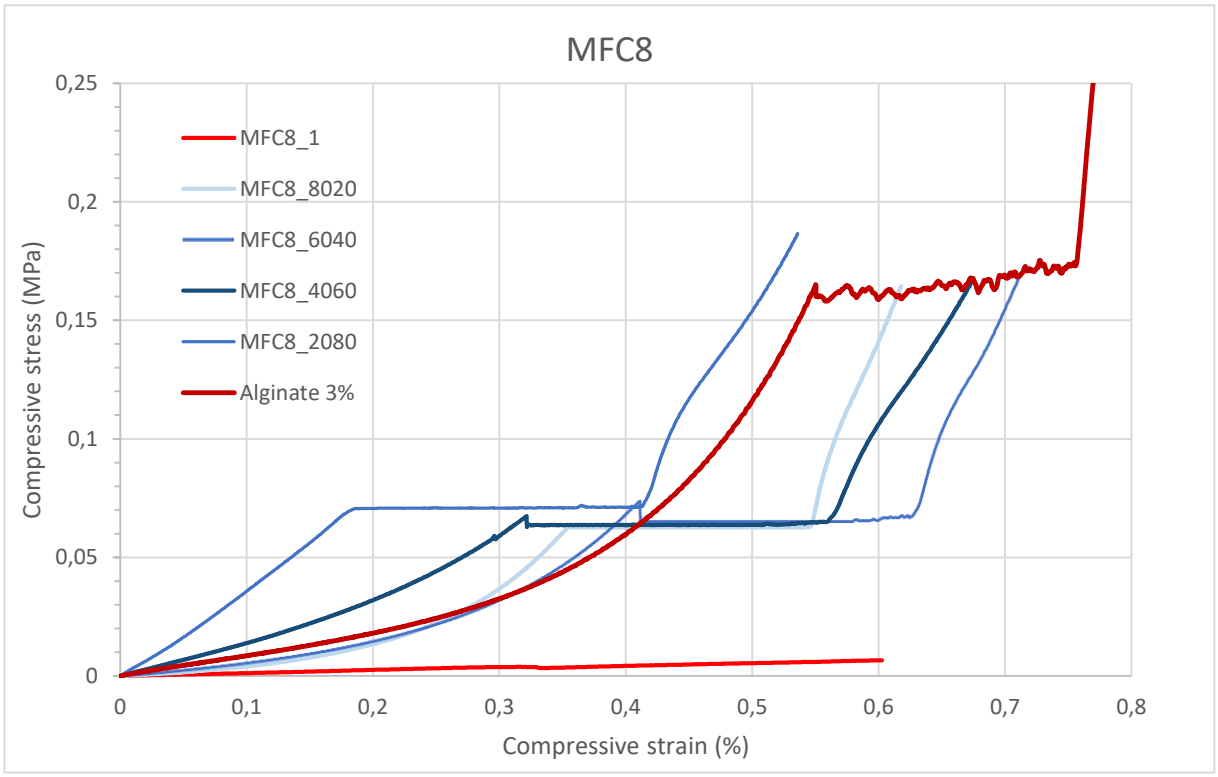

Figure 26. Graph of compression results for the MFC8 derivate hydrogels

After a comparison between the material crosslinked with alginate and without, it was investigated also the mechanical properties (yield strain, yield stress and compressive modulus) of the hydrogel when the amount of alginate increase.

In general, increasing alginate percentage increase compressive modulus and yield stress while yield strain is decreased, this trend is clear for the MFC1, where the compressive modulus pass from 28.9 ± 3 kPa of the MFC1_8020 to 318.2 ± 69 kPa of the MFC1_2080, and the yield strain goes from 49.9 ±3% of the MFC1_8020 to 20.8±4% of the MFC1_2080, while the yield stress follows this trend for MFC1_8020, MFC1_6040 and MFC1_4060 but not for MFC1_8020 (72,4±4kPa, 86,7±5 kPa, 97.9±13 kPa and 82.9±4 kPa respectively). Regarding MFC8 composition, the increase in compressive modulus is seen when the amount of alginate is increased from 20% to 80%, 34,8±5 kPa and 297.4±54 kPa respectively, and same trend is seen for the yield stress, from 56.7±8 kPa to 74.2±5 kPa. However, the yield strain decreasing is not so clear as for MFC1, where yield strain varies from 39.3±4 % to 36±3 % of MFC8_8020 and MFC8_4060 respectively, and decrease drastically for the MFC8_2080, 21.3±9 %.

The test was also conducted on a composition of 3%w/v of pure alginate and compressive modulus of 63.5±8 kPa was founded with a yield stress of 143±20 kPa and yield strain of 64.1±6 %, showing high mechanical properties.

From this test, results show the necessity of having a strong network that give good mechanical properties. Looking at to the graphs it is possible to guess the material rigidity when strain increase, it can be done analysing the compressive modulus increase when the compressive strain increase. MFC8_8020 has a higher increase respect MFC1_8020.

5.1.4. Rheological test

Viscosity inks test

The inks viscosity is mainly dependent from the dry mass percentage in the composition, as the in the preparation of inks the percentage of the hydrogels is kept constant adding alginate include increasing the solid mass. However, all inks prepared show shear thinning properties, essential for 3D printing process.

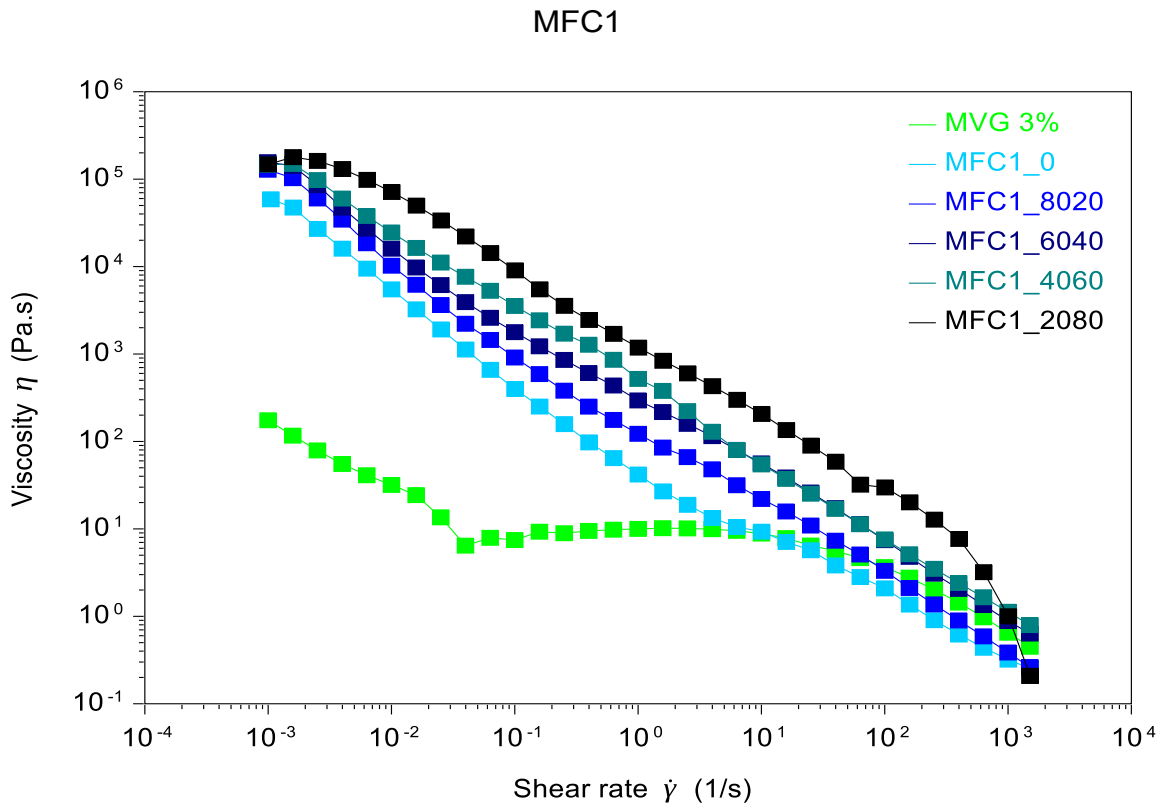

Figure 27. Viscosity properties of MFC1 hydrogels

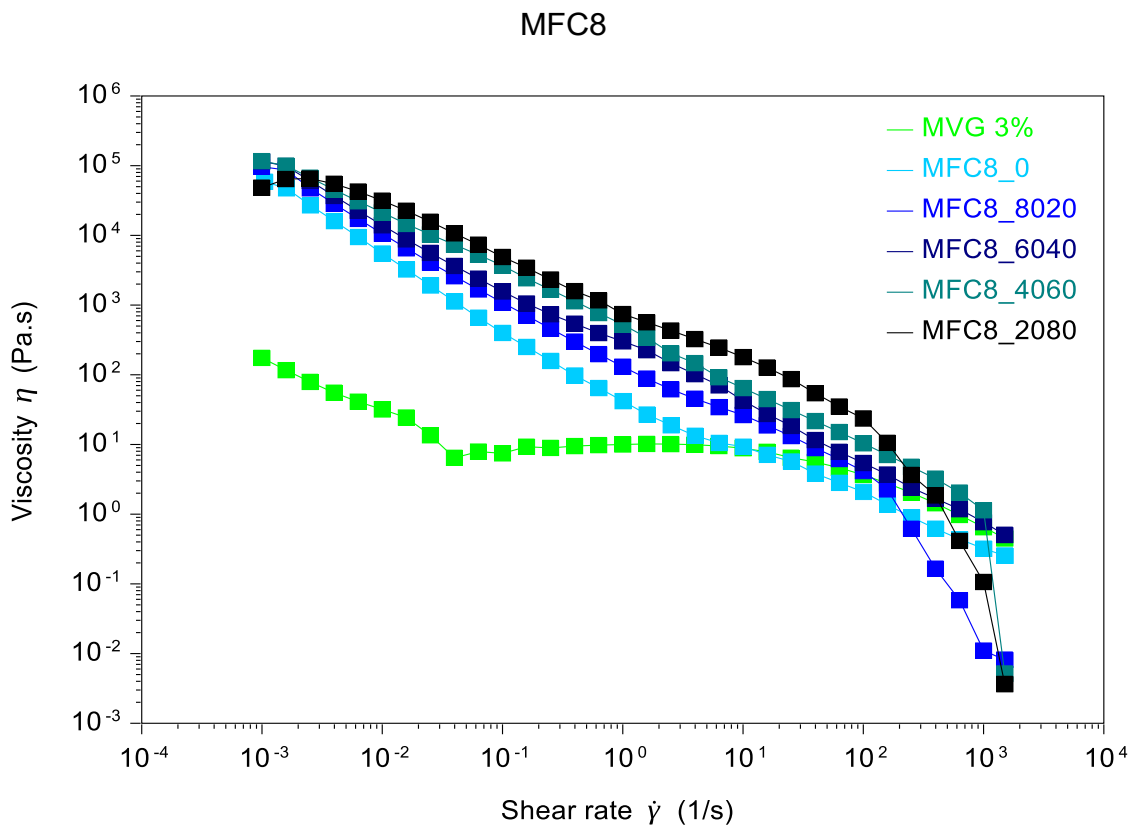

Figure 25.Viscosity properties of MFC8 hydrogels

As show in Figure 27 and Figure 28, both MFC1 and MFC8 show shear thinning properties, with increasing of viscosity if amount alginate increases, thus these results confirmed what expected from the beginning, demonstrating that all the inks, under adequate pressure, can be used as ink in a 3D printing process.

Crosslinking kinetics

In this test the crosslinking kinetics has been tested and as it is possible to see from the graph, after crosslinker addition ($CaCl_2$ 0.5 M) at t=60sec, the G' increase fast, meaning that the alginate network starts to form quickly, and the structure became more rigid.

It is possible to divide the graph in two section, first one before the addition of crosslinker and the second after that. In the first part it is noticeable different value of G', since inks with more alginate have storage modulus higher, while after the crosslinker addition, inks show a fast crosslink, in within 5-6 minutes, and then G' is kept constant. This means that crosslinker doesn't have more influence on the structure when this is complete crosslinked. It is also shown that G', after crosslinker addition, increases with the amount of alginate.

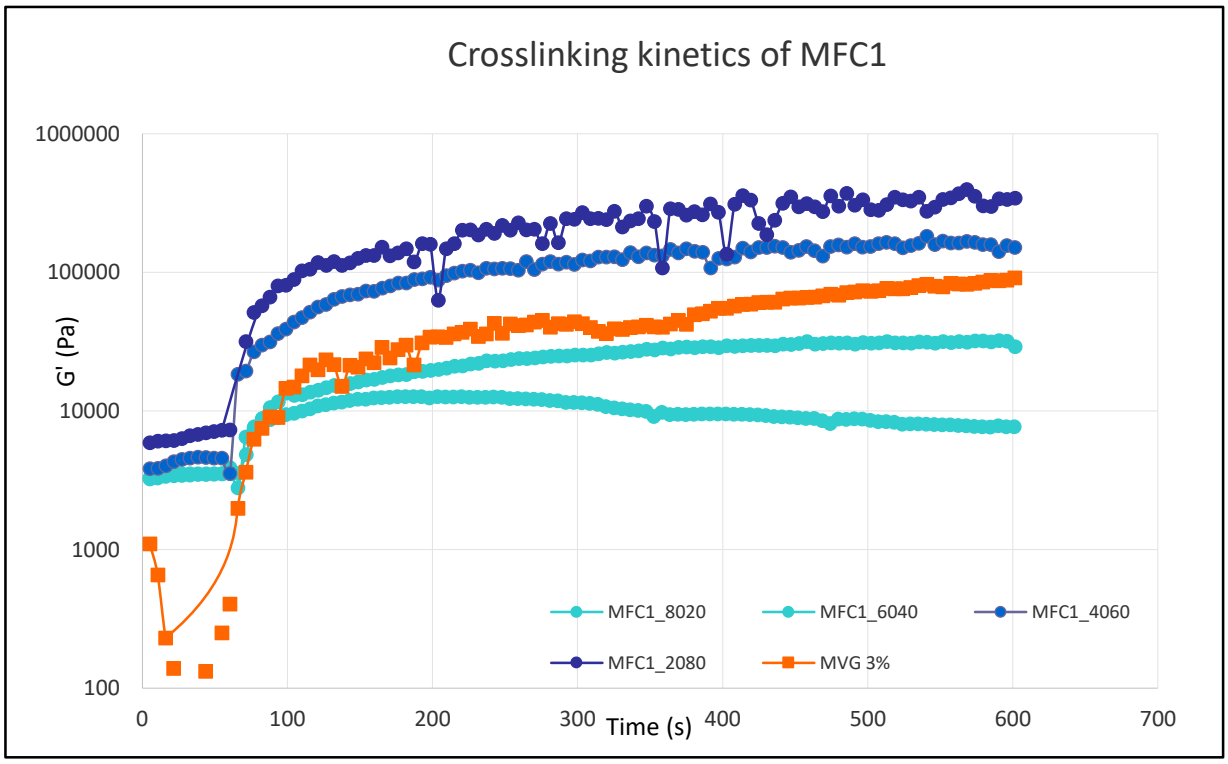

Figure 26. Crosslinking kinetics results of MFC1 hydrogels

For the alginate solution, the crosslinking process take more time, about 15 minutes, when the crosslinking process starts, the network starts to form and G' increases fast and reaches values between composition of 40% and 60% of alginate with MFC. The results are shown in Figure 29 and Figure 30.

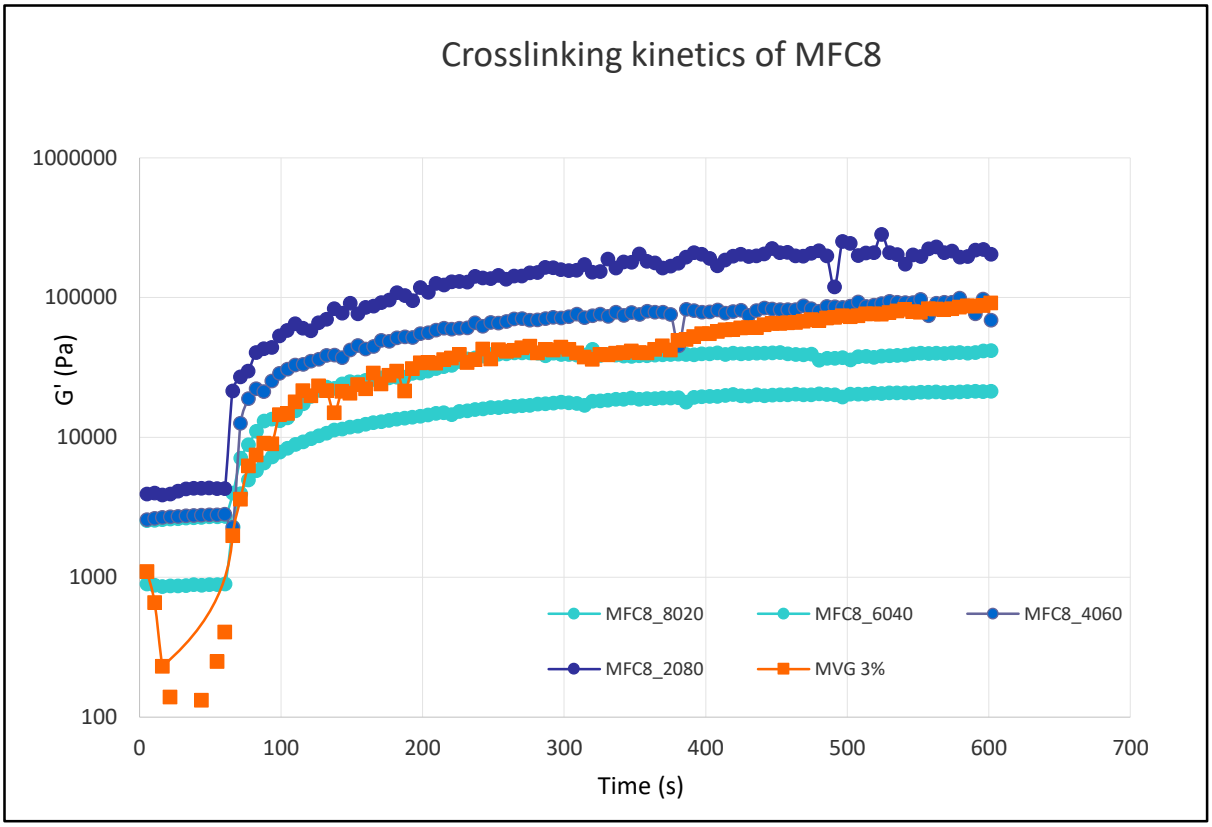

Figure 30. Crosslinking kinetics results of MFC1 hydrogels

Shear resistance

The shear resistance test could give us some information about the maximum forces withstand from the materials. The point where the loss modulus (G'') overcame the storage modulus (G') is the 'break point', it is the stress values that the crosslinked network can stand without breaking and start to flow.

In Figure 31 and Figure 32, it is possible to see that during this test for MFC1_8020 and MFC1_6040 the break point is reached at 4,5 kPa and 5,5 kPa respectively, while for the composition with 60 and 80% of alginate the break point is not reached, the test was stopped at 10 kPa. Regarding the MFC8 the break point is reached both for 20, 40 and 60% with values of 3,8 kPa, 5 kPa and 8,5 kPa respectively, while for the composition with 80% the break point is higher than 10 kPa.

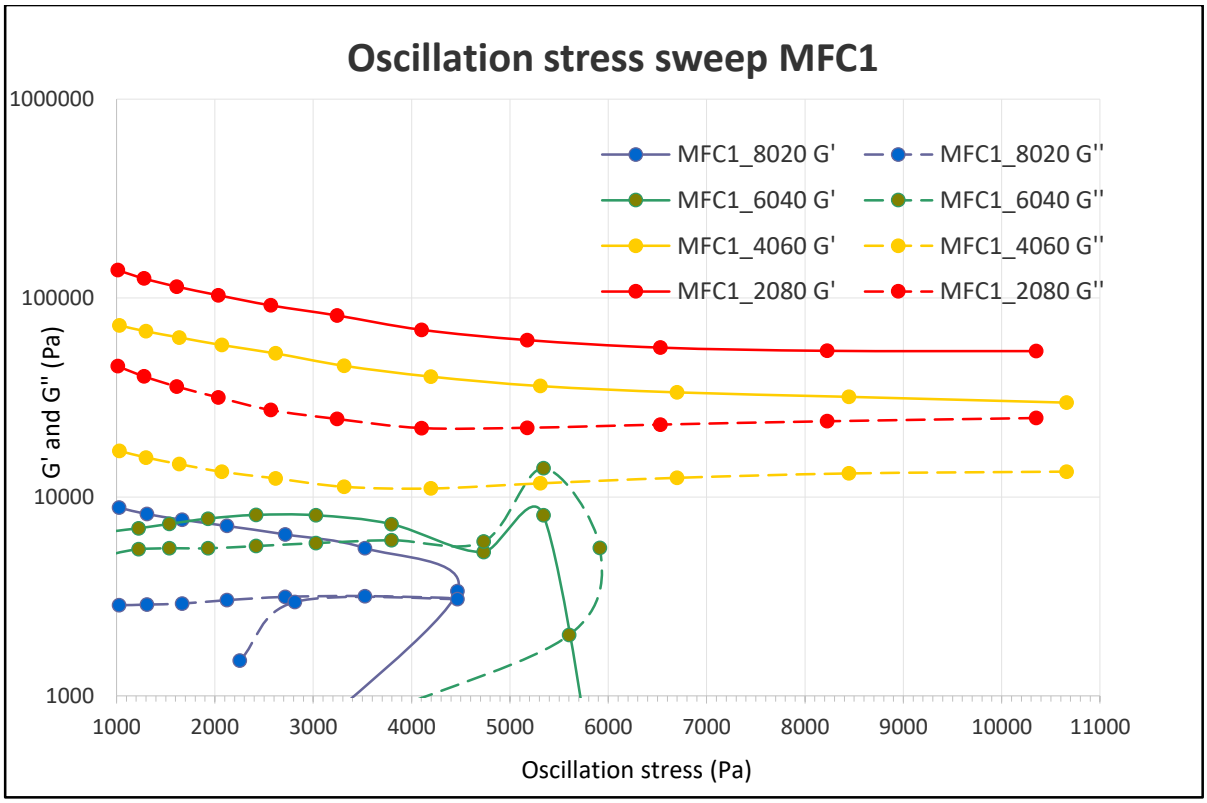

Figure 27. Oscillation stress graph of MFC1 hydrogels

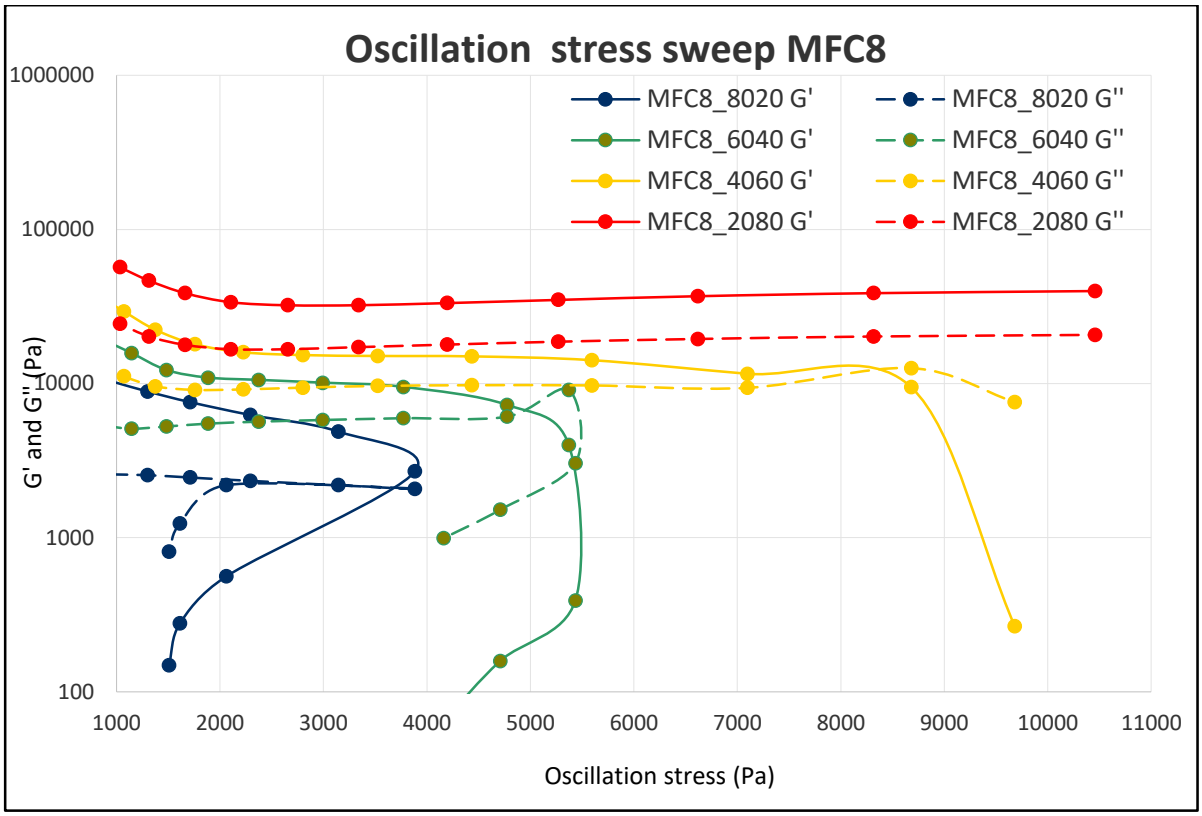

Figure 28.Oscillation stress graph of MFC8 hydrogels

5.1.5. Cytotoxicity

Test specimens and controls were run in triplicate in the agar diffusion assay and their effects on human fibroblast scored, see Table 13. Also, the solutions that hydrogels were soaked in were tested to assess if any cytotoxic substance may have leaked to the surrounding HBSS solution.

All hydrogel based prototypes and their respective HBSS solutions showed viable cells below and beyond the specimens, equal to the negative control and cells only reference. The positive control yielded malformed and degenerated cells below and beyond the specimen. The evaluation was photo documented, Figure 33 and Figure 34.

Table 13. Results from the cytotoxicity experiment

Test specimen	Cytotoxicity score
Negative control	**0**
Positive control	**4**
Cells only	**0**
MFC8_8020	**0**
MFC1_8020	**0**

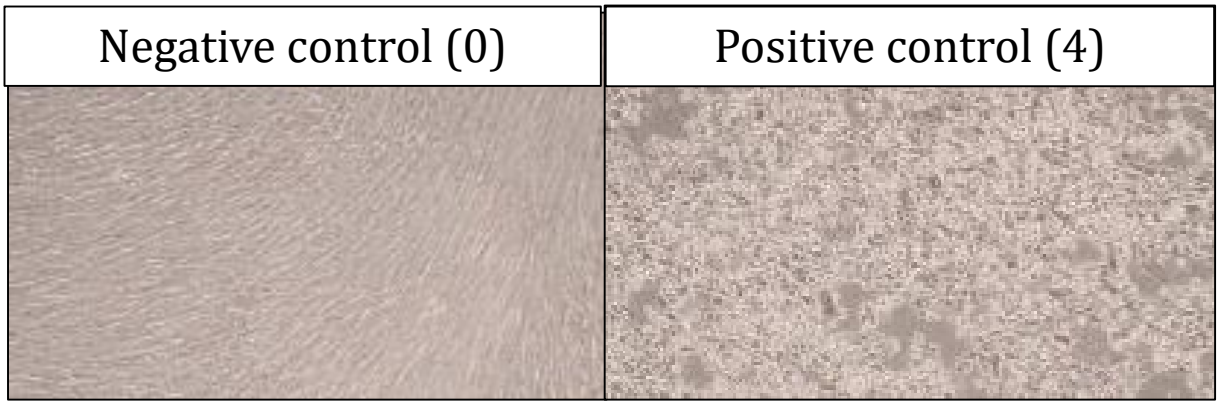

Figure 33. Reference in the cytotoxixity results

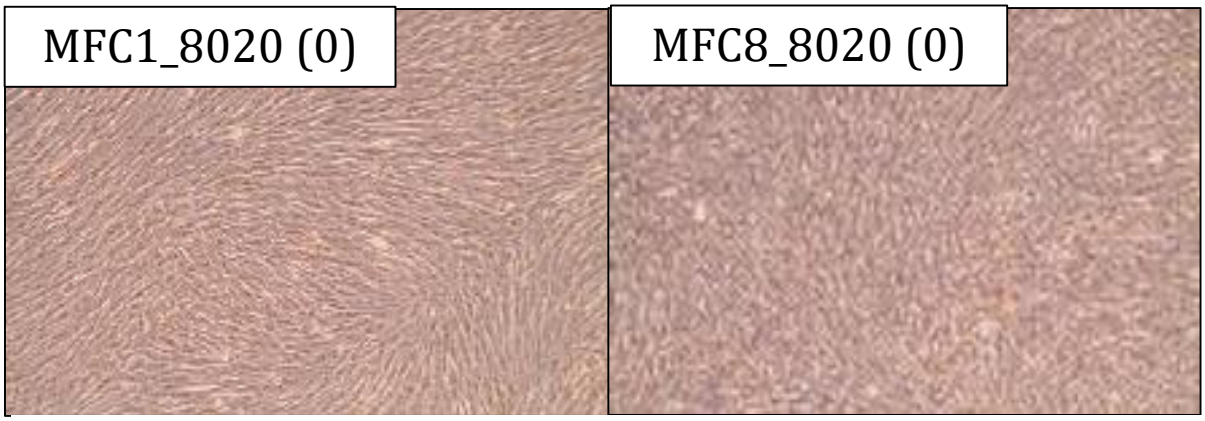

Figure 34 Cytotoxicity results of MFC1_8020 and MFC8_8020

5.1.6. Stability in SWF and NaCl

The stability test demonstrate that the structure is not degraded by synthetic wound fluid (SWF) or from neutral salt solution (NaCl). Indeed, the structure is kept in both cases without losing of elasticity or detriment formation.

In SWF the samples appear coloured after 24 hours meaning that there is a small diffusion of SWF into the hydrogel, but the structure is not influenced and the channels are still visible after the test, as shown in Figure 35. The white particles seen in the channels are from SWF degradation, they don't belong to the hydrogels.

The samples that were putted in the NaCl, Figure 36, show the same results meaning that the crosslinking is stable and there is not exchange between the Ca^{2+} ions and Na^{+} ions. Indeed, after the test the hydrogel present still the same elasticity and shape at the beginning of the test.

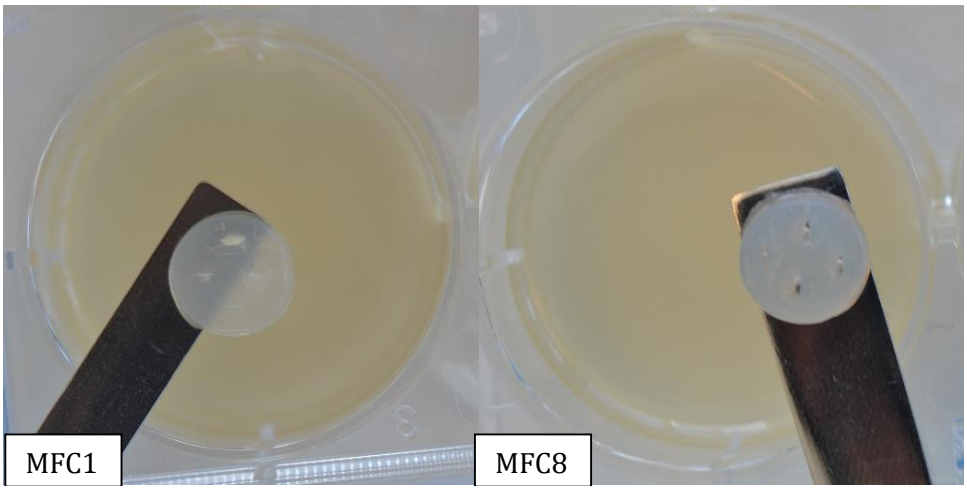

Figure 35. Sample of MFC1_8020 and MFC8_8020 of the stability test in SWF

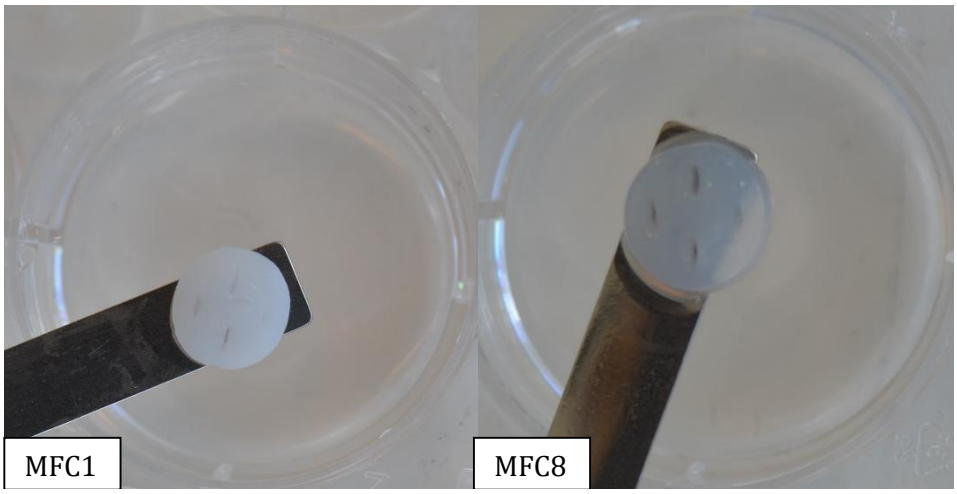

Figure 29. Sample of MFC1_8020 and MFC8_8020 of the stability test in NaCl

5.2. Structure characterization

5.2.1. Interaction between the modules

The moisturizer module was prepared with two different materials, MFC1_8020 and MFC8_8020. The loss of weight could be due to evaporation or from absorption of liquid from the absorbent module. The two causes can be deduced from the samples weight separate and together.

Looking to the data of moisturizer module weight it is possible to see a fast decrease of weight during the first day, Figure 37 and Figure 38, and then a trend to became more linear for long time. The absorption is higher for MFC1_8020 meaning that this material loose water easily than MFC8_8020. Both materials after 197 hours still present 60% and 65%, MFC1 and MFC8 respectively, of initial weight, meaning that only around 40% of initial water is evaporated or absorbed from the second layer.

The evaporation is evaluated measuring the total weight it is possible to see in Figure 38 that the weight decrease at almost the same way for both materials. After 197 hours the total weight is still around 87%, even if MFC1 is a little bit lower than the MFC8. This mean that only around the 13% of the total water evaporate and leave the system.

With a close observation to the absorbent module it is seen the first layer was wet while the rest was dry, and also it becomes less rigid, since the water made as plasticizer.

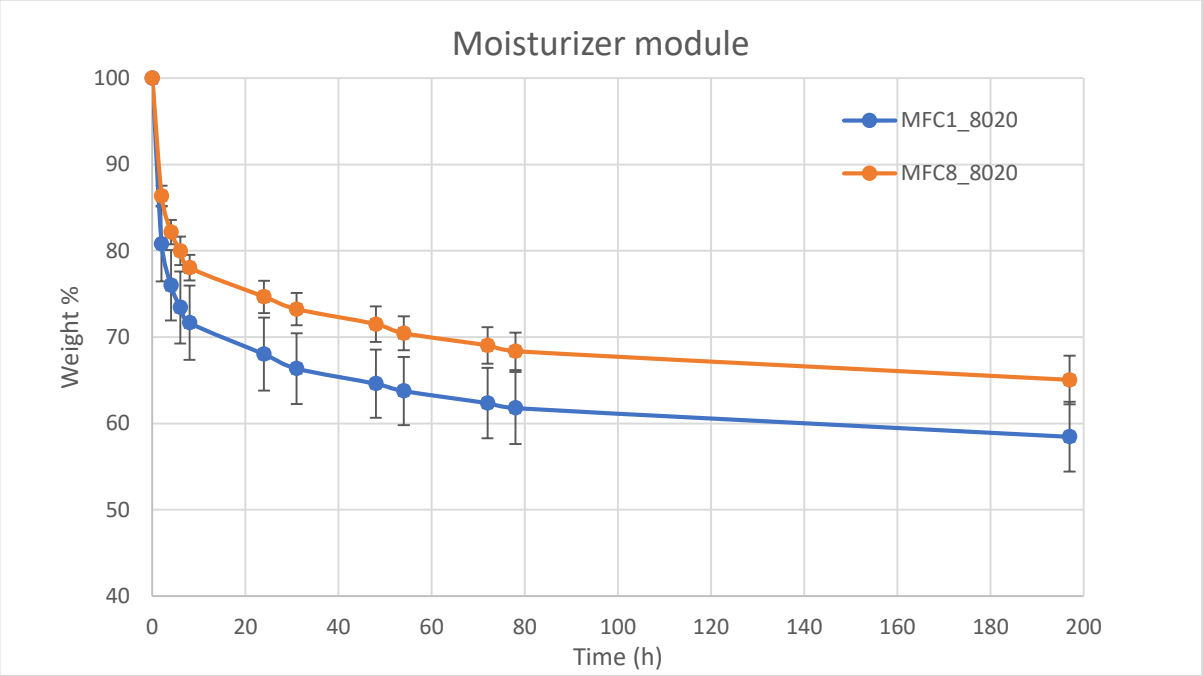

Figure 37 Weight change in the moisturizer module

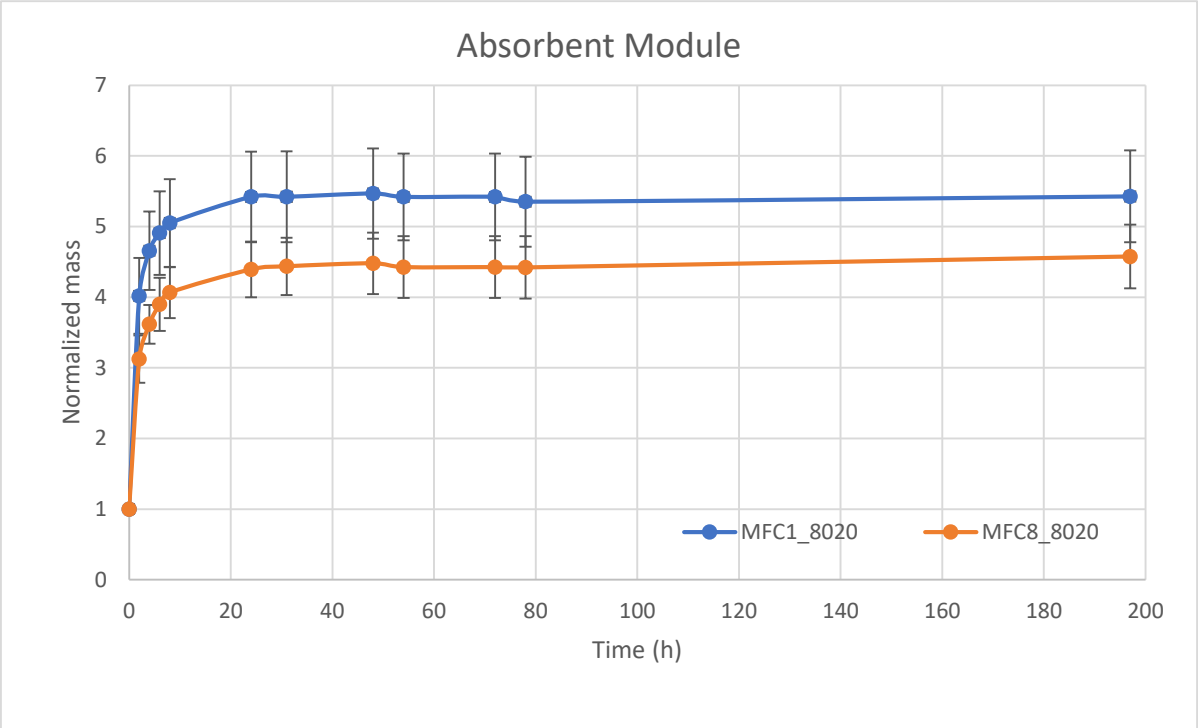

Figure 38. Weight change in the absorbent module

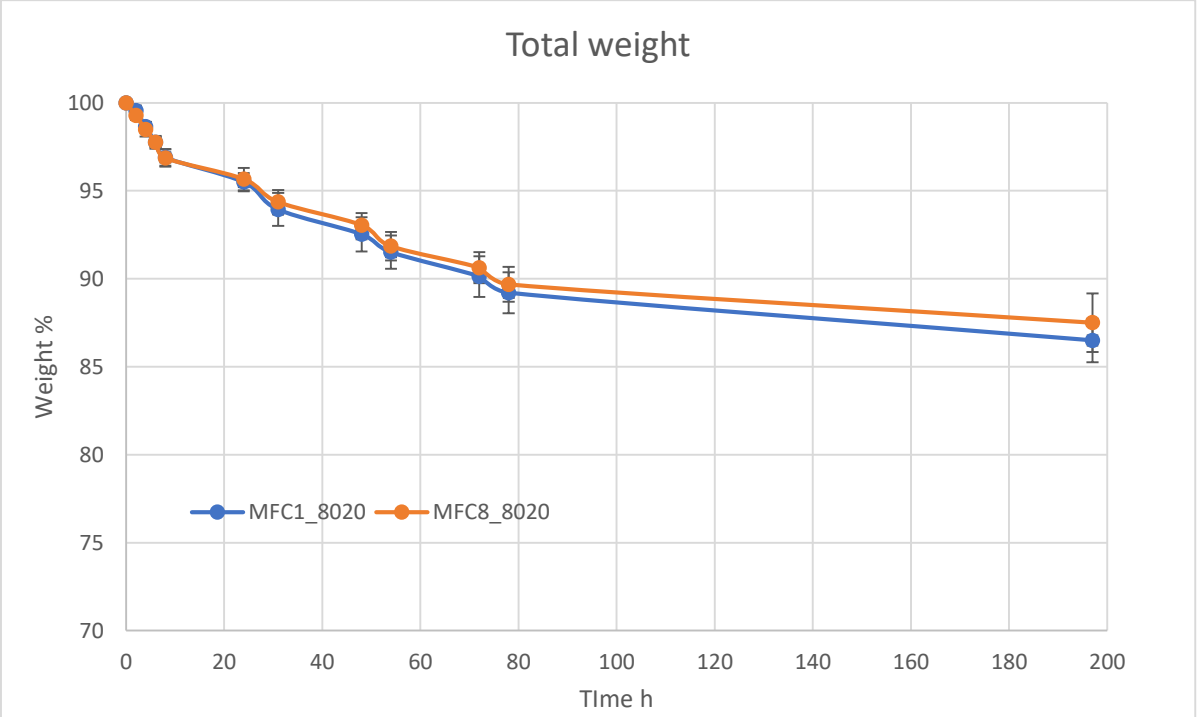

Figure 39 Total weight change, from this graph it is possible to evaluate the total evaporation

5.2.2. Printability

The printability test consists mainly in many prints to examine material behave during the printing process.

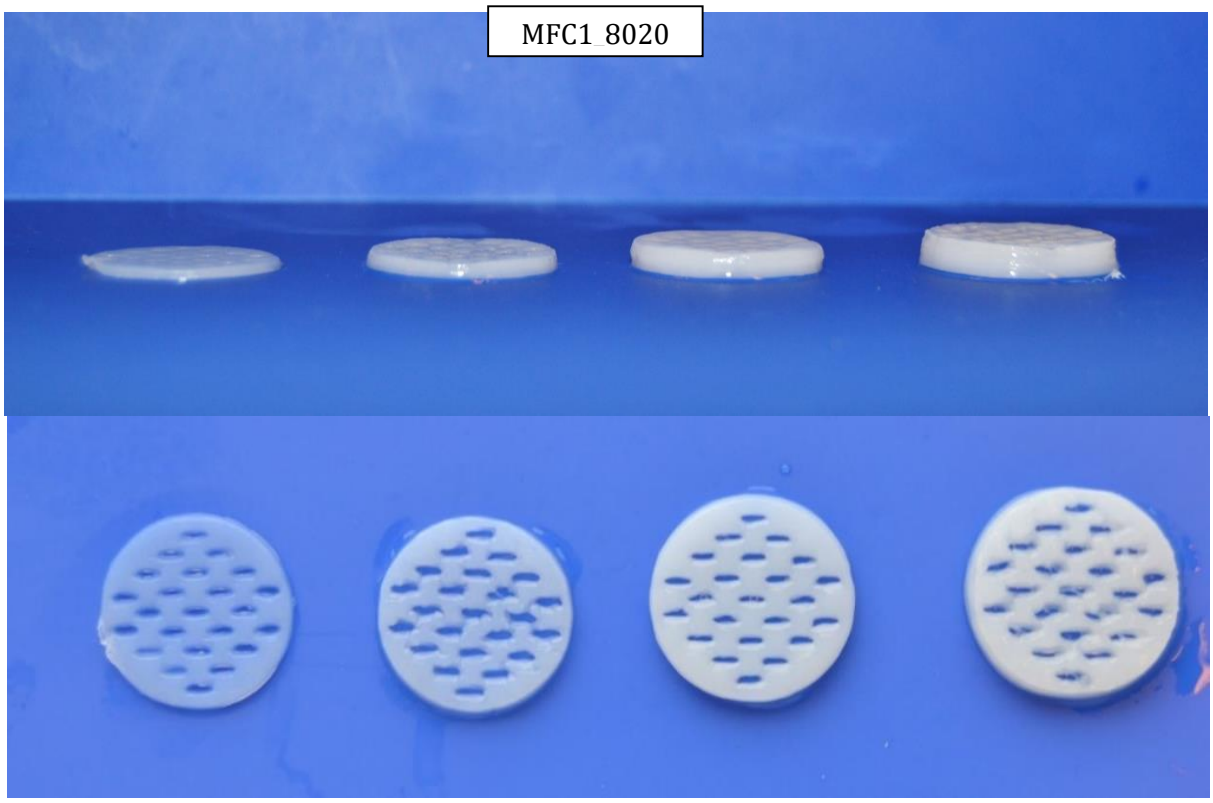

Figure 30. Moisturizer module printed with different height with MFC1_8020

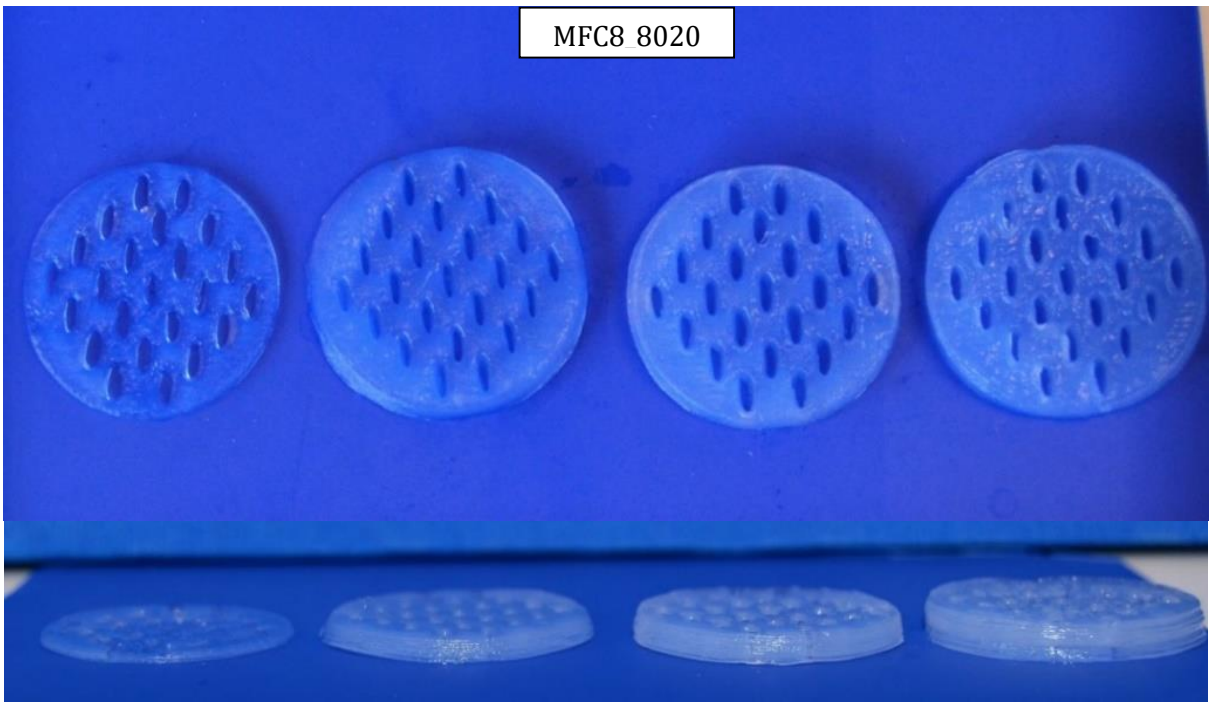

Figure 31. Moisturizer module printed with different height with MFC8_8020

The first experiment was printing with different height starting from 1mm up to 4 mm, the structures printed showed different rigidity, structures with 4mm were too much rigid, therefore unsuitable to cover all body surface uneven, while structures with 1 mm height were weak and it could be used in case the wound exudates is not in high quantity and the surface is highly uneven.

The structures with 2 and 3 mm were considered optimal for this application since they have combination of elasticity and stiffness in the right ratio. The channels formation is possible to achieve for all the structures with a good resolution until 3 mm but when the height reaches 4 mm, the channels start to collapse and close. The maximum height achievable suggested from this test is 3 mm.

The samples printed are shown in Figure 40 and Figure 41.

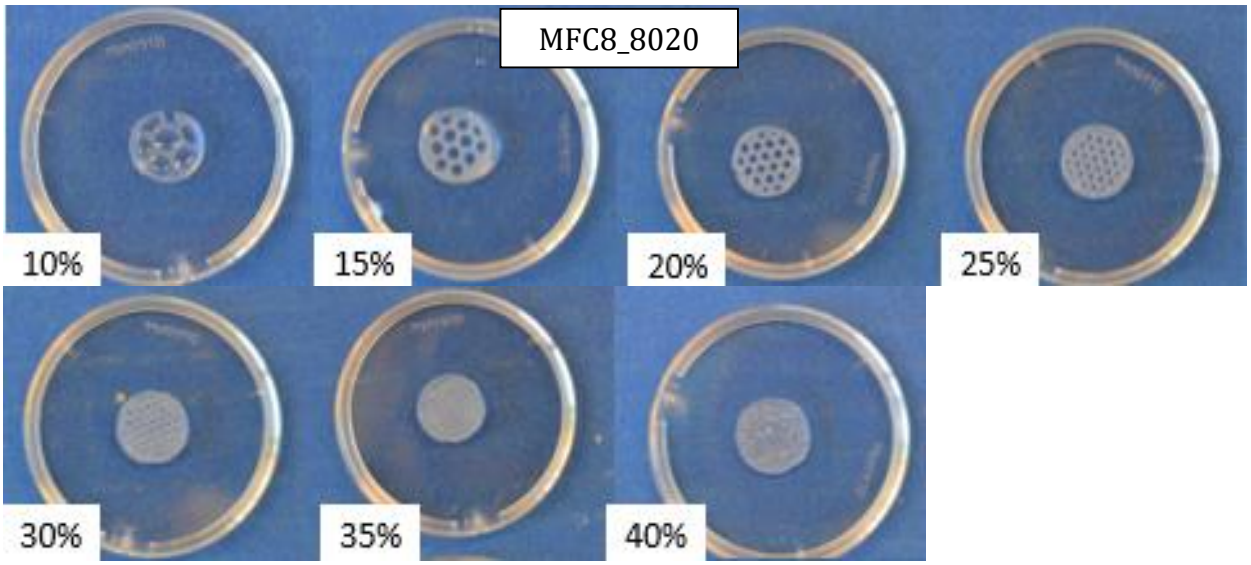

Figure 33. Printability samples to test the optimal infill, printed with MFC8_8020

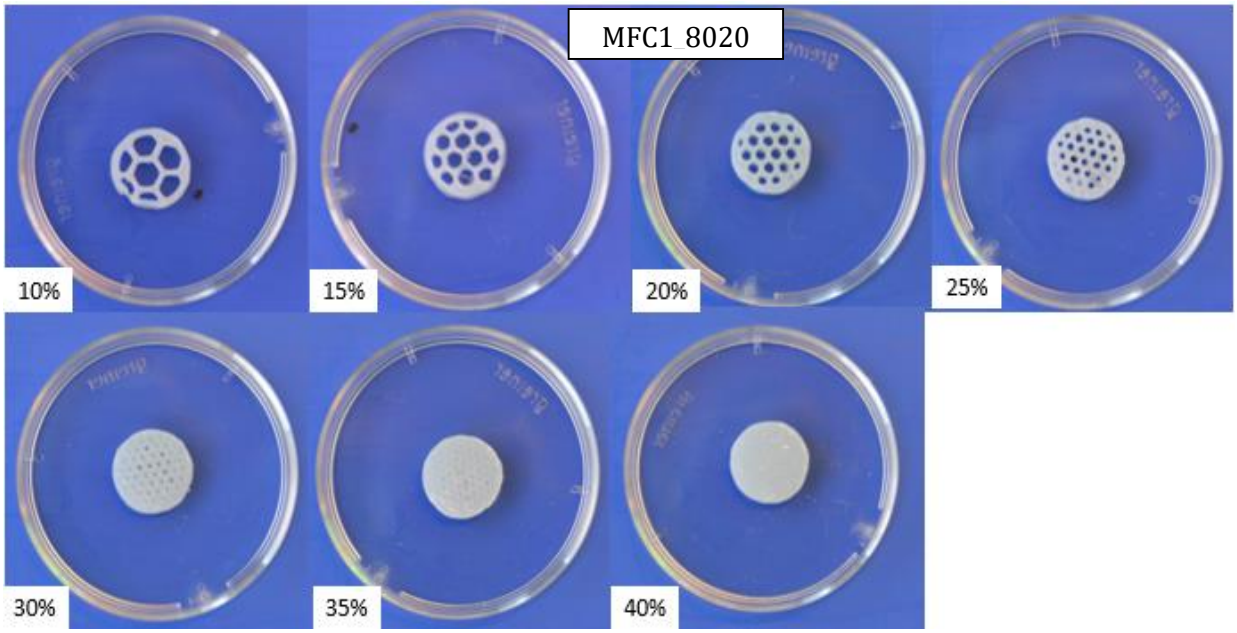

Figure 32. Printability samples to test the optimal infill, printed with MFC1_8020

In the printing test with different infill it is possible to see structures printed with different size and amount of channels depending form the infill chosen, see Figure 42 and Figure 43. For MFC8_8020 there is formation of holes for the structures printed with 10, 15, 20, 25 and 30 %. Structures with 35% of infill still have some channels but the pattern starts to be dense and some channels start to close. With 40% infill the structures are completely without channels. With MFC1_8020 the structures printed showed the same results, in the end to select the optimal infill it is take in consideration the mechanical stability of the structures. For this reason, structures with only 10% and 15% of infill are reject. The optimal infill was identified between 20 and 25%, since the high amount of channels with proper dimensions, homogenously distribution of channels and good mechanical stability of the structure.

5.2.3. Liquid exudate extraction test

In the test different structures were tested as active module to transport liquid from the bottom side to the top and to the absorbent module. The two main goals are to prove the effective functionality of the channels as liquid extractor and to evaluate different rate if the structure changes.

The evaluation was made weighting the absorbent module after 10 minutes from the adding. The results are shown in the Figure 44. The test was made on 4 samples for each series and looking at average value it seems that the liquid absorption is higher for the first structure, but the standard deviation error is very high for the second structure. Therefore, this conclusion is impossible to confirm. The deviation is high because during the experiment it was noticed two samples were not complete in contact with all the channels, preventing full absorption.

For the structure with 23 channels the absorbent module gains around 9 times of the initial weight after 10 minutes of the test, and, even after 10 minutes, the absorbent modules were not yet saturated. While the absorbent layer changes his weight during the absorption, the moisturizer module was not affect from the liquid, indeed it didn't gain weight and it didn't change shape or color of the structure.

From Figure 45 it is possible to see the change of the absorbent module during the test, it is noticeable that already after 1 min there some liquid which reaches the top of the module, from this result we can assume that the initial absorption is quite fast.

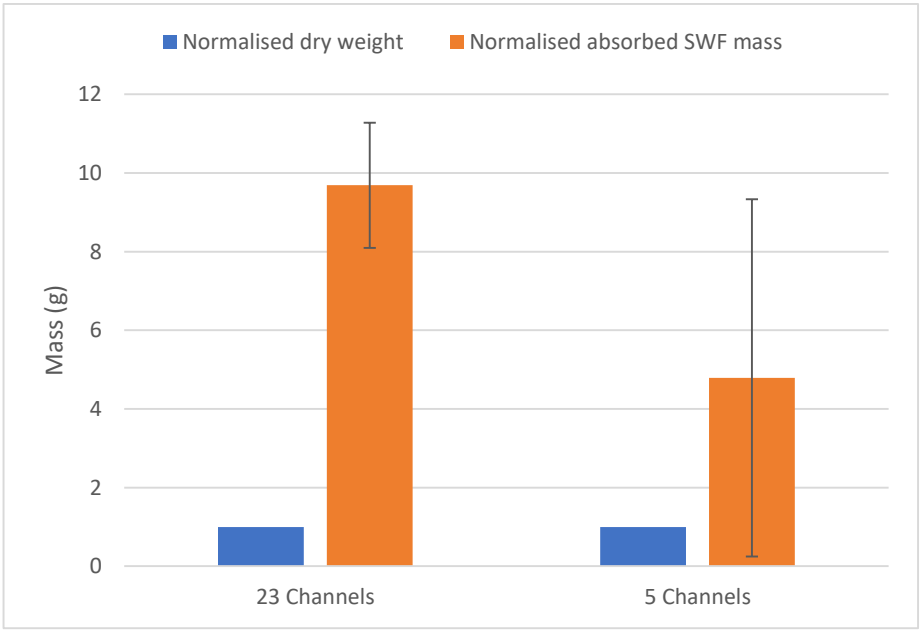

Figure 34. Graph of the absorbent weight during after the test in case the moisturizer module has 23 or 5 channels

For future work it would be important to test and evaluate the rate in order to have information to the structures and absorption rate related to have a better customization of the dressing.

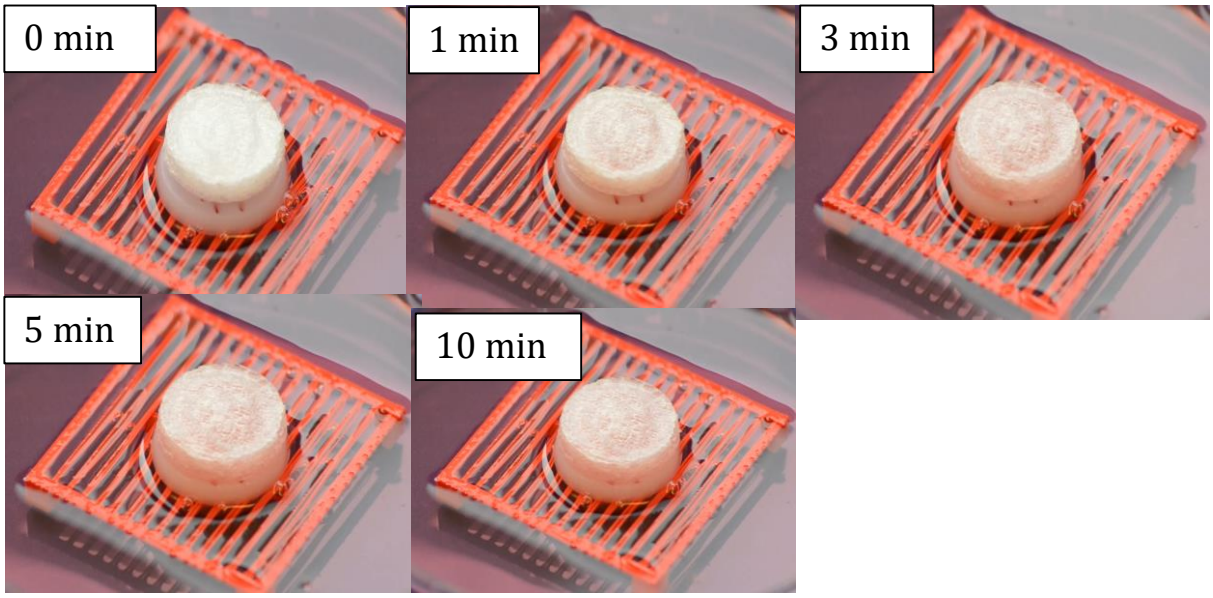

Figure 35. Pictures of the experiment taken at 0, 1, 3, 5 and 10 minutes.

Chapter 6

6. Discussion

Analysing the results from the tests above it is possible to deduce which is the best material to create the prototype. First of all, the hydrogel must be 3D printable, and therefore have shear thinning properties, in the viscosity analysis is shown that all compositions are 3D printable but some are easier to print than other, except the alginate solution, where it is show low viscosity at low shear rate. The compositions with higher alginate shown a higher viscosity, meaning that during the printing process is necessary to use higher pressure and low extruder speed, indeed for the composition with around 80% of alginate the pressure used was in the range of 170 kPa while for the composition with 20% of alginate only 20-30 kPa is necessary. The pressure during printing depends also from the friction between pistons and cartridges, but for a defined couple cartridge-piston the pressure depends only from the material viscosity.

The first requirement to satisfy is listed in Table 1 and it is: to keep moist the wound bed for at least 7 days. Currently Aquacel® is used in chronic wound to maintain the moisture level in the wound bed during healing. Thanks to the water retention test is shown that all hydrogels have better WRT_{value} than Hydrofiber® dressing. Between the composition with MFC1 and MFC8 and 20% of alginate the second one has slightly higher values, but the test shows that both materials are suitable for the application to keep the wound bed with a proper moisture level. The capacity to hold water depends from the hydrogen bonds creates between fibrils, most correctly from the surface substituent, and water molecules, groups with higher polarity create stronger hydrogen bond.

Correlated to the water retention test is the shrinking test, where shrinking is mainly due to water evaporation and the network strength, indeed from the result is shown crosslinked materials have higher ST_{value}, this makes MFC1_8020 and MFC8_8020 promising materials for this application.

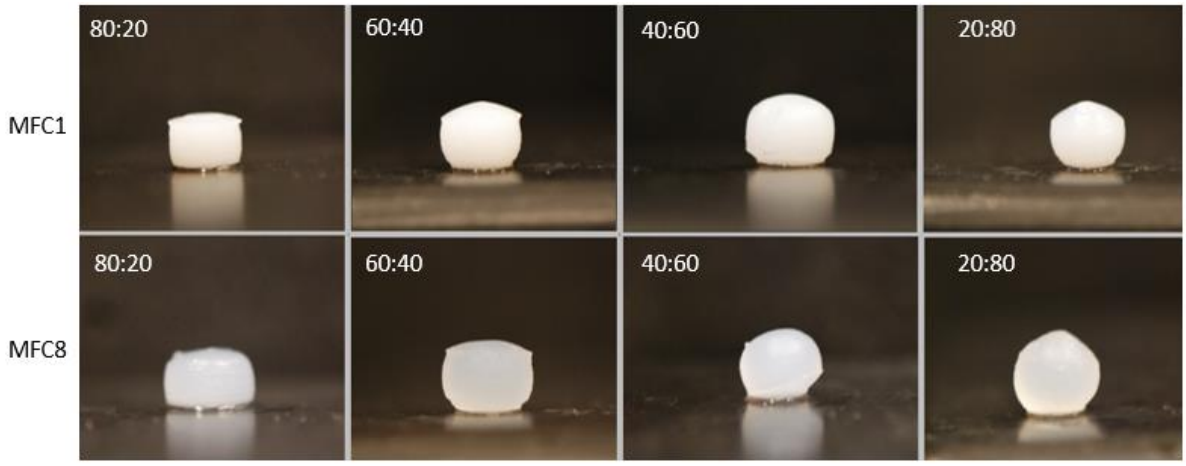

Figure 36. Samples for the compression test. The swelling behaviour is greater for higher alginate content

Regarding the mechanical properties is shown that compressive modulus is higher if alginate increase, while generally yield strain decrease. The first deduction from the compressive results is that the material without alginate (MFC8_1) is not suitable for this application since the poor mechanical properties, see Table 12. From visual inspection is important to report higher swelling for compositions with higher alginate amount, as shown in Figure 46 below.

The composition with only the 20%w/v of alginate show a good flat surface with low swelling, which will result in better reproducibility of the structure to print. The meaning of the higher compressive modulus for higher values of alginate content it is supposed to be caused by the alginate network formation that give strength to the structure and consequently lock the fibrils. Higher amount of alginate will create a network denser and stronger, indeed load is primarily supported by the matrix, in this case the alginate network, and after the fibril network will keep the structure but in this test the fibrils break point is not reached. The only alginate structures show higher yield stress and yield strain with a compressive modulus in the range of 60 kPa, in this material there are not fibrils. The composition with 60% and 80%w/v show high rigidity, which makes the materials not suitable for this application since high rigidity and low elasticity. Considering the composition with 20%w/v of the two materials, MFC1_8020 and MFC8_8020, the yield strain is the most suitable for the application with values of 49% and 39% respectively, while the MFC8_8020 shows higher compressive modulus, 35kPa compare to 29kPa, but lower yield stress, 57kPa compared to 72kPa.

Thanks to the crosslinking kinetics test is possible to evaluate the crosslinking time evaluating the storage modulus increasing, G'. In Figure 29 and Figure 30, it is shown the increasing of G', which is very fast, meaning that the crosslinking is a fast reaction. The crosslink starts from the surface, forming a skin outside of the material, which limit the crosslinker diffusion in the bulk for the structure complete crosslink, indeed alginate solution will take around 25 minutes to have complete crosslink, as shown in Figure 47 below. The composition with microfibrillated cellulose and alginate have a faster time to reach the complete crosslink. Therefore, the fibrils presence facilitated the crosslink, probably due to the lower presence of alginate on the surface and more distributed in all the material. Furthermore, analysing the G' before the crosslink is possible confirm the results already seen in the viscosity test where hydrogels with higher alginate % have higher viscosity. As last result is possible to see that MFC8_8020 has higher final G' than MFC1_8020, as in the same way in the compressive results.

The mechanical properties trend is also confirmed by the shear resistance where is possible to see the break point for the materials MFC1_8020, MFC1_6040, MFC8_8020, MFC8_6040 and MFC8_4060, while for the others, MFC1_4060, MFC1_2080 and MFC8_2080 is not visible since the test is stopped at 10kPa of oscillation stress. Regarding the interested composition MFC1_8020 and MFC8_8020, the value where the G'' intersect G' correspond to the break point of the solid structure under shear forces, this values has the same trend of the yield stress in the compression test, since it is 4,5 kPa and 4 kPa respectively.

Cytotoxicity test confirm the skin friendly behaviour of the material.

During the structure characterization the printability test show that height higher than 3 mm make the structure too rigid and unable to fulfil uneven wound surface, thus height between 1,5 and 2 mm are suggested for the prototype. The infill test suggests a honeycomb infill with a percentage between 20 and 25% to have well defined channels and enough strong structure to be hand able.

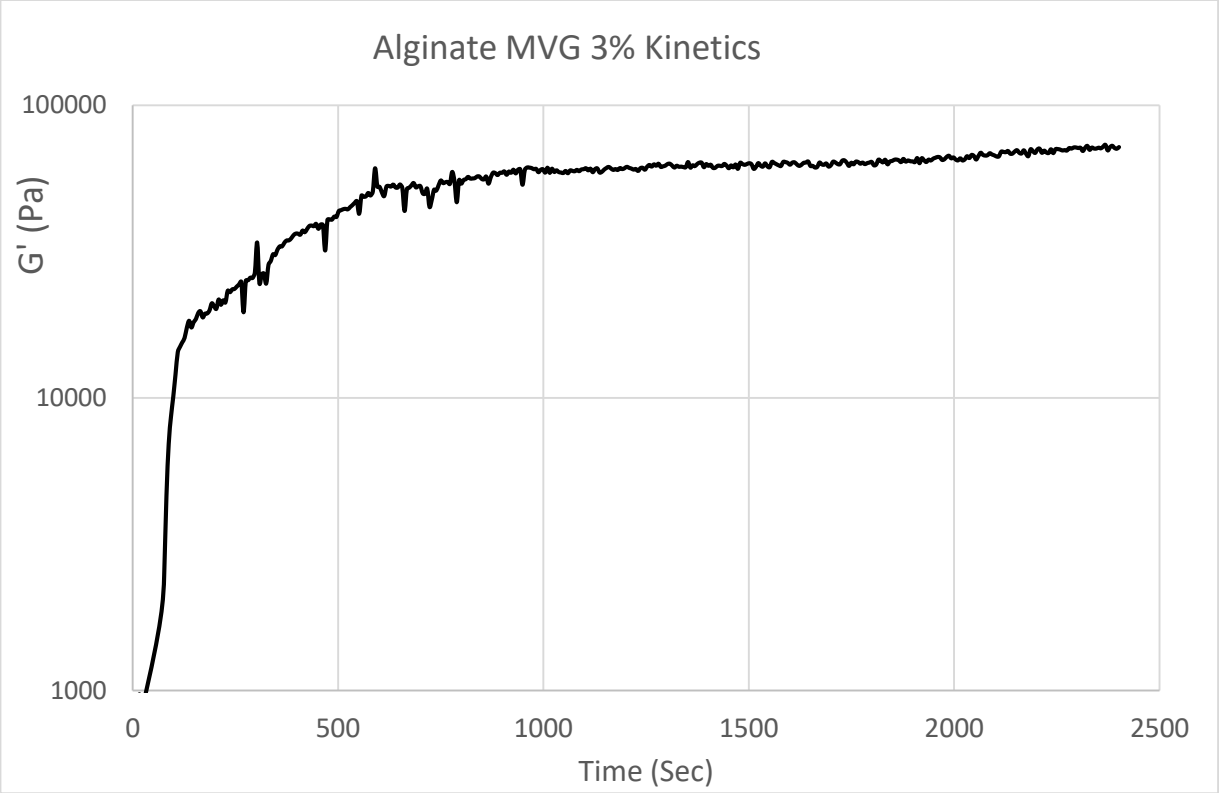

Figure 37. Alginate crosslinking kinetics test.

The combination of the two first modules in the interaction test help to evaluate drying process done by the second module to the first one. This tests show that the drying is fast for the first 20 hours but then is almost saturated, probably because the second module absorb the free water on the higher layer of the module but once that is saturated the first layer of the absorbent module, the drying is slowly and mainly due to the evaporation since the samples are open when they have to be weighted. This test shows also that MFC8_8020 is the material that dry less between the two compositions tested.

In the liquid extraction test, the results are difficult to interpret since it is impossible to find an extraction rate for the different structures, but it is proven that the structures can extract liquid and bring it to the absorbent module. In a future work is recommended to define the extraction rate of the structures.

In the end, two microfibrillated cellulose with different amount of alginate were tested and mechanical and other properties are reported. Both MFC1_8020 and MFC8_8020 are suitable for the application to create the prototype. However, for the next stage, the prototype printing, was used only MFC8_8020, also because it satisfies the desire described to be transparent, useful to help wound bed visual inspection without the full dressing removal. In the next section the description of the prototype construction is done.

Chapter 7

7. Prototype development

In the end, after material development and characterization a prototype was develop and tested combined with the other modules. Two type of prototypes were developed. The develop start from the design and ended with the printing of a dressing for a simulated wound on the intern part of a simplify elbow, to show that is possible to create these kind of dressing also on concave surfaces.

7.1. Design of the prototype

The structure designed were two main group:

1. Flat prototype: structure reproduces a hypothetical wound and is printed with a height of 1.5 mm and two design of the channels, a honeycomb infill with 22% and with 23 elliptical channels;
2. Concave prototype: the structure reproduces the uneven surface of a hypothetical wound with designed channels and is printed with support ink to reproduce the exact surface.

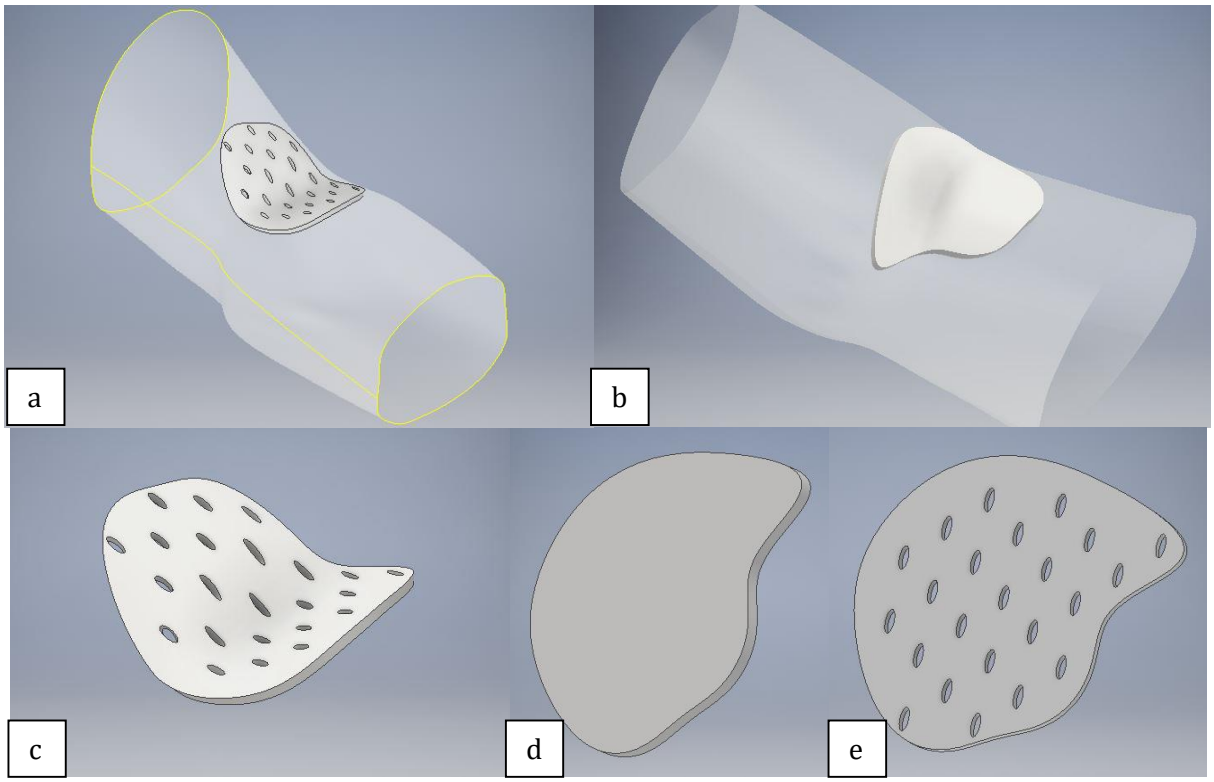

Figure 38. Prototype design: a) and b) Elbow structure used as model for the simulated wound, with and without designed channels c) Concave prototype model, d) Flat model used for the printing with low infill, e) Flat model with designed channels

In Figure 48 are shown the different model used for the prototype printing.

7.2. Printing process

For the printing it was used the BioX printer supplied from CELLINK, Figure 49, and it was used CELLINK start as support ink for the concave structure, Figure 50. A conical nozzle of 0.41mm was used for the concave structure while a conical nozzle of 0,25 mm was used for the flat structure, to have a better resolution. The time printing was around 7 hours for the convex structure while only 30 min for the slat structure.

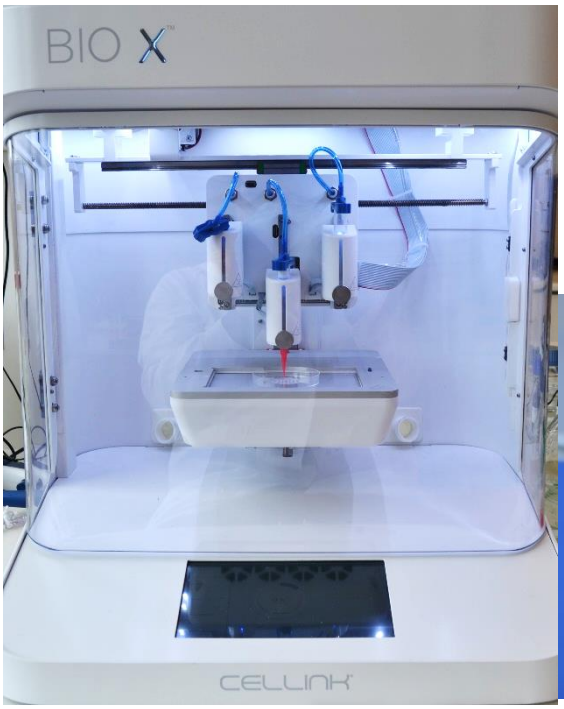

Figure 39. BioX printer

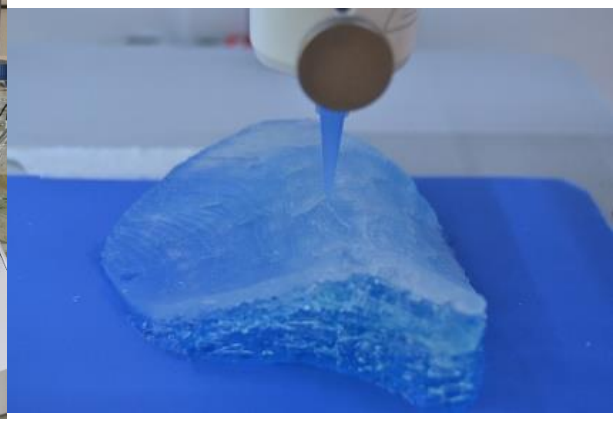

Figure 50. Printing process of the concave prototype

In Figure 50 it is showed the concave prototype. This solution presents some disadvantages:

- Long-time printing, around seven hours.
- Low resolution if used 0,41 mm nozzle, to have higher resolution it is necessary to use smaller nozzle but the printing time will increase even further.
- The channels need to be designed from the STL file, they cannot be created automatically by the printing process.

For the reasons listed above this solution is rejected for the final prototype choice.

Figure 40. Concave prototype, with and without the support structure

In Figure 52 are showed the flat prototype model. The show good mechanical properties and, contrary to the concave prototype, they are fast to produce with good resolution, 30 min with 0,25 mm. These are the solutions that will be considered the best choice for the final prototype model.

In the end the flat prototype was chosen as the most suitable for the application since it has the advantage of being faster when printed and it is flexible enough, Figure 53, to fulfil the uneven surface of the elbow.

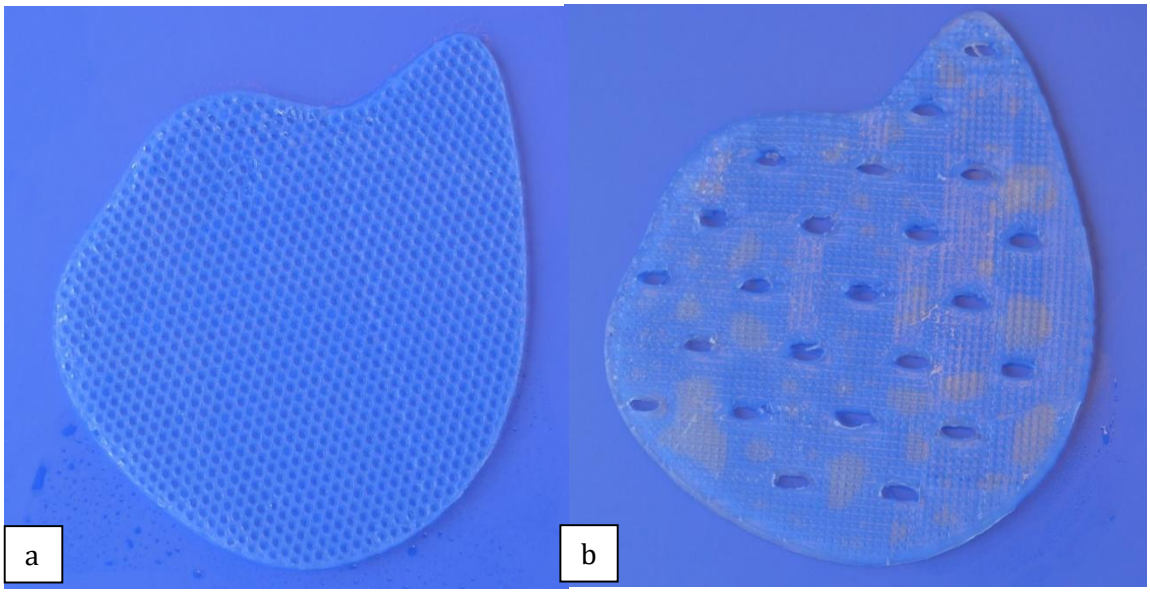

Figure 41. Flat prototype, a) with channels designed and b) with low infill and honeycomb pattern

Chapter 8

8. Conclusion and future work

In the end, it is shown in this work the hydrogel MFC/alginate based characterization with rheological and mechanical test. The MFC1 and MFC8 properties were evaluated and compared with different amount of alginate in the compositions. The material chosen for this application is a combination of microfibrillated cellulose, enzymatic or carboxylmethylated, and alginate with a ratio 80:20. After the material assessment, a structure characterization showed the best solution for a prototype development. The best solution was found in the flat prototype with 22% of infill and honeycomb pattern, the final prototype is show in Figure 51. To conclude, the possibility of using MFC as material for wound dressing applications and 3D printing processes as method was proven. The requirements listed in Table 1 are satisfied both from the material and from the structure, as shown in Table 14.

Table 14. Requirements of the moisturizer module

Number	Requirement	Description
1	Keep moist	The wound bed must to be kept moist for at least 7 days to have a proper healing
2	Remove wound exudate	The wound exudate produced from the wound must to be removed
3	Mechanically stable under moderate compression and shear forces	The material must be stable under moderate compression and shear forces to maintain the structure
4	Retain the shape to prevent the maceration	The material must not shrink to much to stay in place and maintain the wound bed moist all the time
5	Be 3D printable	The material must be 3D printable in order to have the possibility of create a structure that reproduce the wound shape and preventing maceration and lifting of the skin transplant
6	Be skin friendly	The material must not cause allergic reaction or irritation to the patient's skin
7	Be Sterile	The material must be sterilize before the use
8	Be applied without causing any pain to the patient	The module must to be easy to apply without causing pain to the patient
9	Available on demand	The module must be available to caregiver immediately after surgery
10	Allow the daily tasks of the patient	The module must not be invasive to allow daily activities to the patients to reduce the medical cost and improve the living during the wound healing

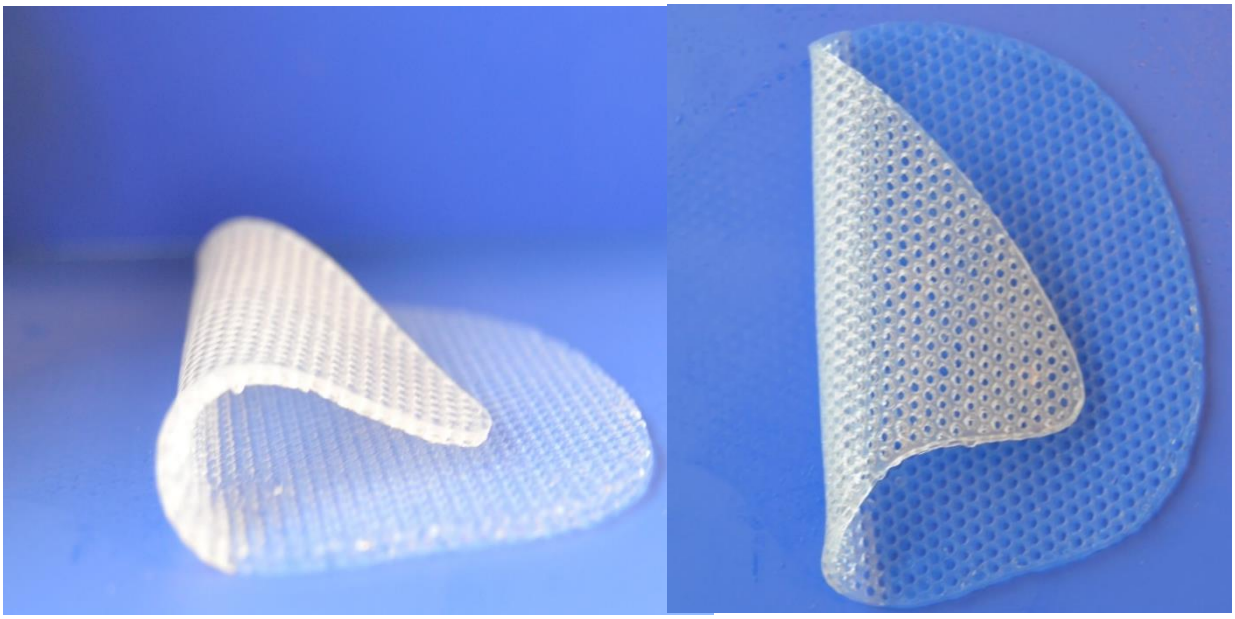

Figure 42. Flat prototype with 22% of infill, it is so flexible that it is foldable

Furthermore, regarding the desires listed in Table 2, it is possible to see that one desires is achieved using MFC8_8020 as material, since it is more transparent than MFC1_8020, as shown in Figure 54. The other three desires; (i) customized moisture level, (ii)customized exudates removal and (iii) prevent bacterial growth, could be use as inspiration for future work. Indeed, there are already on market some material that prevent bacterial growth, as Aquacel Ag®, but could be very useful the possibility to combine these properties with a customized moisture level of the material that could be used on demand thank to the 3D printing technology. To achieve this goal is important first to investigate and define the right moist level necessary for a correct wound healing. Last, a customized exudate removal could be achieved but it is necessary to investigate more the transport phenomena of the liquid through the moisturizer module, indeed in this work it has been proven the functionality but we didn't characterize quantitatively the exudates removal.

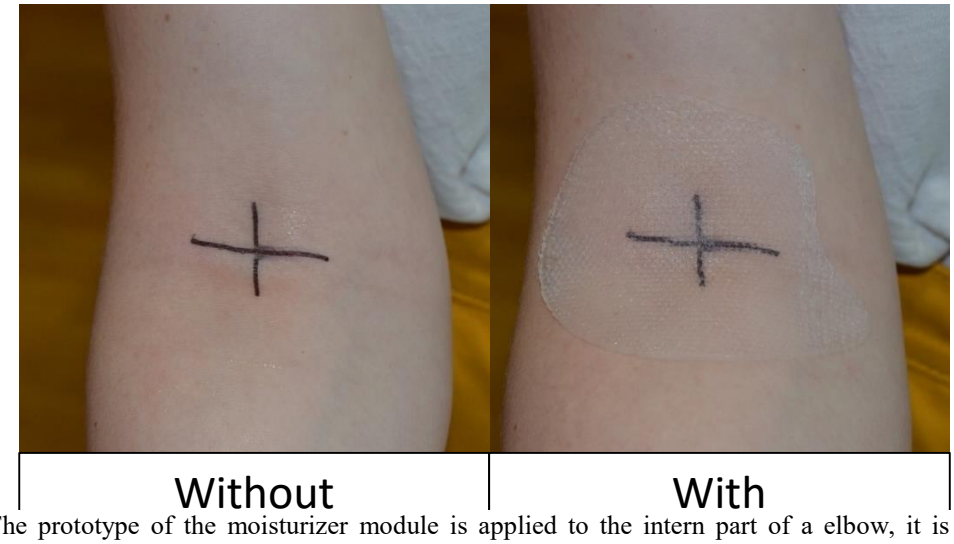

Figure 54. The prototype of the moisturizer module is applied to the intern part of a elbow, it is shown its transparency

9. Bibliography

[1] *Behovsstudie om sårläkning vid hudtransplantationer* **2017**.

[2] O. Nechyporchuk, M.N. Belgacem, J. Bras, *Ind. Crops Prod.* **2016**, *93*, 2.

[3] D. Klemm, B. Heublein, H.P. Fink, A. Bohn, *Angew. Chemie - Int. Ed.* **2005**, *44*, 3358.

[4] T. Lindström, C. Aulin, A. Naderi, M. Ankerfors, *Encycl. Polym. Sci. Technol.* **2014**, 1.

[5] T. Lindström, C. Aulin, *Scand. J. For. Res.* **2014**, *29*, 345.

[6] Y. Habibi, *Chem. Soc. Rev.* **2014**, *43*, 1519.

[7] V.K. Varshney, S. Naithani, **2011**, 43.

[8] C. Aulin, E. Johansson, L. Wågberg, T. Lindströ, **2010**, 872.

[9] C. Aulin, S. Ahok, P. Josefsson, T. Nishino, Y. Hirose, M. Österberg, L. Wågberg, *Langmuir* **2009**, *25*, 7675.

[10] A. Isogai, *J. Wood Sci.* **2013**, *59*, 449.

[11] G. Siqueira, S. Tapin-Lingua, J. Bras, D. da Silva Perez, A. Dufresne, *Cellulose* **2011**, *17*, 1147.

[12] K.R. Turbak, A.F.; Snyder, F.W.; Sandberg, *J. Appl. Polym. Sci. Appl. Polym. Symp.; (United States)* **1983**, *37*.

[13] K.R. Herrick, F.W.; Casebier, R.L.; Hamilton, J.K.; Sandberg, *J. Appl. Polym. Sci. Appl. Polym. Symp.; (United States)* **1983**, *37*.

[14] H.R. Nordli, G. Chinga-Carrasco, A.M. Rokstad, B. Pukstad, *Carbohydr. Polym.* **2016**, *150*, 65.

[15] T. Saito, M. Hirota, N. Tamura, S. Kimura, H. Fukuzumi, L. Heux, A. Isogai, *Biomacromolecules* **2009**, *10*, 1992.

[16] J.M.B. Fernandes Diniz, M.H. Gil, J.A.A.M. Castro, *Wood Sci. Technol.* **2004**, *37*, 489.

[17] M. Spinu, N. Dos Santos, N. Le Moigne, P. Navard, *Cellulose* **2011**, *18*, 247.

[18] S. Janardhnan, M.M. Sain, *Cellul. Microfibril Isol. Bioresour.* **2006**, *1*, 176.

[19] M. Henriksson, G. Henriksson, L.A. Berglund, T. Lindström, *Eur. Polym. J.* **2007**, *43*, 3434.

[20] H. Fukuzumi, T. Saito, A. Isogai, *Carbohydr. Polym.* **2013**, *93*, 172.

[21] A. Isogai, T. Saito, H. Fukuzumi, *Nanoscale* **2011**, *3*, 71.

[22] K. Markstedt, A. Mantas, I. Tournier, H. Martínez Ávila, D. Hägg, P. Gatenholm, *Biomacromolecules* **2015**, *16*, 1489.

[23] K. Markstedt, A. Escalante, G. Toriz, P. Gatenholm, *ACS Appl. Mater. Interfaces* **2017**, *9*, 40878.

[24] K.L. Spence, R.A. Venditti, O.J. Rojas, J.J. Pawlak, M.A. Hubbe, *BioResources* **2011**, *6*, 4370.

[25] N. Øyvind Eriksen, Norwegian University of Science and Technology, Trondheim, Norway, Kristin Syverud, Paper and Fibre Research Institute, Trondheim, Norway, Øyvind Gregersen, Norwegian University of Science and Technology, Trondheim, *Nord. Pulp&Paper* **2008**, *23*, 299.

[26] M. Pääkko, M. Ankerfors, H. Kosonen, A. Nykänen, S. Ahola, M. Österberg, J. Ruokolainen, J. Laine, P.T. Larsson, O. Ikkala, T. Lindström, *Biomacromolecules* **2007**, *8*, 1934.

[27] M. Pääkkö, et al, *Biomacromolecules* **2007**, *8*, 1934.

[28] T. Saito, A. Isogai, *Colloids Surfaces A Physicochem. Eng. Asp.* **2006**, *289*, 219.

[29] T. Zimmermann, E. Pöhler, T. Geiger, *Adv. Eng. Mater.* **2004**, *6*, 754.

[30] M. Henriksson, L.A. Berglund, P. Isaksson, T. Lindström, T. Nishino, *Biomacromolecules* **2008**, *9*, 1579.

[31] N.J. Davis, S.L. Flitsch, *Tetrahedron Lett.* **1993**, *34*, 1181.

[32] R.K. Johnson, A. Zink-Sharp, W.G. Glasser, *Cellulose* **2011**, *18*, 1599.

[33] U.J. Kim, S. Kuga, *J. Chromatogr. A* **2001**, *919*, 29.

[34] A. Tejado, M.N. Alam, M. Antal, H. Yang, T.G.M. van de Ven, *Cellulose* **2012**, *19*, 831.

[35] H. Liimatainen, N. Ezekiel, R. Sliz, K. Ohenoja, L. Berglund, O. Hormi, *ACS Appl. Mater. Interfaces* **2013**, *5*, 13412.

[36] L. Wågberg, G. Decher, M. Norgren, T. Lindström, M. Ankerfors, K. Axnäs, *Langmuir* **2008**, *24*, 784.

[37] C. Eyholzer, N. Bordeanu, F. Lopez-Suevos, D. Rentsch, T. Zimmermann, K. Oksman, *Cellulose* **2010**, *17*, 19.

[38] W. Lars, L. Winter, L. Dberg, T.O.M. Lindstrom, **1987**, *27*, 163.

[39] H. Dai, S. Ou, Y. Huang, Z. Liu, H. Huang, *Cellulose* **2018**, *25*, 593.

[40] O. Aarstad, E.B. Heggset, I.S. Pedersen, S.H. Bjørnøy, K. Syverud, B.L. Strand, *Polymers (Basel).* **2017**, *9*.

[41] A. Saarai, V. Kasparkova, T. Sedlacek, P. Saha, *J. Mech. Behav. Biomed. Mater.* **2013**, *18*, 152.

[42] Ý.A. Mørch, S. Holtan, I. Donati, B.L. Strand, G. Skjåk-Bræk, *Biomacromolecules* **2008**, *9*, 2360.

[43] A. Basu, J. Lindh, E. Ålander, M. Strømme, N. Ferraz, *Carbohydr. Polym.* **2017**, *174*, 299.

[44] A.B.G. Lansdown, F.R.C. Path, *Wound Repair Regen.* **2002**, *10*, 271.

[45] T. Hakkarainen, R. Koivuniemi, M. Kosonen, C. Escobedo-Lucea, A. Sanz-Garcia, J. Vuola, J. Valtonen, P. Tammela, A. Mäkitie, K. Luukko, M. Yliperttula, H. Kavola, *J. Control. Release* **2016**, *244*, 292.

[46] K. Vowden, P. Vowden, *Br. J. Community Nurs.* **2003**, *8*, 4.

[47] G.D. Winter, *Nature* **1962**, *193*, 293.

[48] N.J. Trengove, M.C. Stacey, S. Macauley, N. Bennett, J. Gibson, F. Burslem, G. Murphy, G. Schultz, *Wound Repair Regen.* **1999**, *7*, 442.

[49] M. Benbow, *Nurs. Stand.* **2016**, *30*, 40.

[50] K.F. Cutting, *Br. J. Community Nurs.* **2003**, *8*, S4.

[51] S.S. Scherer-pietramaggiori, G. Pietramaggiori, P. Dennis, *Plast. Surg.* **2013**, 319.

[52] A. Ag, *In Vitro* **1997**, 14.

[53] A. Rees, L.C. Powell, G. Chinga-Carrasco, D.T. Gethin, K. Syverud, K.E. Hill, D.W. Thomas, *Biomed Res. Int.* **2015**, *2015*.

[54] G. Chinga-Carrasco, *Bioengineering* **2017**.

[55] N. Hong, G.-H. Yang, J. Lee, G. Kim, *J. Biomed. Mater. Res. Part B Appl. Biomater.* **2017**, 1.

[56] A. Rees, L.C. Powell, G. Chinga-Carrasco, D.T. Gethin, K. Syverud, K.E. Hill, D.W. Thomas, *Biomed Res. Int.* **2015**, *2015*.

[57] L. Greenspan, *J. Res. Natl. Bur. Stand. -A. Phys Ics Chem.* **1977**, *81*.